UNIVERSITY OF CALIFORNIA,
IRVINE

The role of Myoglianin in *Drosophila* metamorphosis

DISSERTATION

submitted in partial satisfaction of the requirements
for the degree of

DOCTOR OF PHILOSOPHY

in Biological Sciences

by

Maribel Alvarez

Dissertation Committee:
Professor Kavita Arora, Chair
Professor Todd C. Holmes
Professor Diane K. O'Dowd
Professor Thomas F. Schilling

2015

TABLE OF CONTENTS

LIST OF FIGURES

LIST OF TABLES

ACKNOWLEDGEMENTS

I would like to express my deepest gratitude towards my thesis advisor, Kavita Arora for her guidance. Her passion for science was an inspiration. I would like to thank my thesis committee members: Dr. Todd Holmes, Dr. Diane O'Dowd, and Dr. Thomas Schilling for their advice and suggestions. I thank Dr. Michael Mulligan who has supported me throughout every step of this PhD. I would also like to thank the Minority Science Program and directors, Dr. Marlene de la Cruz and Dr. Luis Mota-Bravo for all their support. I would like to express my appreciation towards Dr. Doug Bornemann and Debra Mauzy-Melitz for their advice. I would like to acknowledge AGEP/DECADE, graduate division, and Tom Angell for their support during trying times.

I would like to thank former members of the Arora lab: Dr. Jeremy Ellis, Dr. Jane Cho, Dr. Joseph Pentek, Dr. Rebecca Dunning and Brittany Ross for their suggestions. To my undergraduate students Eric, Tiffany, Huy, Jila, Billy, Nicole, Alfred, Shirin, Katherine, and Priyanka, thank you for permitting me to teach you. I consider you not only my students but also friends. I would like to specially thank my friends Celina, Faby, and Vaishali for always being there for me.

Finally, I would like to thank my family for their unconditional support. Este logro no es solo mío. También es de ustedes. My parents, Jesus and Juana, taught me that I could accomplish anything if I work hard and have the determination to follow my dreams. I would like to thank my siblings Jorge, Elizabeth, and Angelica for their support. My boys, Junior and Elvis, need to be recognized as they have been by my side every moment through this journey.

CURRICULUM VITAE

Maribel Álvarez

EDUCATION

2015 Ph.D. in Biological Sciences, University of California, Irvine

2005 B.A. in Biology and Minor in Spanish Language, California State University Northridge, Northridge

PROFESSIONAL EXPERIENCE

Graduate Student, Developmental and Cell Biology, University of California, Irvine, Irvine, CA, June 2008-Present.
Thesis Advisor: Dr. Kavita Arora
Project: The role of Myoglianin in *Drosophila* metamorphosis

Minority Health and Health Disparities International Research Training (MHIRT), University of California, Irvine, California; Neurobiology Institute, National University of Mexico (UNAM), Querétaro, México, Summer 2006

- Program Director: Dr. Luis Mota-Bravo
- Associate Director: Dr. Marlene de la Cruz
- UNAM Faculty Mentor: Dr. Carmen Clapp
- Project Goals: Investigate the proangiogenic actions of the GH/IGF-1 axis and their interaction with VEGF. Determine whether the intravitreal injection of GH induces the expression of IGF-1 and VEGF in the retina and results in retinal vasodilation.

UCLA Post-Baccalaureate Research Scholar, University of California Los Angeles, Los Angeles, CA, July 2005- June 2006.

- Program Director: Dr. Richard L. Weiss
- UCLA faculty mentor: Dr. Kathy Sakamoto
  Project Goals: Characterization of interacting molecules with cAMP response element binding protein (CREB).

Undergraduate Research Assistant, NIH MBRS RISE program, California State University Northridge, Northridge, CA, June 2004-August 2005.

- Program Director: Dr. Maria Elena Zavala
- Faculty Mentor: Dr. Steve Oppenheimer
  Project Goals: Characterization of molecules in sea urchin disaggregation supernatant.

Undergraduate Research Assistant, Center for Cancer and Developmental Biology, California State University Northridge, Northridge, CA, June 2003- June 2004.

- Faculty Mentor: Dr. Steve Oppenheimer
  Project Goals: Investigate the interaction between mannose-rich yeast to concanavalin A, a mannose-binding lectin, in the presence of 30 different carbohydrates and under 9 different pH conditions.

Teaching Experience

Teaching Assistant:

DNA to Organisms (Bio 93): Fall 2009
Instructors: Drs.Diane O'Dowd and Rahul Warrior

Developmental Biology (D104): Winter 2009, Winter 2011, Winter 2014
Instructors: Drs. Kavita Arora and David Gardiner

Scientific writing (Bio 100): Spring 2012, Fall 2012, Winter 2013, Spring 2014.
Instructor: Dr. Debra Mauzy-Melitz

Santa Ana high school 2010-2011
GK-12 Fellowship
Program directors: Drs. Luis M. Mota-Bravo, Michael Mulligan, and Marlene de la Cruz.

PUBLICATIONS

Journal Publications:

- Alvarez, M., Nnoli, J., Carroll, E. J., Hutchins-Carroll, V., Razinia, Z. and Oppenheimer, S. B. (2008) Exogenous hyalin and sea urchin gastrulation, part II: Hyalin, an interspecies cell adhesion molecule. Zygote. 16, 73-78
- Oppenheimer, S. B., Alvarez, M. and Nnoli, J. (2008) Carbohydrate-based experimental therapeutics for cancer, HIV/AIDS and other diseases. Acta Histochem. 110, 6-13
- Zem, G. C., Badali, O., Gaytan, M., Hekmatjou, H., Alvarez, M., Nnoli, J., Katus, E. and Oppenheimer, S. B. (2006) Microbead analysis of cell binding to immobilized lectin: An alternative to microarrays in the development of carbohydrate drugs and diagnostic tests. Acta Histochem. 108, 311—317

ABSTRACT OF THE DISSERTATION

Role of Activin signaling in the *Drosophila* nervous system

By

Maribel Alvarez

Doctor of Philosophy in Biological Sciences

University of California, Irvine, 2015

Professor Kavita Arora, Chair

Signaling by the Transforming Growth Factor-β (TGF-β) superfamily is essential for many cellular processes and is required throughout the life of many organisms. TGF-β signaling triggers distinct developmental programs and cellular processes, thus disruption of the pathway is associated with defects in development and growth of the organism. Signaling specificity is achieved through the use of distinct pathway components and combinatorial action with other cell signaling pathways. The main goal of my thesis project was to understand the roles of two ligands of the TGF-β superfamily, Maverick (Mav) and Myoglianin (Myo), and their mechanism of action in *Drosophila*. We first characterized several mutant alleles for *mav* and *myo* that were previously generated in the lab. Next, we investigated the role of *mav* at the neuromuscular junction (NMJ). Loss-of-function analysis suggests that *mav* has no affect on growth of the NMJ. However, ectopic expression of *mav* in glial cells does have

an affect on the NMJ, suggesting that while not essential, NMJ growth may be sensitive to changes in levels of Mav. Phenotypic analysis of mutations in *myo* that encodes an activin ligand, revealed a wide range of metamorphosis phenotypes reminiscent of loss of the steroid hormone ecdysone. We investigated the role of *myo* in several tissues that undergo specific changes during metamorphosis. We determined that *myo* is selectively required for expression of the ecdysone receptor EcR-B1 isoform in a diverse group of neurons in the central nervous system, but not in other EcR-B1 expressing tissues, for example gut, fat body and salivary glands. Therefore one of the roles of Myo is to regulate the ability of specific cells to respond to ecdysone. Importantly, we found that salivary gland destruction in response to ecdysone signaling is dependent on activin signaling, but this occurs through regulation of EcR-B1 in specific cells in the brain, rather than in the salivary gland itself. Our data argue for a model in which ecdysone signaling utilizes both direct and indirect inputs to coordinate salivary gland destruction during pupal metamorphosis. The work presented here provides insights into the requirement of Myo/activin signaling in regulation and coordination of steroid dependent biological processes in animals.

Chapter 1

Introduction

Cell-cell communication and the TGF-β signaling pathway

In all multicellular organisms, cell-cell communication is critical for cell growth, division, cell fate specification, differentiation and the ability of the cell to carry out specific functions. Cell communication can occur through short or long-range signals that are essential for survival of the organism. The TGF-β superfamily is part of a larger network of signaling pathways that together regulate many biological processes. For example, cell proliferation, differentiation, embryonic patterning, stem cell maintenance, and organogenesis are all regulated by inputs not only from the TGF-β pathway, but also Wingless (Wg)/Wnt, Hedgehog (Hh), Notch/Delta, and mitogen-activated protein kinase (MAPK) signaling (Guo and Wang, 2009). Studies in *Drosophila* have proven to be very useful in understanding the function of these pathways and dissecting cross talk between signaling pathways. These studies have also provided valuable insights into the possible roles and mechanism of action of these pathways in higher organism as the pathways and signaling components are conserved across species.

The TGF-β superfamily of ligands can be further subdivided into three subfamilies based on sequence homology. The three major branches are TGF-βs, Bone Morphogenetic Proteins (BMPs), and activins (Massague, 1998; Parker et al., 2004). There family includes other divergent members such as growth differentiation factors (GDFs), glial derived neurotrophic factors (GDNFs), Nodal, and Müllerian inhibiting substance (MIS). TGF-β superfamily ligands contain characteristics that are hallmarks of the pathway. The ligands are synthesized as

precursor proteins, that contain a secretion signal sequence, a proteolytic cleavage site, and a C-terminal ligand domain with seven or nine cysteine residues at specific positions (Parker et al., 2004). Disulfide linked homodimeric or heterodimeric ligands bind to a complex of serine/threonine kinase transmembrane receptors. Upon ligand binding, the type II receptor phosphorylates the type I receptor, activating the type I receptor kinase, and allowing it to phosphorylate intracellular receptor-regulated R-Smads. The phosphorylated R-Smads associate with a co-Smad and accumulate in the nucleus to regulate gene expression.

Vertebrate BMPs were identified as factors required for bone formation. However, since this initial discovery, many more functions have been identified for BMPs, such as in embryonic axis specification, gastrulation, organogenesis, neurogenesis, chondrogenesis, and interdigit apoptosis (reviewed in Massague 1996). Activins were identified as endocrine factors required for follicle-stimulating hormone (FSH) biosynthesis and secretion in the fly reproductive organs (Ling et al., 1986). Vertebrate activins are also essential for induction of axial mesoderm and anterior structures in the embryo, and for erythroid differentiation (reviewed in Carcamo et al., 1994). Inhibins have the opposite affect compared to activins, as they prevent FSH synthesis. Five representatives of the TGF-β subfamily have been identified TGF-β 1, 2, 3, 4 (identified only in the chick), and 5 (identified only in *Xenopus*). These ligands are important for cell cycle arrest of epithelial and hematopoietic cells and for proliferation and differentiation of mesenchymal cells (reviewed in Massague, 1990). Nodals are

important for left-right asymmetry and mesoderm induction (Hogan, 1996). GDNF is a glial derived factor important for dopaminergic neuron survival and for kidney development (reviewed in Massague, 1996).

TGF-β pathway in *Drosophila*

The fruit fly is favored as a model organism for studies of signaling pathways and analysis of gene regulatory networks because of significant gene conservation with vertebrates and low functional redundancy. It is estimated that 75% of disease related genes found in humans are also found in *Drosophila* (Reiter et al., 2001). Analysis of the TGF-β pathway in *Drosophila* has also proven useful in understanding the more complex pathway in mammals. Over thirty different TGF-β superfamily ligands, seven type I receptor, and five type II receptors, have been identified in mammalian systems. In contrast, seven ligands, three type I receptor, and two type II receptors have been identified in *Drosophila* (Parker et al., 2004; Massague 2012; Wrana 2013). The fly BMP ligands Decapentaplegic (Dpp), Glass bottom boat (Gbb), and Screw (Scw) are important for embryonic and larval development, while the activin-related ligands Activin-β (Act β), Dawdle (Daw) and Myoglianin (Myo), have been linked to various aspects of nervous system development. Maverick (Mav) shows low homology to all three subfamilies and remains to be assigned to a pathway. There are no *Drosophila* ligands belonging to the TGF-β subfamily (Parker et al., 2004; Pentek et al., 2009).

Extensive studies of the TGF-ß pathway genes in *Drosophila* have

revealed the mechanism of action of the core components of the signal transduction pathway and the extent to which they are shared between the BMP and activin pathways (such as the type II receptors Punt (Put) and Wishful thinking (Wit) and the co-Smad, Medea). However, other components are specific to a single pathway resulting in different biological responses. BMP and activin ligands signal through different type I receptors. BMP ligands signal through Thickveins (Tkv) or Saxophone (Sax) and activin ligands through Baboon (Babo). The R-Smads Mad and dSmad2/Smox are also specific to the BMP and activin pathways, respectively. The Mad-Medea complex can cooperate with the cofactor Schnurri to regulate gene transcription in response to BMP signaling. Cofactors that cooperate with dSmad2-Madea have yet to be identified (Parker et al., 2004). The activity of both groups of ligands can be modulated or restricted by specific inhibitors. Short gastrulation (Sog) is known to inhibit BMP ligands (Parker et al., 2004); and previous work from our laboratory showed that *Drosophila* Follistatin (dFs) can inhibit the *Drosophila* activin pathway in a manner similar to what has been shown in vertebrates (Pentek et al., 2009).

The most extensively studied BMP ligand in the fruit fly is Dpp. Dorsal patterning of the *Drosophila* embryo is dependent on a gradient of Dpp and Scw (Ferguson and Anderson, 1992a,b; Wharton et al., 1993; Arora et al., 1994). There is evidence suggesting that this patterning is dependent on a Dpp/Scw heterodimer (Shimmi et al., 2005). Growth and patterning of imaginal discs require Dpp activity and a gradient of Dpp is critical for establishing cell fate in

the wing disc (Nellen et al., 1996). Germ line stem cell maintenance in the *Drosophila* ovary is dependent on Dpp signaling (Xie and Spradling, 1998); while Gbb is essential for germ line stem cell maintenance in the testis (Kawase et al., 2004; Spradling et al., 2011). Gbb was named based on its transparent larval phenotype, in which the fat body opacity is reduced (Khalsa et al., 1998). The transparent fat body phenotype has been reported for nutrient-deprived larvae (Britton and Edgar, 1998), and subsequent studies have shown that Gbb is important for nutrient storage and energy homeostasis during development (Ballard et al., 2010). Gbb plays a critical role in retrograde signaling for synaptic growth and function (McCabe et al., 2003). Recent studies from our lab and others have shown that activin signaling can also influence synaptic growth through regulation of *gbb* transcript levels in larval muscle (Ellis et al., 2010; Fuentes-Medel et al., 2012). A synergistic relationship between activin and BMP signaling has been observed in many other processes, including in vertebrate digit chondrogenesis (Montero et al., 2008). There are several examples in *Drosophila* of a synergistic relationship between different TGF-β components. There is evidence of a synergistic interaction between BMP type I receptors, Tkv and Sax for dorsal–ventral patterning in the early embryo and for wing patterning in the larva. Likewise, a synergistic relationship between the ligands that bind to these receptors Dpp (to Tkv) and Screw (to Sax) in the early embryo and the ligands Dpp (to Tkv) and Gbb (to Sax) for wing patterning (Haerry et al., 1998; Neul and Ferguson, 1998; Nguyen et al., 1998).

Evidence of an activin signaling pathway in flies came through cell culture

experiments in which the *Drosophila* type I and II receptors, Baboon (babo) and Put were shown to bind vertebrate activin (Wrana et al., 1994). This interaction also led to the phosphorylation of dSmad2 (Das et al., 1999; Brummel et al., 1999). Subsequently, studies from our lab showed that Daw initiates the activin pathway and is able to signal through Babo and phosphorylate dSmad2 (Parker et al., 2006; Ellis et al., 2010). These studies also showed that Daw is required for embryonic neuronal pathfinding and growth of the neuromuscular junction (Parker et al., 2006; Ellis et al., 2010). TGF-β signaling has also been implicated in synaptogenesis in vertebrates where TGF-β1 increases the number of neurotransmitter receptor clusters in the developing NMJ (Feng and Ko, 2008). In addition to synaptogenesis defects, *daw* mutants display multiphasic lethality and growth defects that can be reversed by supplementing their nutrition (Parker et al., 2006; Ellis et al., 2010; Zhu et al., 2008). Recent studies in our lab and others have revealed that Daw is required for carbohydrate and mitochondrial metabolism and for insulin secretion (Bai et al., 2013; Ghosh and O'Connor, 2014; Chng et al., 2014; K. Arora, personal communication). Interestingly, disrupting vertebrate TGF-β/Smad3 signaling affects insulin levels and promotes the development of metabolic diseases such as diabetes (reviewed in Tan et al., 2012). *daw* mutants have also been shown to affect neuronal proliferation and photoreceptor axon targeting. A similar defect has been described for mutations in Act β, which acts redundantly with Daw in neuronal proliferation in the brain (Zhu et al., 2008). Act β was initially shown to be required for neuronal remodeling through regulation of ecdysone receptor B1 isoform (EcR-B1)

expression in the brain (Zheng et al., 2003). However, work described in this thesis and by others (Awasaki et al., 2011) provides evidence that neuronal EcR-B1 expression is dependent on Myo and not Act β.

Myo has two vertebrate orthologous, GDF-11 and Myostatin (MSTN), also known as growth differentiation factor 8 (Figure 1.1). Myo shares 46% identity with both BMP-11 and MSTN. GDF-11 is known to play a role in rostrocaudal patterning during embryogenesis and in chondrogenesis (Liu, 2006; Gamer et al., 2001), while MSTN is expressed in skeletal muscles and a negative regulator of muscle growth. MSTN mutations in mice and cattle display increased muscle mass due to hypertrophy and hyperplasia (McPherron et al., 1997; Lee, 2004). However, Myostatin has additional roles, such as in preadipocyte and osteogenic differentiation (Hamrick et al., 2007; Li et al., 2011 Prior to initiation of these studies both Mav and Myo were considered orphan ligands. However, it has since been shown that Myo acts through Babo and is therefore an activin-type ligand (Awasaki et al., 2011). The signaling components that Mav acts through remain unclear.

mav is expressed from early embryonic development to adulthood. During later stages of embryogenesis, *mav* is expressed in the developing gut, visceral mesoderm, and endoderm. *mav* transcripts have also been detected in reproductive tissues, testis and oocyte (Nguyen et al., 2000; Schulz et al., 2004). Recent studies indicate that like *daw*, *mav* also plays a role in NMJ growth by increasing *gbb* transcription. Decreased *gbb* transcript levels and NMJ growth

defects were observed when Mav was depleted from glial cells (Fuentes-Medel et al., 2012).

Myo is important for regulation of nervous system processes, however a role in other tissues is unclear. Myo is expressed in the developing embryonic somatic and visceral muscle, larval glial cells, and in the female reproductive system (http://flybase.org/reports/FBgn0026199.html; Lo and Frash, 1999). Our initial phenotypic analysis of Myo revealed phenotypes similar to that observed with overexpression of Fs. The morphological pupal phenotypes indicate that *myo* mutant larvae fail to undergo metamorphosis with defects similar to those seen in ecdysone pathway mutants. Studies by Awasaki et al. (2011) and data presented in this thesis show that mushroom body γ-neuron remodeling is disrupted in *myo* mutants due to loss of EcR-B1 expression, and failure to respond to ecdysone. However, it remains to be determined if a similar mechanism is in place to ensure the proper response of all tissues to ecdysone signaling. Interestingly, TGF-β1 and TGF-β2 regulate the response to follicle-stimulating hormone (FSH) signaling through upregulation of the FSH receptor in the rat ovary during prepubertal development (Dunkel et al., 1994), similar to the requirement of Myo in regulating EcR-B1 expression during metamorphosis, suggesting that this may be a conserved aspect of TGF-β/activin signaling.

In addition to receptor regulation, activin signaling has also been shown to regulate ecdysone biosynthesis. In *Drosophila*, the major larval endocrine tissue in which ecdysone is produced, is the ring gland (Harvie et al., 1998). However the midgut and nervous system are also endocrine tissues that produce peptide

and/or steroid hormones (Veenstra, 2009; Park et al., 2011). The ring gland, which lies adjacent to the brain, is comprised of the prothoracic gland (PG), corpus allatum (CA) and corpus cardiacum (CC). The active form of ecdysone derives from cholesterol obtained from dietary sources (Marchal et al., 2010). Cholesterol is converted to ecdysone by a group of cytochrome450 enzymes, encoded by the Halloween genes, in the prothoracic gland. Upon release from the prothoracic gland into the hemolymph, ecdysone is converted to the active form 20-hydroxyecdysone (Mcbrayer et al., 2007). During metamorphosis the PG is degraded (Dai and Gilbert, 1991). However in the adult fly the reproductive organs are believed to be the sites of ecdysone synthesis (Riddiford, 1993; Hentze et al., 2013). It is unknown if other larval tissues can also provide a source of ecdysone.

The active form of ecdysone binds to a nuclear heterodimeric receptor complex, comprised of ecdysone receptor (EcR) and Ultraspiracle (USP). There is only one isoform of USP, but there are three EcR isoforms: A, B1, and B2. The ecdysone, EcR, and USP complex directly binds to ecdysone response elements on target genes to spatially and temporally activate primary response genes E93, E74, and BR-C and secondary response genes *rpr*, *hid*, and *dronc* that are important for establishing biological responses during metamorphosis. The Ashburner model proposes that the complex binds to primary response genes, which in turn regulates not only the expression of secondary response genes that control biological responses but also feed back to the receptor complex to modulate self expression. This model was based on the observation of a

sequence of temporally induced chromosomal puffs in the *Drosophila* salivary gland polytene chromosomes (Ashburner et al., 1974; Karim et al., 1993).

Recently, the activin pathway was shown to affect ecdysone biosynthesis through regulation of receptors in the PTTH and insulin signaling pathways. Knockdown of *dSmad2* in the prothoracic gland resulted in decreased ecdysone titers, developmental delay, and growth defects (Gibbens et al., 2011), similar to phenotypes observed when PTTH and insulin signaling are disrupted (Quinn et al., 2012). *Drosophila* insulin–like proteins and PTTH hormone are synthesized in neurosecretory cell and act on the prothoracic gland, the site of ecdysone synthesis (Mcbrayer et al., 2007 and Gibbens et al., 2011). Ecdysone, PTTH, and the insulin pathways all cooperate to regulate growth and developmental timing to determine the final body size (Orme and Leevers, 2005). The activin ligand(s) required for ecdysone biosynthesis remains to be determined.

Endocrine tissues produce two major classes of hormones: steroid and peptide hormones that regulate growth and development, metabolism, sexual function, reproduction, and sleep across the animal kingdom (Toivonen and Partridge, 2009). In addition, the insect endocrine system also regulates water balance, salivary gland secretion, molting, and cuticular synthesis (Nijhout, 1998; Boyd and Ashburner, 1977; Riddiford, 1976). Plants also use a steroid signaling system that interestingly, shares many similarities with the ecdysone pathway in insects. Ecdysosteroids have only been identified in insects and plants (phytoecdysteroid) (Adler and Grebenok, 1995). Plant and insect ecdysteroids are structurally similar, however a role in hormonal regulation for

phytoecdysteroid has yet to be identified (Bathori et al., 2008). The function for phytoecdysteroids is to protect plants, as they are toxic to predators (Thummel and Chory, 2002). *Drosophila* ecdysosteroid and *Arabidopsis* brassinsteroid (BR) biosynthesis are both controlled by a similar series of cytochrome P450 enzymatic reactions. Although their mechanism of signaling differs both ecdysone and BR signaling are required to elicit cell changes required to form a mature organism (Thummel and Chory, 2002).

Androgens, estrogens, and progesterone are examples of steroid hormones in vertebrates. No vertebrate homologs for ecdysone have been identified, however ecdysone receptor Ultraspiracle (USP), has a vertebrate homolog, the nuclear RXR receptor (Hall and Thummel, 1998). RXR forms a heterodimer with retinoic acid receptors (RAR), which are bound by retinoids. RXR can also form heterodimers with receptors for thyroid hormone and vitamin D (Kliewer et al., 1992). Steroid hormone signaling mechanisms are conserved between flies and vertebrates. Thus analysis of ecdysone signaling mechanisms and their biological outcomes is likely to lead to novel insights into the regulatory input signals that control steroid hormone responses in higher organisms. There are several mechanisms in place that ensure specific tissues responses to ecdysone signaling and activin signaling is known to regulate several aspects, including ecdysone biosynthesis and receptor expression (Figure 1.2). We are interested in identifying additional roles of activins in steroid hormone signaling regulation.

Thesis objectives

As stated previously, the main objective of this thesis is to elucidate the role of two TGF-β/activin ligands Mav and Myo, with particular emphasis on aspects of neuronal function. To assess the contribution of these two specific TGF-β/activin ligands, we generated multiple reagents, including loss of function mutant alleles, transgenic RNAi lines, deficiency stocks, and targeted gene knockouts. My first objective was to investigate the role of *mav* in the neuromuscular junction. We used two approaches (gain and loss-of-function analysis) to determine if *mav* function is required for synaptic growth and development. My second objective was to determine the role of *myo*. Analysis of mutant alleles revealed a significant role for *myo* in pupal metamorphosis. *myo* mutants are pupal lethal and display a range of morphological defects consistent with disruption of ecdysone signaling. This is supported by gain-of-function studies where excess Myo resulted in precocious development and lethality. We found that Myo regulates ecdysone responsiveness during metamorphosis through regulation of ecdysone receptor B1 expression specifically in the nervous system. Interestingly, we find that through regulation of EcR-B1 expression in the brain, Myo impacts the production of other signals that in turn, also promote tissue metamorphosis.

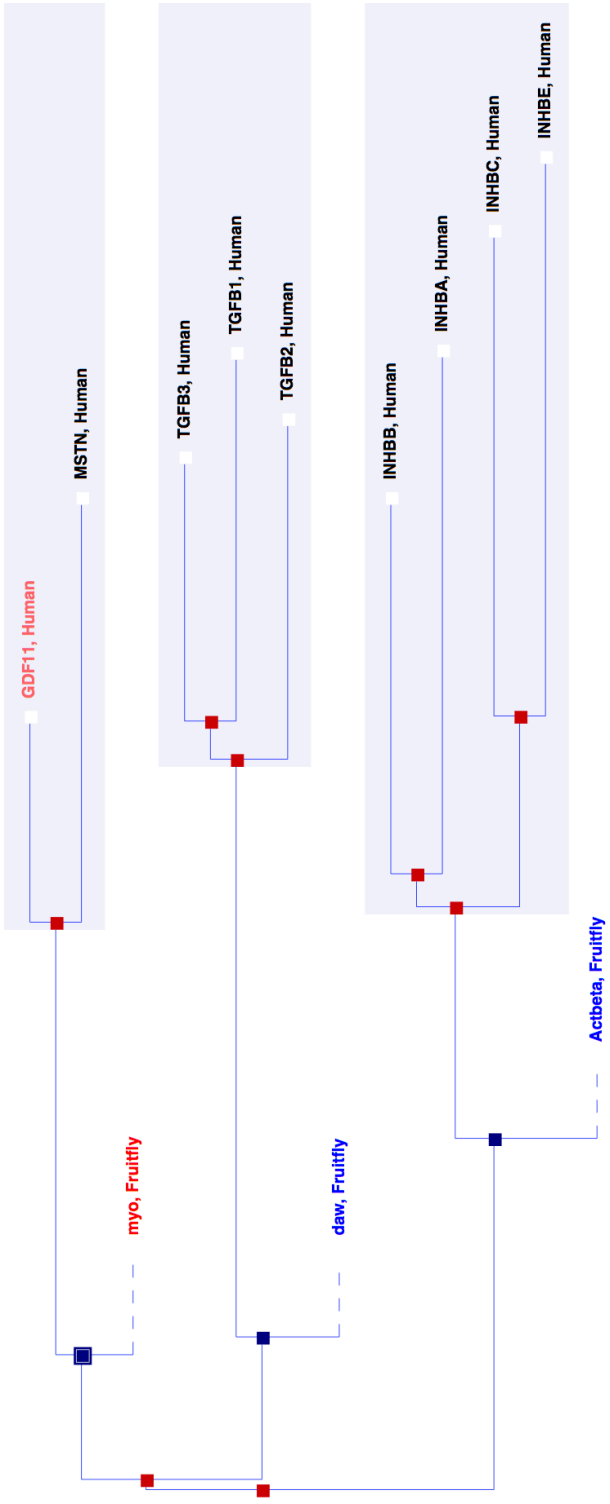
GDF11, Human
MSTN, Human
TGFB3, Human
TGFB1, Human
TGFB2, Human
INHBB, Human
INHBA, Human
INHBC, Human
INHBE, Human
myo, Fruitfly
daw, Fruitfly
Actbeta, Fruitfly

Figure 1.1 Phylogenetic tree of activin ligands

Phylogenetic tree derived from protein alignments of the activin pathway ligands in humans and *Drosophila melanogaster* (fruit fly) using ENSMBL.

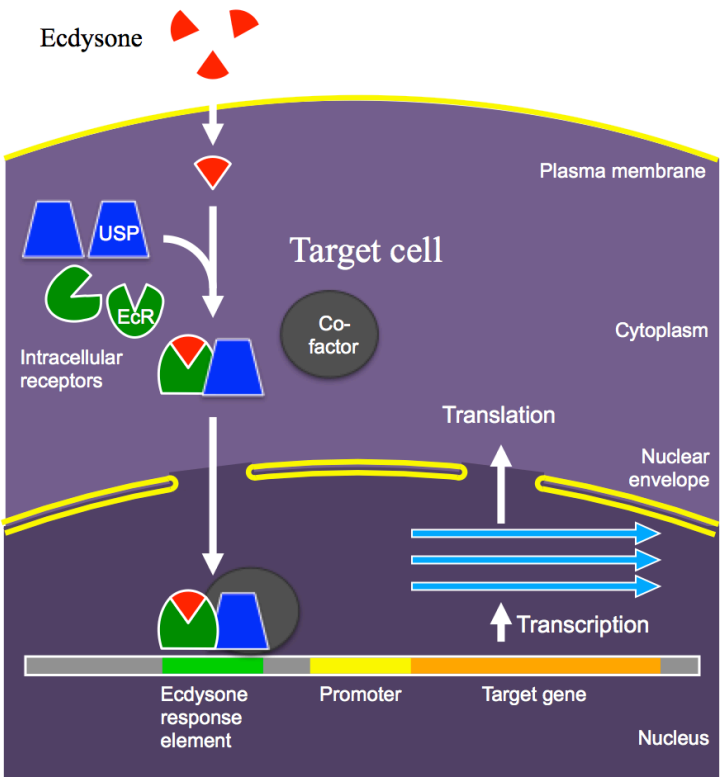

1. Ecdysone Biosynthesis

2. Receptor expression
3. Co-factor expression

.

Figure 1.2 Ecdysone signaling regulation

Diagram of the ecdysone signaling pathway. On the right, are three different mechanisms used to regulate the response to the pathway: ecdysone biosynthesis, ecdysone receptor, and co-factor expression. Currently, it is known that activin signaling can regulates ecdysone biosynthesis and ecdysone receptor expression.

Chapter 2

The role of Maverick, a TGF-β Ligand, in the *Drosophila* Neuromuscular Junction

Abstract

The TGF-β superfamily regulates a wide range of cellular functions, from proliferation and differentiation to apoptosis. Activin signaling is important in many vertebrate and invertebrates biological processes including embryonic and nervous system development, wound repair, hormone regulation, and metabolism. In *Drosophila,* the activin pathway regulates growth of the neuromuscular junction (NMJ), as well as ecdysosteroid and neuroendocrine signaling. In this chapter, we focus on requirements for a novel TGF-β/activin ligand, Mav, in regulating synaptic growth of the larval NMJ. We generated *mav* knockout mutants and examined larval NMJs, but observed no difference in *mav* knockout mutants. Specifically, in the numbers of boutons in synapses of abdominal segments 2 and 5. However, increasing the levels of *mav* in glia increased bouton numbers, suggesting that while not necessary, Mav is sufficient to promote NMJ growth.

Introduction

The nervous system communicates with other neurons and muscles through chemical signals that are released at specialized junctions known as synapses. The *Drosophila* larval NMJ has served as a model system for understanding the formation and function of synapses in higher organisms as many of the molecular and physiological aspects are conserved. Additionally, several *Drosophila* mutants that affect NMJ growth and development parallel human diseases that affect the NMJ and result in defective muscle function (Lloyd and Taylor, 2010). Thus, analysis of the *Drosophila* NMJ can provide new insight into the molecular mechanisms that regulate NMJ development and disease.

Studies in *Drosophila* have revealed the involvement of several signaling pathways including Wnt, MAPK, and TGF-β. Mutations in components of these signaling pathways display NMJ growth defects (Miech et al., 2008). The first evidence that TGF-β signaling is required for NMJ development came from analysis of the Type II BMP receptor Wit. Mutations in *wit* display smaller synapses, morphological defects in the bouton active zones, and reduced bouton counts (Aberle et al., 2002; Marques et al., 2002). Subsequent studies showed that muscle-derived Gbb, is required for retrograde signaling and shows identical phenotypes as *wit* mutants (McCabe et al., 2003). Loss of BMP inhibitors has the opposite affect and results in larger NMJs with satellite boutons that bud of from existing boutons (Keshishian and Kim, 2004; Menon et al., 2013).

Subsequent studies from our lab identified a role for the activin pathway in growth of the NMJ. Parker et al., (2006) showed that Daw acts via a canonical activin signaling pathway to control motoneuron pathfinding during embryogenesis in *Drosophila*. Subsequently, Ellis et al., (2010) showed that Daw signaling was required to up-regulate *gbb* expression in the larval muscle. Loss of Daw and mutations in its downstream signaling components, *babo* and *dSmad2,* result in lower numbers of boutons at NMJs. Furthermore*, daw* mutants exhibit locomotor defects during larval development and as do the few adult escapers. Loss of *babo* results in a stronger NMJ phenotype compared to the *daw* mutants, therefore it was argued that a second TGF-β/activin ligand that signals through *babo* could also be required for NMJ growth.

mav is expressed throughout embryogenesis; and is expressed in neuronal and muscle cells (Nguyen et al., 2000), leading us to hypothesize that it could have a potential role in neural development and more specifically, in regulation of synaptic growth. We tested this hypothesis through loss-of-function and gain-of-function analysis of Mav. We expected that absence of Mav would lead to smaller NMJs and decreased numbers of boutons. In contrast, misexpression of *mav* in either glia, muscle, or motoneurons, was expected to increase the number of boutons.

Surprisingly, we did not find defects in bouton counts in *mav* knockout mutants. However, over expression of Mav led to increased bouton numbers demonstrating that it is sufficient to promote synaptogenesis. Subsequent studies by Fuentes-Medel et al. (2012) have identified a requirement for *mav* at the NMJ.

These authors showed that like Daw, Mav also regulates *gbb* expression in the muscle. We discuss possible reasons that would explain the differences in our data. Finally, *mav* transcripts are expressed at extremely high levels in the adult male accessory gland (http://flybase.org/reports/FBgn0039914.html) raising the possibility that *mav* has additional roles in *Drosophila.*

Material and Methods

Drosophila stocks and genetics

Stocks were obtained from the Bloomington Stock Center unless otherwise stated. $mav^{ko\ 75/75}$ and $mav^{ko\ 14/14}$ were generated by FLP-*FRT* recombination (K. Arora and Allison Wu, personal communication); and UAS-*mav* transgenic lines were generated by K. Arora (personal communication).

Molecular Analysis of mav^{ko} allele

Two pairs of primers *mav*_3111F/ *mav*_3616R and *mav*_2193F/ *mav*_32646R were used to amplify different regions of the *mav* genomic region from control $y^{-}w^{-}$ *and* homozygous mav^{ko} animals. Control RP49 was amplified using primer pairs RP49F and RP49R. 5PRIME MasterMix was used to PCR amplify regions following manufacturers instructions. Multiple independent samples were tested.

Primer sequences:

RP49F: 5’-TGACCATCCGCCCAGCATACAGG-3’

RP49R: 5’-TGGCGCTCGACAATCTCCTT-3’

*mav*_3111F: 5’-TGATTTCAGCCCGTCAACACC-3’

*mav*_3616R: 5’-CTGCATATCACTCCATGTCGA-3’

*mav*_2193F: 5’-TGAAACCAGACTAAAGCACCTCG-3’

*mav*_32646R: 5’-CATTGTATCCTGTTCGCCACG-3’

Immunohistochemistry

Animals were raised at 29°C on 4% orange juice-agar plates supplemented with yeast. Third instar larvae were dissected in fresh 1X PBS and fixed in a solution containing 4% formaldehyde and 0.4% IGEPAL detergent for 30 minutes. The larval fillets were stained with fluorophor conjugated antibodies mouse anti-horseradish peroxidase (HRP), which labels the presynaptic component of boutons. The post-synaptic terminals were visualized with mouse anti-disc large (Dlg) (DSHB: 4F3) and the secondary antibody anti-mouse Alexa 488. Larvae were stained with primary anti-Dlg (1:100) overnight at 4°C, followed by secondary antibody Alexa 488 (1:200) overnight at 4°C. On day 3, larvae were stained with anti-HRP (1:500) over night at 4°C. Larvae were washed with 1XPBS; 0.4% IGEPAL after fixation and each antibody staining. The larval fillets were mounted in Vectashield (Vector Labs).

Imaging and quantification

Larval preparations were imaged with a Zeiss LSM 510 META laser-scanning confocal microscope. LSM files were converted to JPEG using IMAGE J and assembled in Photoshop. In each experiment, boutons were counted in the synapse that forms at the boundary of muscle 6/7 in the second and fifth abdominal segments (A2 and A5). The muscle size was measured and the number of boutons normalized to correct for variations in muscle area. Statistical analysis was performed using a Students *t*-test. Error bars represent standard deviation.

Results

To better understand the requirement for different components of the TGF-β/activin pathway in *Drosophila* neuronal development, the Arora lab generated mutations in several components of the pathway. *mav* knockout lines were generated using site directed homologous recombination, FLP-FRT (K. Arora and Allison Wu, unpublished). A knockout construct was engineered containing a mini w^+ (*white*) marker P{w^+Mav-KO} and a genomic sequence that flanked the *mav* open reading frame. To recover transgenic animals, the construct was injected into w^- embryos, which lack eye color pigment. This fragment of DNA was expected to undergo homologous pairing and recombine with the endogenous *mav* gene replacing it with the mini w^+ marker gene, hence creating a *mav* knockout mutation. Successful recombination events were detected by the presence/absence of mini w^+ marker in progeny. Two lines,

mav$^{ko14/14}$ and *mav*$^{ko75/75}$, which displayed the mini w^+ cell marker, were recovered. We used PCR analysis to confirm that *mav* was eliminated from these lines. We extracted genomic DNA from control y^-w^- and *mav*$^{ko14/14}$ (two different stocks) and *mav*$^{ko75/75}$. We amplified control RP49 from all three samples (Figure 2.1, lanes 2-5). Two sets of primer pairs were used to amplify two different regions from the *mav* locus. While we recovered *mav* PCR products from the y^-w^- controls, we failed to observe PCR products in the *mav* knockout lines (Figure 2.1, lanes 6-13). This data indicates that lines represent true knock out lines. In this study I used the *mav*$^{ko75/75}$ allele to determine the functional role of *mav* at the NMJ.

Lethal phase analysis of homozygous *mav*^{ko} mutant animals revealed that 100% of mutants were viable. Furthermore, adult morphological defects were not detected. These results suggest that the function of Mav is not essential for development of the animal. However, with respect to synapse development there are examples of genes such as Neurexins and Neuroligin 2, cell adhesion molecules, that are required for NMJ growth and function, but are adult viable (Sun et al., 2011). Therefore it is possible that there is a requirement for Mav at the NMJ, although it is not essential for progression through life.

To determine if *mav* is required at the NMJ, we studied NMJ growth and morphology in *mav*$^{ko75/75}$ mutants. Most studies on the *Drosophila* NMJ focus on analysis of terminal bouton counts. Motonuerons innervate muscles to form synapses that branch out and terminate in specialized structures called boutons. Within the bouton there are several active zones that house neurotransmitters,

which upon release bind to receptors on the adjacent muscle. Binding of the neurotransmitter to its receptors causes a change in calcium influx that causes muscle contractions (Bayat et al., 2011). By the end of embryonic development, the NMJs have formed, but contain only a few boutons. As the animal develops, the NMJ grows and increases the number of boutons. Although several pathways (Wnt and BMPs) have geen implicated in synapse development and growth, the mechanisms that regulate bouton formation remain poorly understood (Menon et al., 2013). There are three major types of boutons. The type I, which secret glutamate can be subdivided into large (Ib) and small (Is) based on size. The type II boutons house octopamine neurotransmitters and the type III release insulin (Prokop, 2006). At third instar larval stage, about 20-50 type I boutons can be identified in each muscle fiber. Muscle 6/7 is composed of two muscle fibers therefore between 40-100 boutons are observed. In addition to bouton counts, other aspects can be analyzed such as morphology, bouton size, synaptic transmission, neurotransmitter receptor expression, and the development of satellite boutons and ghost bouton (*de novo* boutons that do not have an active zone).

There are 8 abdominal hemisegments A1-A8, each with 30 muscles (Campos-Ortega and Hartenstein, 1985; Menon et al., 2013). The abdominal hemisegments A2-A7 are very similar in shape and are innervated by 32-35 different motoneurons. Motoneurons can innervate one muscle fiber (muscle 4) or pairs of muscles (muscle 6/7 and 12/13). Synapse formation is most often analyzed in muscle 6/7 that is innervated by the RP3 motor neuron, and muscle

4 that is targeted by RP2 motor neurons (Aberle et al.,2002; Ruiz-Canada and Budnik, 2006; Choi et al., 2004; Nose, 2012). Most studies focus on abdominal segments A2-A5. In our studies, we focused on muscle 6/7 in abdominal segments A2 and A5.

We examined NMJ growth and morphology in *mav*$^{ko75/75}$ mutants. Third instar larva were dissected and the presynaptic membrane component of boutons were stained with fluorescently conjugated antibodies to detect horseradish peroxidase (HRP) and anti-disc large (Dlg), a scaffolding protein that localizes to the postsynaptic muscles and imaged with a Zeiss LSM 510 confocal microscope. We analyzed the number of type I boutons in *mav*$^{ko75/75}$ mutants and control *y*$^{-}$*w*$^{-}$. In each experiment, boutons were counted in the synapse that forms at the boundary of muscle 6/7 in the second abdominal segment (A2) and in the fifth abdominal segment (A5). The muscle size was measured and the numbers of boutons were normalized to correct for variation in muscle area. We observed 62.27±14.75 boutons in control *y*$^{-}$*w*$^{-}$ NMJ (n=10) versus 60.36±12.77 boutons in *mav*$^{ko75/75}$ NMJ (n=16) in the abdominal segment A2. For the abdominal segments A5, 32.25±6.02 boutons were observed in *y*$^{-}$*w*$^{-}$ NMJ (n=10) and 37.77±17.46 boutons in *mav*$^{ko75/75}$ NMJ (n=15). No significant difference was observed between *y*$^{-}$*w*$^{-}$ and *mav*$^{ko75/75}$ bouton counts in either the A2 and A5 segments of muscle 6/7 (Figure 2.2 E).

The synapse at A2 from control *y*$^{-}$*w*$^{-}$ is long, branched, and has an “X” shaped morphology. The morphology of the A5 segment is unbranched and linear in *y*$^{-}$*w*$^{-}$ (Figure 2.2 A, B). While morphology of the NMJ of *mav*$^{ko75/75}$

appears unaltered and maintains a similar appearance to the $y^{-}w^{-}$ control NMJs at A5 segments, A2 segment NMJ arbors have a different appearance (Figure 2.2 C, D). Further analysis is required to determine if Myo regulates formation of synaptic arbors at the A2 segment. These data suggested that *mav* is not required at the NMJ to regulate synaptic bouton development. However it leave open the possibility that *mav* may regulate other aspects of NMJ development.

In parallel with loss-of-function analysis, we also investigated the effects of misexpression of Mav on the NMJ to see if bouton numbers or bouton morphology were affected. A series of simple crosses were used to generate larvae in which Mav was expressed in specific tissues using the GAL4-UAS system. We selected several GAL4 drivers to express *mav* in glia, motoneurons, or muscles. To express *mav* in glial cells, we used the *repo*-GAL4 driver. We crossed *repo*-GAL4 flies to UAS-*mav* or $y^{-}w^{-}$ (control) flies and selected F1 third instar larvae. Bouton counts in controls (*repo*-GAL4/+) animals in A2 segments were 42.17±15.93 (n=13) versus 67.2±14.49 (n=16) when *mav* was expressed in glia (*repo*-GAL4>UAS-*mav*). For the abdominal segments A5, we quantified 28.26±11.9 boutons in control NMJs (n=13) and 41.14±7.81 boutons in *repo*-GAL4>UAS-*mav* animals (n=15). A difference in bouton counts is observed between control and glial *mav* expression in both the A2 and A5 segments of muscle 6/7 (Figure 2.3 A-D), however analysis indicates it is not statistically significant ($P>0.05$). These data raise the possibility of a functional role for Mav at the NMJ, however we need a greater sample size to demonstrate the relationship.

We also examined the effects of presynaptic (motoneuron) expression of UAS-*mav* on growth of the NMJ. *ok6*-Gal4>UAS-*mav* animals showed no significant effect on either bouton number (A2: 76.78±16.34; n=17 and A5: 50.61±10.26; n=15) or morphology compared to controls (*ok6*-Gal4/+) (A2: 80.39±11.5; n=19 and A5: 42.43±9.32; n=10) (Figure 2.4 A-D).

Lastly, we decided to test the effects of expression of *mav* in muscles, a tissue known to secrete TGF-β ligands involved in NMJ growth. Again, postsynaptic expression of UAS-*mav* in the muscle (*dmef2*-Gal4/UAS-*mav*) had no significant effect on either bouton number (A2: 67.24±15.65; n=16 and A5: 39.94±10.74; n=15) or morphology compared to controls (*dmef2*-Gal4/+) (A2: 67.92±20.0; n=17 and A5: 67.24±15.65; n=17) (Figure 2.5 A-D). While the loss-of-function analysis did not reveal a requirement for Mav for NMJ growth, the gain-of-function experiments indicate that increased levels of Mav from the glia are sufficient for NMJ growth.

Discussion

TGF-β/ activin signaling is essential for many nervous system processes in *Drosophila* such as axonal pathfinding in the embryo and neuroblast proliferation of the larval brain. In an effort to better understand the role of TGF-β and activin signaling in the nervous system, we analyzed the role of Mav at the NMJ. The Arora lab generated mutations in all of the TGF-β/activin ligands, including Mav. In the present study, we confirmed that two lines, expected to delete *mav* through homologous recombination, indeed successfully deleted the

gene. My data argued that loss of *mav* had no significant affect on bouton counts at muscle 6/7. However, increased expression of *mav* in glia, had an effect on NMJ growth. These studies suggest that while not critical for synaptic growth, a Mav signal is sufficient for synapse development.

A subsequent study by Fuentes-Medel et al., (2012) identified a requirement for Mav in growth of the NMJ. The authors depleted *mav* using two RNAi contructs, which target different regions of *mav* and found decreased bouton numbers when *mav* was depleted in glial cells. Analysis of bouton numbers was done in a different hemisegment (A3) of muscle 6/7, while our analysis focused on segments A2 and A5. While there is no evidence that mutations can cause segment specific phenotypes, each abdominal muscle fiber is innervated by specific motoneurons from the CNS, raising the possibility that there may be differences in innervation of the same muscle between different abdominal segments. For example, type III motoneurons that innervate muscle 12 do so only in four of the abdominal segments, implying that innervation varies from segment to segment in muscle fibers (Berke and Keshishian, 2009; Berke et al., 2013; Keshishian et al., 1996). This may provide an explanation for why we failed to see a phenotype. Expression of *mav* in muscle 6/7 did not reveal an NMJ over growth phenotype in Fuentes-Medel et al., 2012. However, they did find increased bouton counts in muscle 4, a muscle type we did not analyze. Studies reveal that environmental factors influence NMJ growth such as rearing temperature and population density. Wild-type animals reared at 29°C versus 25°C have increased boutons counts (Sigrist et al., 2003; Stewart and McLean,

2004). It is also possible that our rearing conditions differ, which could explain the differences in our data. One possibility is that Daw is the major player at the NMJ that promotes retrograde signaling by regulating Gbb expression and Mav has minor role in the same process. Analysis of double mutants may provide a better insight into the requirement for these ligands at the NMJ.

Interestingly, a recent study by (Kim and O'Conner, 2014), reports that neither *babo* nor *dsmad2* mutants exhibit a significant difference in normalized bouton counts compared to wild-type controls. However, they find that activin signaling is required for other aspects of NMJ development, such as expression of the glutamate receptor and regulation of miniature excitatory junction potentials (*mEJPs*). These authors argue that the *babo* allelic combination used by Ellis et al., 2010, $babo^{32/52}$, may contain a background mutation that results in lower bouton counts, not observed with other *babo* alleles. However, studies by Ellis et al., 2010 showed that cell-autonomous RNAi depletion of *babo* receptor also affects NMJ growth, arguing that Babo signaling is in fact required for NMJ growth.

Currently, there is no biochemical evidence to support if *mav* triggers activin or TGF-β signaling. Fuentes-Medel et al., (2012), present evidence that P-Mad levels are affected in motoneurons when Mav is depleted in the glia. However, since depletion of *mav* affects retrograde BMP signaling through regulation of post-synaptic Gbb expression, the levels of P-Mad in motoneurons, reflect Gbb signaling.

Mutations in cell adhesion molecules, cytoskeletal proteins, ligands, transcription factors, potassium and calcium channels, involved at the NMJ are characterized by having one or several of the following phenotypes: formation of satellite or ghost boutons, defects in synaptic transmission, bouton size, and levels of glutamate receptors. While our analysis suggest that Mav is required but not critical for NMJ growth (based on bouton counts), Mav may regulate other aspects of NMJ development and may display other NMJ phenotypes, based on the fact that loss activin signaling has been implicated in the regulation of many of the aspects listed above. Further analysis may reveal that *mav* is essential for other aspects of NMJ development.

Interestingly, Mav is highly expressed in several organs of the adult male reproductive system. Mav is expressed in the testis, where TGF-β signaling is required for stem cell maintenance (Schulz et al., 2004; Decotto and Spradling, 2005). In addition, flybase reports extremely high expression levels of *mav* in the accessory glands (paragonia) (http://flybase.org/reports/FBgn0039914.html). The accessory glands secret seminal proteins, which along with sperm are transferred to the female during mating and regulate female mating behaviors (Wolfner, 1997; Wolfner, 2002). Recently, it was shown that accessory gland secondary cells exosomes require BMP signaling for secretion (Corrigan et al., 2014). One area of future study in the lab is to examine whether *mav* plays a role in some aspect of male reproductive behavior.

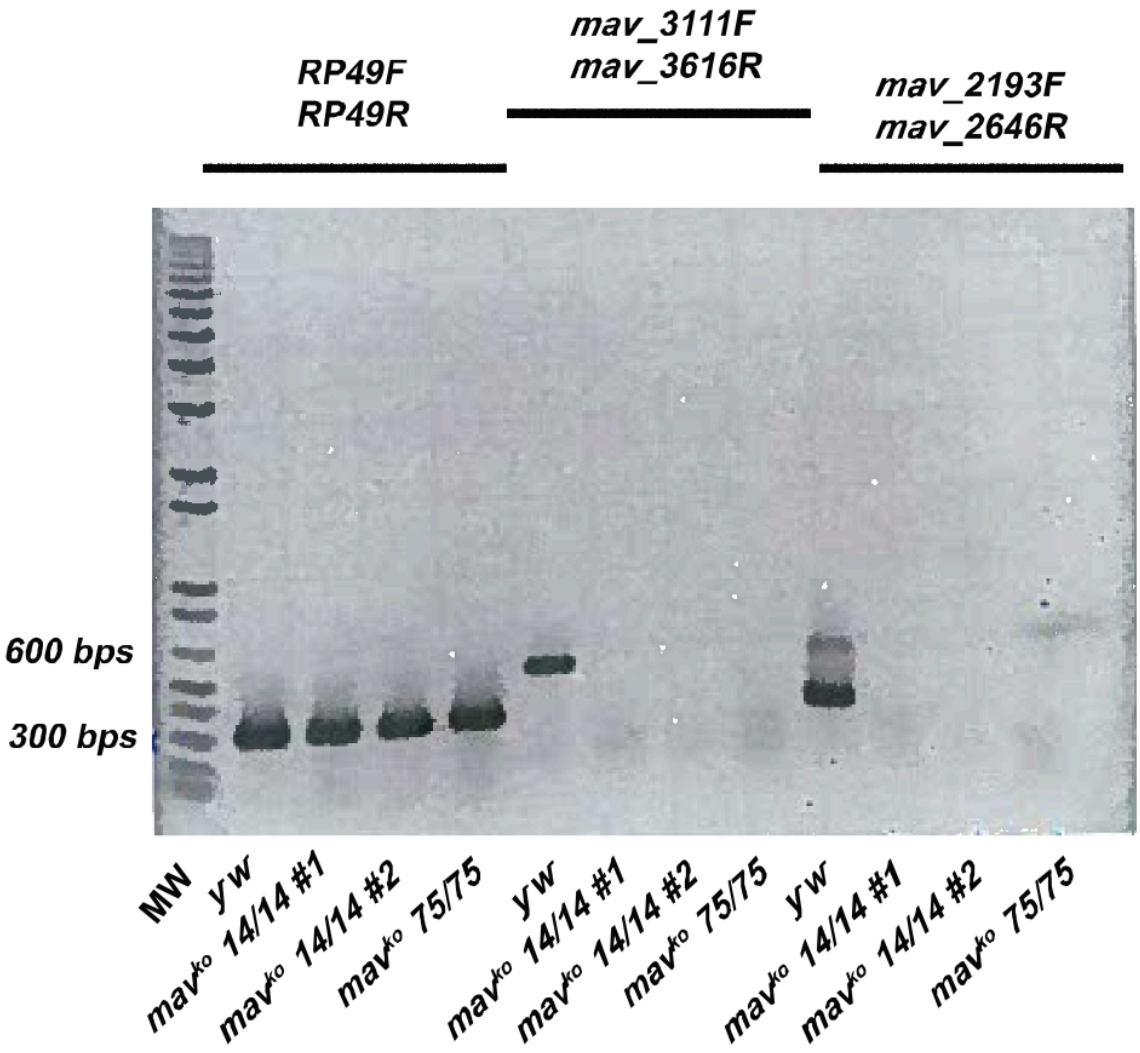
RP49F
RP49R
mav_3111F
mav_3616R
mav_2193F
mav_2646R
600 bps
300 bps
MW
yw
mavko 14/14 #1
mavko 14/14 #2
mavko 75/75
yw
mavko 14/14 #1
mavko 14/14 #2
mavko 75/75
yw
mavko 14/14 #1
mavko 14/14 #2
mavko 75/75

Figure 2.1 Molecular verification of *mav* knockout mutants.

Genomic DNA collected from $y^{-}w^{-}$ *and* homozygous mav^{ko} mutants were PCR amplified using primers specific for RP49 or *mav*. Lane 1 contains molecular weight markers. Sizes have been indicated next to several bands. Lane 2-5, PCR amplification of RP49 in $y^{-}w^{-}$; $mav^{ko14/14}$ sample #1; $mav^{ko14/14}$ sample #2, $mav^{ko75/75}$. RP49 PCR products were obtained from genomic DNA extracted from both $y^{-}w^{-}$ and *mav* knockout mutants. Lane 6-9, PCR amplification of *mav* in $y^{-}w^{-}$; $mav^{ko14/14}$ sample #1; $mav^{ko14/14}$ sample #2, $mav^{ko75/75}$. *mav* PCR products were obtained in from genomic DNA extracted from $y^{-}w^{-}$ but not from *mav* knockout mutants. Lane 10-13, PCR amplification of different region of the *mav* locus in $y^{-}w^{-}$; $mav^{ko14/14}$ sample #1; $mav^{ko14/14}$ sample #2, $mav^{ko75/75}$. *mav* PCR products were obtained in from genomic DNA extracted from $y^{-}w^{-}$ but not from *mav* knockout mutants confirming that the mav locus had been deleted.

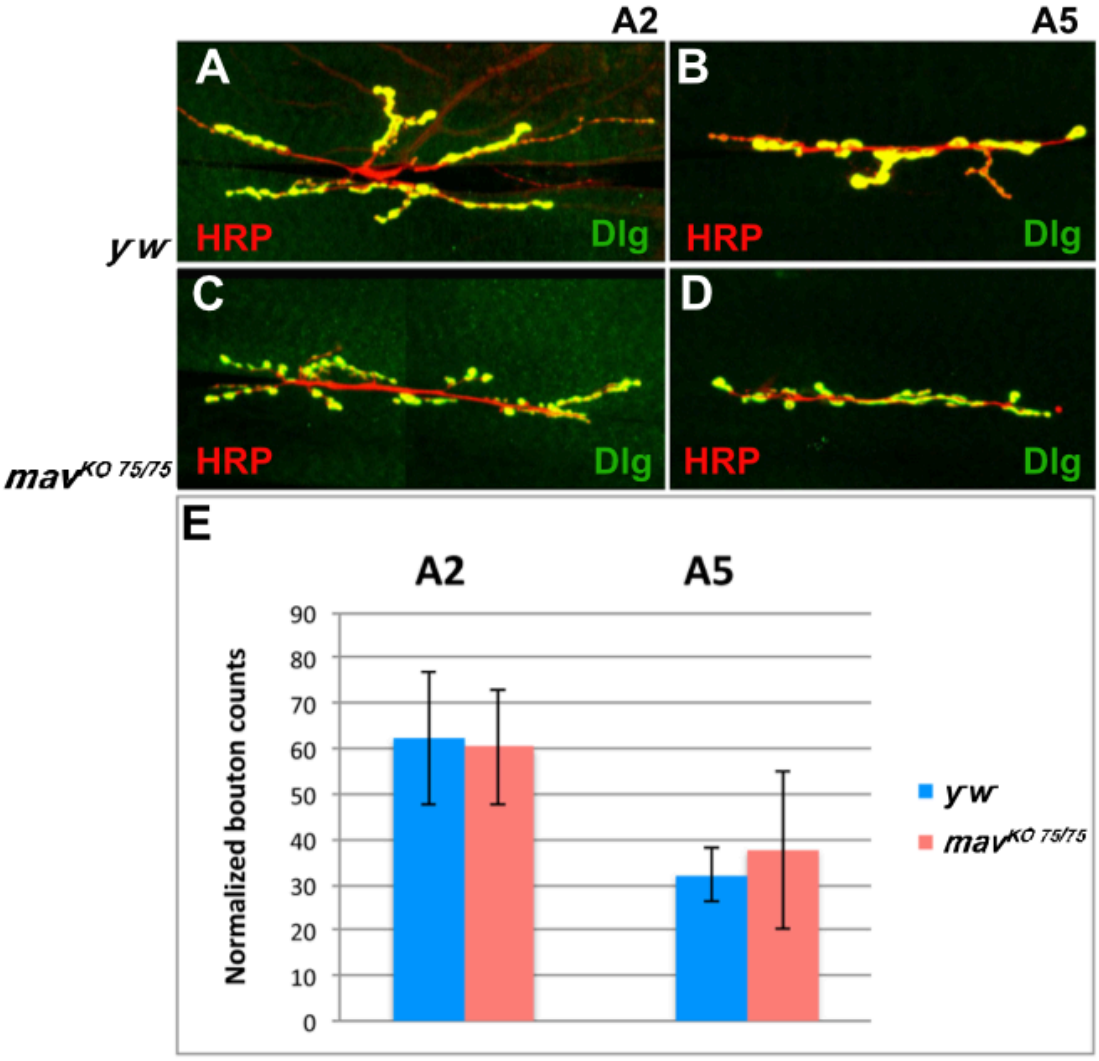
A2
A5
A
B
yw
HRP
Dlg
HRP
Dlg
C
D
mavKO 75/75
HRP
Dlg
HRP
Dlg
E
A2
A5
Normalized bouton counts
90
80
70
60
50
40
30
20
10
0
yw
mavKO 75/75

Figure 2.2 *mav* knockout mutants do not display defects in bouton numbers.

(A-D) Representative confocal images of the NMJ at muscle 6/7 abdominal segments A2 (A,C) and A5 (B,D). Third instar larvae were stained with post-synaptic marker anti-Dlg (green) and pre-synaptic marker anti-HRP (red). (A) A control y^-w^- NMJ (n=10), with a branched "X" shaped synapse with many boutons in muscle 6/7 of segment A2. (B) A control y^-w^- NMJ (n=10), with a linear shaped synapse with many boutons in muscle 6/7 of segment A5. (C) The NMJ at segment A2 in $mav^{ko75/75}$ mutant (n=16). The morphology of segment A2 appears altered as fewer arbors are observed in muscle 6/7 compared to y^-w^- controls. (D) The NMJ at segment A5 in $mav^{ko75/75}$ mutant (n=15), maintains a linear shaped synapse with many boutons similarly as y^-w^- controls. (E) Quantification of boutons in y^-w^- and $mav^{ko75/75}$ mutants in abdominal regions A2 and A5. Bouton counts were normalized to correct for muscle size differences. A students *t*-test revealed no significant difference between control and *mav* mutant bouton numbers. Error bars represent standard deviation.

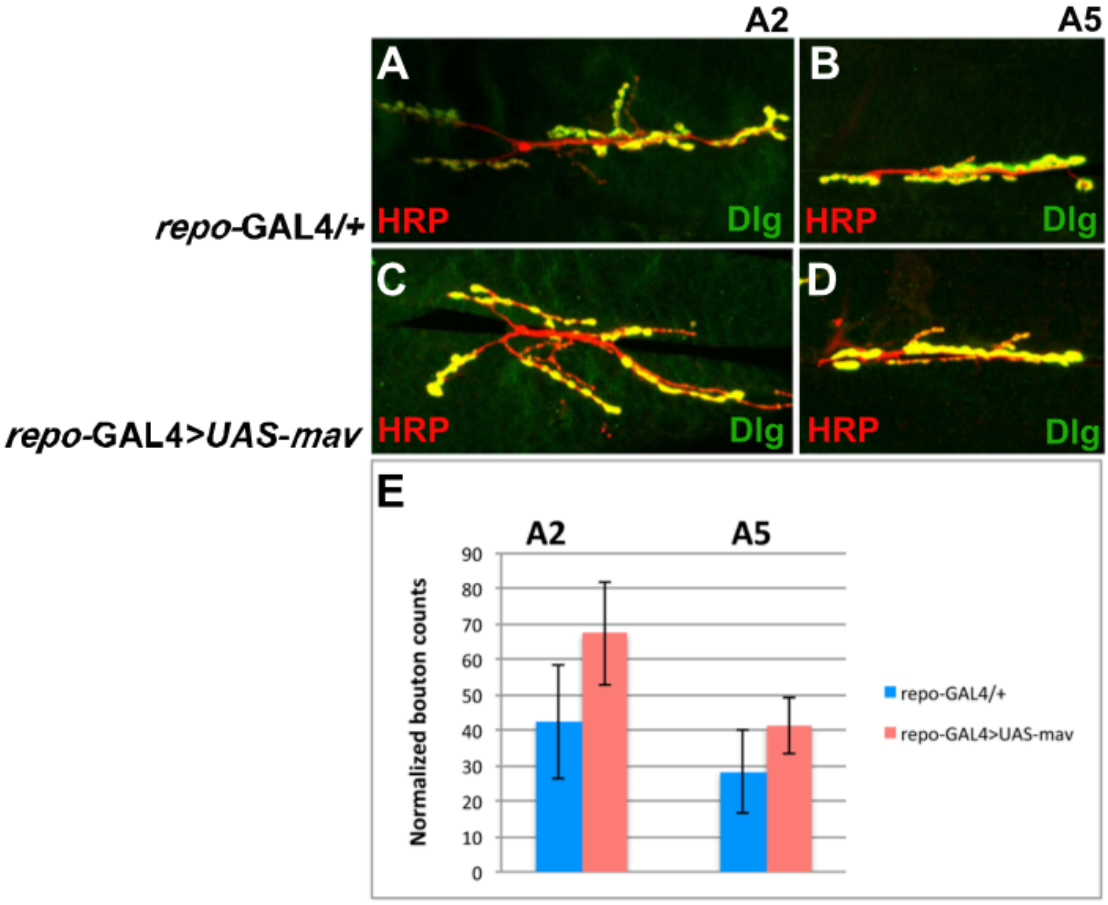
A2
A5
A
B
repo-GAL4/+
HRP
Dlg
HRP
Dlg
C
D
repo-GAL4>UAS-mav
HRP
Dlg
HRP
Dlg
E
A2
A5
Normalized bouton counts
90
80
70
60
50
40
30
20
10
0
repo-GAL4/+
repo-GAL4>UAS-mav

Figure 2.3 Expression of *mav* in glia had an affect on NMJ growth.

(A-D) Representative confocal images of the NMJ at muscle 6/7 abdominal segments A2 (A,C) and A5 (B,D). Third instar larvae were stained with post-synaptic marker anti-Dlg (green) and pre-synaptic marker anti-HRP (red). (A) The NMJ of a control animal, *repo*-GAL4 crossed to $y^{-}w^{-}$ (*repo*-Gal4/+) (n=13), with a branched "X" shaped synapse with many boutons at muscle 6/7 of segment A2. (B) The NMJ of a control animal (*repo*-Gal4/+) (n=13), with a linear shaped synapse with many boutons in muscle 6/7 of segment A5. (C) The NMJ at segment A2 in animals in which *mav* has been expressed in glial cells (*repo*-GAL4>UAS-*mav*) (n=16), maintain a branched "X" shaped synapse with many boutons in muscle 6/7 similarly as controls. (D) The NMJ at segment A5 in glial expression of *mav* (*repo*-GAL4>UAS-*mav*) (n=15), maintains a linear shaped synapse with increased boutons compared to controls. (E) Quantification of boutons in control and *mav* glial expression in abdominal regions A2 and A5. Bouton counts were normalized to correct for muscle size differences. A students *t*-test revealed no significant difference between control and glial *mav* expression numbers ($P>0.05$). Error bars represent standard deviation.

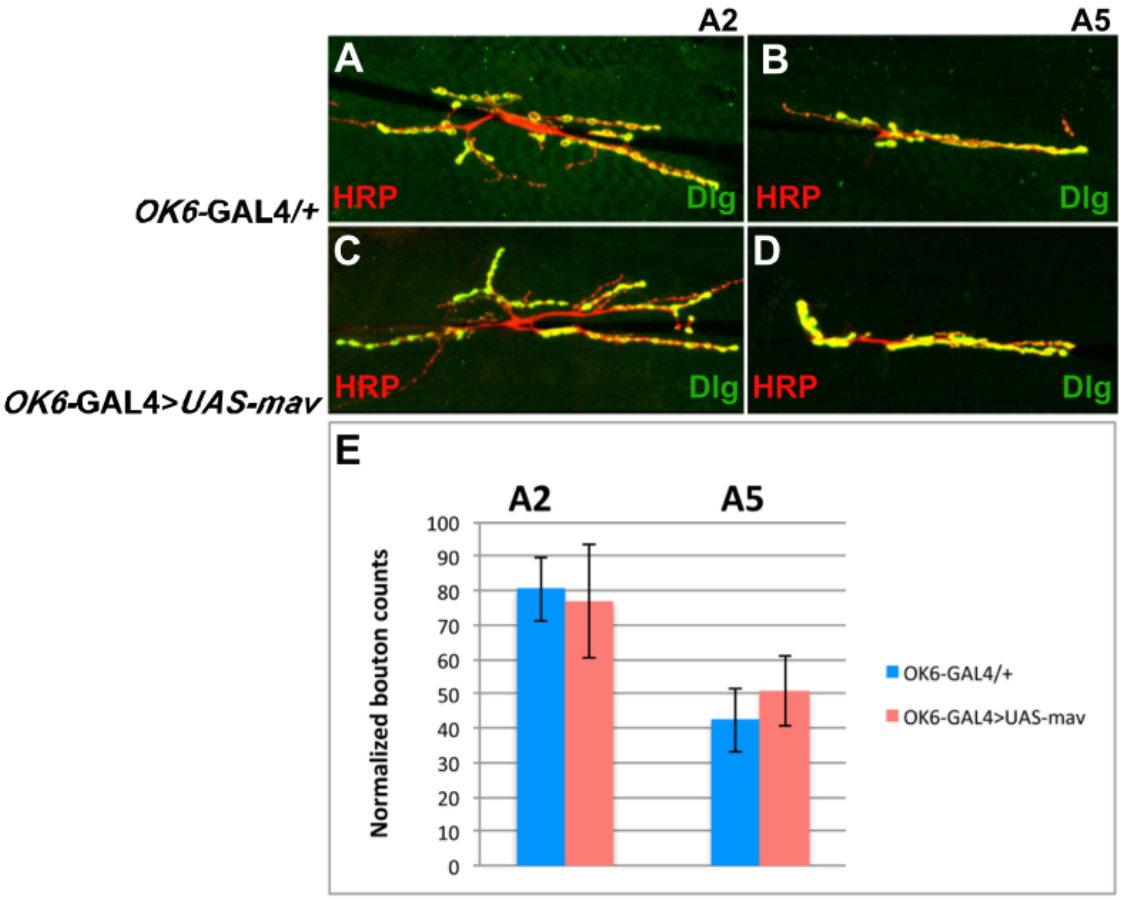
A2
A5
A
B
HRP
Dlg
OK6-GAL4/+
C
D
OK6-GAL4>UAS-mav
E
A2
A5
Normalized bouton counts
100
90
80
70
60
50
40
30
20
10
0
OK6-GAL4/+
OK6-GAL4>UAS-mav

Figure 2.4 Expression of *mav* in motoneuron had no affect on NMJ growth. (A-D) Representative confocal images of the NMJ at muscle 6/7 abdominal segments A2 (A,C) and A5 (B,D). Third instar larvae were stained with post-synaptic marker anti-Dlg (green) and pre-synaptic marker anti-HRP (red). (A) The NMJ of a control animal, *ok6*-GAL4 crossed to *y⁻w⁻* (*ok6*-Gal4/+)(n=19), with a branched "X" shaped synapse with many boutons at muscle 6/7 of segment A2. (B) The NMJ of a control animal (*ok6*-Gal4/+)(n=10), with a linear shaped synapse with many boutons in muscle 6/7 of segment A5. (C) The NMJ at segment A2 in animals in which *mav* has been expressed in motoneurons (*ok6*-GAL4>UAS-*mav*) (n=17), maintain a branched "X" shaped synapse with many boutons in muscle 6/7 similarly as controls. (D) The NMJ at segment A5 in motoneuron expression of *mav* (*ok6*-GAL4>UAS-*mav*) (n=15), maintains a linear shaped synapse with many boutons similarly as controls. (E) Quantification of boutons in control and *mav* motoneuron expression in abdominal regions A2 and A5. Bouton counts were normalized to correct for muscle size differences. A students *t*-test revealed no significant difference between control and glial *mav* expression numbers. Error bars represent standard deviation.

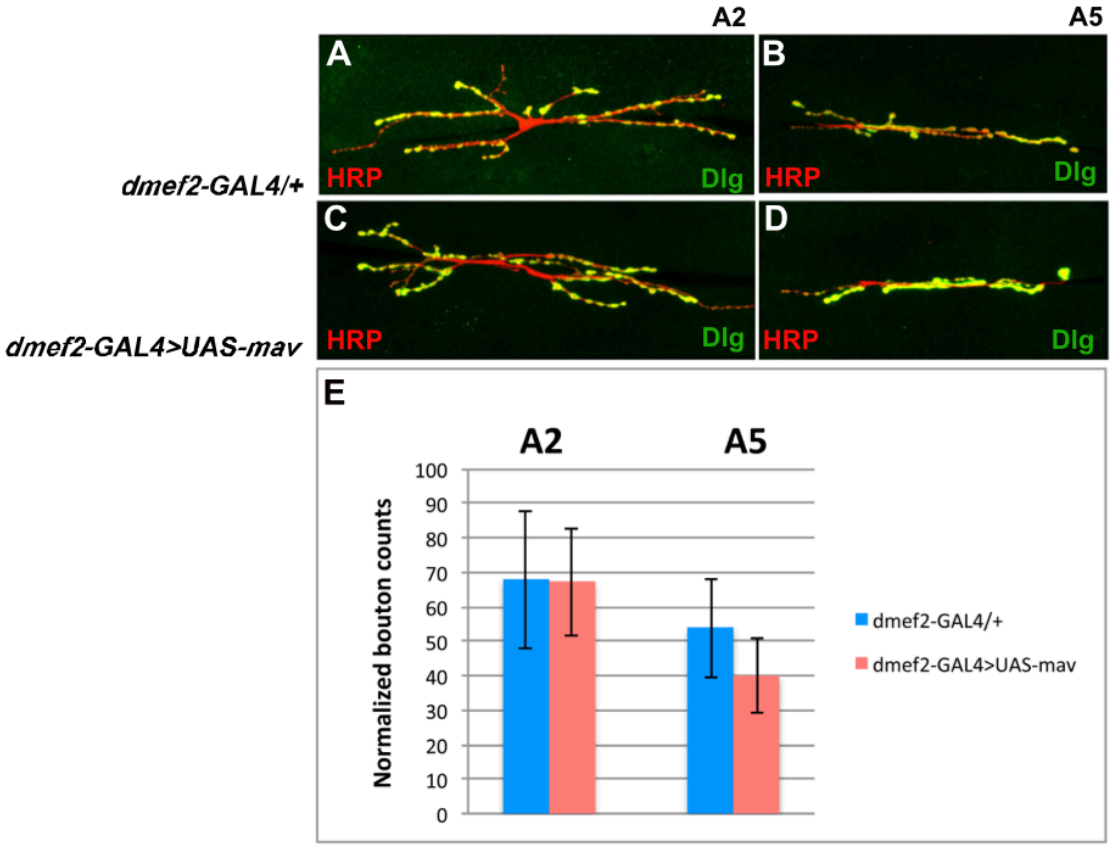
A2
A5
A
B
C
D
HRP
Dlg
dmef2-GAL4/+
dmef2-GAL4>UAS-mav
E
A2
A5
Normalized bouton counts
100
90
80
70
60
50
40
30
20
10
0
dmef2-GAL4/+
dmef2-GAL4>UAS-mav

Figure 2.5 Expression of *mav* in muscle had no affect on NMJ growth.

(A-D) Representative confocal images of the NMJ at muscle 6/7 abdominal segments A2 (A,C) and A5 (B,D). Third instar larvae were stained with post-synaptic marker anti-Dlg (green) and pre-synaptic marker anti-HRP (red). (A) The NMJ of a control animal, *dmef2*-GAL4 crossed to $y^{-}w^{-}$ (*dmef2*-Gal4/+)(n=17), with a branched "X" shaped synapse with many boutons at muscle 6/7 of segment A2. (B) The NMJ of a control animal (*dmef2*-Gal4/+)(n=17), with a linear shaped synapse with many boutons in muscle 6/7 of segment A5. (C) The NMJ at segment A2 in animals in which *mav* has been expressed in the muscle (*dmef2*-GAL4>UAS-*mav*) (n=16), maintain a branched "X" shaped synapse with many boutons in muscle 6/7 similarly as controls. (D) The NMJ at segment A5 in muscle expression of *mav* (*dmef2*-GAL4>UAS-*mav*) (n=15), maintains a linear shaped synapse with many boutons similarly as controls. (E) Quantification of boutons in control and *mav* muscle expression in abdominal regions A2 and A5. Bouton counts were normalized to correct for muscle size differences. A students *t*-test revealed no significant difference between control and glial *mav* expression numbers. Error bars represent standard deviation.

Chapter 3

Myoglianin signaling in the nervous system is required for metamorphosis of the larval salivary gland

Abstract

Metamorphosis is an important developmental stage in the life cycle of many organisms, where the animal undergoes a dramatic change in form and shape. The process occurs through cell growth, death, and differentiation, and requires stringent regulation. In the fruit fly *Drosophila melanogaster,* metamorphosis is under the control of the steroid hormone 20 hydroxyecdysone (20E). Several mechanisms have been identified, which ensure that the multiple tissues undergoing metamorphosis do so in a coordinated manner. The activin/TGF-β signaling pathway is one of several inputs that regulate both ecdysone biosynthesis and the response to ecdysone through regulation of receptor expression (EcR-B1). In the present study, we have characterized two alleles for *myoglianin* (*myo)*, a gene that encodes an activin/TGFβ ligand. Analysis of myo^{2} and myo^{4} null alleles reveals that *myo* is required for progression through metamorphosis. *myo* mutants display a wide range of phenotypes similar to defects encountered in ecdysone pathway mutants suggesting that Myo regulates multiple metamorphic events. Misexpression of Myo induces precocious development that results in lethality. We show that *myo* function is required for destruction of the larval salivary glands, and that expression levels of cell death genes are reduced in *myo* mutants. Loss of the *myo* specific receptor isoform *babo-a* in the nervous system also results in a persistent salivary gland phenotype. We further show that degradation of the salivary glands is dependent on expression of EcR-B1 in the brain.

Introduction

In *Drosophila*, metamorphosis, larval molting, and aspects of embryonic development are all controlled by distinct pulses of the active form of ecdysone, 20E (Riddiford, 1993; Thummel, 1996). Metamorphosis events are controlled by two major pulses. In response to the late larval-prepupal pulse the larva transitions to a prepupal stage. During this period imaginal discs undergo cell proliferation and differentiation, the anterior spiracles evert, and the larval midgut and anterior muscles undergo apoptosis. The following prepupal-pupal pulse of ecdysone triggers transition from a prepupa to pupa, during which the head everts, the legs extend, and abdominal muscles and salivary glands are destroyed (Broadus et al., 1999). Extensive studies have been performed on the larval salivary glands, which are destroyed in response to the prepupal-pupal pulse, to understand the mechanism and regulation of ecdysone signaling responses. The salivary glands are a pair of tubular organs, which secrete glycosylated proteins (glue) necessary for the larva to fix itself to a dry surface during puparium formation. Once the larval salivary glands are no longer required they undergo apoptotic (Type I) programmed cell death and autophagic (Type II) programmed cell death. Previous studies have shown that destruction of the larval glands is a result of both repression of remodeling inhibitor gene *diap2* and activation of cell death genes *reaper* (*rpr*), *head involution defect* (*hid*) and *Drosophila* Nedd2-like caspase (*dronc)*. These genes are transcriptionally regulated by the ecdysone response genes E74A, E93, and BR-C (Jiang et al., 2000). A persistent salivary gland phenotype has been reported for mutations in

these ecdysone response genes (Broadus et al., 1999; Ward et al., 2003).

Many mutants for components of the ecdysone pathway have been characterized and analyzed. Mutations in the Halloween genes, which encode components of the ecdysone biosynthetic pathway are embryonic lethal, while mutations in ecdysone receptors result in lethality at multiple stages. EcR mutations that affect all three isoforms are embryonic lethal. Mutations specific for EcR-B1 and EcR-B2 isoforms display larval molting defects and arrest development as first or second instar larva. EcR-B1 mutant larvae fail to attach to a solid surface, shorten, harden cuticle, evert spiracles, and are pupal lethal. Mutations in downstream components of the ecdysone pathway are characterized by developmental arrest at pupal stages and pupal defects in spiracle eversion, head eversion, leg extension, failure of gas bubble movement to the anterior, and defects in salivary gland cell death (D'Avino and Thummel, 1998; Bender et al., 1997; Schubiger, 1998).

Several mechanisms are in place to ensure that tissue specific responses to ecdysone occur at the right time (see Figure 1.2). First, the response to ecdysone signaling can be controlled through regulation of expression of competence factor βFTZ-F1, coactivators or corepressors such as Fkh, NURF, SMRTER, Bonus, and Brahma. This mechanism allows signaling inputs to provide tissue and temporal specificity in response to ecdysone binding to its nuclear receptors (Yamanaka et al., 2013). A second mechanism in place to control ecdysone signaling responses is by regulating ecdysone receptor expression and/or ecdysone biosynthesis. Currently very little is known about the

factors that regulate EcR-A expression, however several studies have shown there are multiple inputs that spatially and temporally regulate EcR-B1 expression. Currently, three different inputs are known to regulate EcR-B1 expression. Schuldiner et al. 2008 demonstrated that mutations in the cohesin complex result in reduced levels of EcR-B1 in γ mushroom body neurons, which undergo remodeling during metamorphosis. In 2011 Boulanger et al., showed that Ftz-f1, also a nuclear receptor, is required for EcR-B1 expression in γ neurons of the mushroom body. Myo signaling has also been shown to regulate EcR-B1 expression in the γ neurons of the mushroom body (Zheng et al., 2003; Awasaki et al. 2011). Cohesin is believed to be required for initiation of EcR-B1 transcription, while Ftz-f1 and Myo are temporal signals that spatiotemporally upregulate EcR-B1 expression. In the muscle, EcR-B1 expression is dependent on Ftz-f1 and TGF-β signaling for motoneuron retraction during metamorphosis (Boulanger et al. 2012).

Previous studies have shown that activation of neuropeptide networks in the central nervous system results in the release of signals that regulate specific aspects of ecdysone mediated behaviors during metamorphosis, such as cuticle tanning through release of crustacean cardioactive peptide (CCAP) and coordination with circadian locomotor rhythms via the pigment dispersing factor (Pdf) neuropeptide (Nassel and Winther, 2010). Ecdysone biosynthesis is induced by the release of prothoracicotropic hormone (PTTH) *(Nässel, 2002*). In addition to the above mentioned role for Myo in regulation of EcRB1 expression in the γ neurons of the mushroom body, previous studies have shown that activin

signaling can also regulate the response to PTTH by regulating PTTH receptor, *torso*, expression in the ring gland. Loss of *dsmad2*, the canonical activin signal transducer, results in lower titers of ecdysone. This was a result of decreased expression levels of PTTH and insulin receptor expression, important for transcription of ecdysone biosynthetic enzymes (Gibbens et al., 2011). However, the activin ligand and receptor involved remain unknown. Together, these finding suggest that activin signaling can impact different aspects of ecdysone signaling.

In this study we analyzed loss of function mutations in *myo* to determine if *myo* is required for ecdysone signaling dependent responses in tissues other than the mushroom body. We show that loss of Myo results in a wide range of pupal defects indicative of a broad role in metamorphosis. We focused our attention on analysis of specific tissues that express high levels of the B1 isoform of ecdysone receptor and undergo a morphological change in response to ecdysone signaling. We find that *myo* mutants show defects in salivary gland destruction, correlated with decreased levels of apoptotic cell death genes. Furthermore, depletion of the Myo isoform specific receptor Babo-a and EcR-B1 in the nervous system, mimics this phenotype. Thus our study identifies a novel role for Myo signaling in non-cell autonomous control of salivary gland degradation via induction of EcR-B1 in the nervous system. Based on these findings, we propose that Myo regulates EcR-B1 in the brain to regulate multiple biological responses or behaviors during metamorphosis.

Methods

Drosophila stocks

Stocks were obtained from Bloomington Stock Center unless listed otherwise: Df (4)*myo* (M. Frash); *babo*^{Fd4}/CyO (Zheng et al., 2003), Df(2)*babo*/CyO (Brummel et al., 1999), *UAS-babo-a-miRNA*, (M. B. O'Connor, HHMI, University of Minnesota, MN), *fkh*-GAL4 (E.H. Baehrecke, University of Massachusetts Medical School, MA). *myo*^{2} and *myo*^{4} are EMS alleles generated in a y^{-}, w^{-}; p[KG y^{mini}, w^{+}] background (J. Ellis and K. Arora; unpublished data). Generation of UAS-Myo and UAS-Myo-RNAi are described in Ellis, 2010.

Sequencing of *myo alleles*

To determine lesions generated through EMS mutagenesis we collected homozygous *myo*^{2} and *myo*^{4} mutant larva. Genomic sequencing was performed by Genewiz. We PCR amplified the entire *myo* genomic region from wild type and mutant chromosomes. PCR products from multiple independent PCR reactions were sequenced. Primer sets used are listed below:

*myo*seqF2 5′-CGTGGTTGGGATTGGATAAGTGCTCA-3′

*myo*seqR4 5′-CCTGACGGAATACTATGTCG-3′

ROdirect 5′-GGAAAGCATTGACGAATCTCA-3′

*myg*4check 5′-TCCATATTCCTTTGCGTTAA-3′

Lethal phase and phenotypic analysis

Egg lays from *myo*^{2}/actin-GFP flies crossed to Df(4)*myo*/actin-GFP were collected on 3% grape agar plates at 25°C in 70% humidity. Hatched larvae were counted and transheterozygous mutants were transferred to a fresh plate daily. Dead larvae were staged by mouth hook morphology. For morphological analysis, animal were transferred to a slide, scored, and imaged using a Zeiss Axioplan microscope.

Immunohistochemistry

Animals were staged and dissected in 1x PBS. Tissues were fixed in 4% formaldehyde in PBS and 0.1% Triton X-100 for 30 minutes. EcR-B1 was detected using AD4.4 (1:100) from Developmental Studies Hybridoma Bank (DSHB) and with a α-mouse Alexa 488 secondary. Larva were incubated in primary antibody overnight at 4°C and in secondary antibody for 2h at room temperature. Tissues were counter stained with 0.5 µg/ml DAPI for 10 minutes and rinsed. Tissues were mounted in Vectashield (Vector). Preparations were analyzed sing an Olympus FluoView FV1000 scanning laser confocal or LSM780 confocal.

Imaging of GFP expression in salivary glands of living animals

Animals were staged and collected at 0 APF. Animals were placed on a slide that was placed in a humid chamber at 25°C. Animals were imaged throughout pupariation and pupation. A Zeiss Axioplan2 microscope was used to capture

epiflourescence. Salivary gland morphology was analyzed at 12, 15, and 24 APF.

qRT-PCR Analysis

Salivary glands were dissected from 13.5 APF control and *myo* mutants. Total RNA was extracted using Trizol (Invitrogen) according to the manufacturer's instructions. First-strand cDNA was synthesized from 1µg total RNA using SuperscriptTMIII reverse transcriptase (Invitrogen). Primers listed below were used to amplify cDNAs for *hid, rpr, dronc* and *rp49* control, respectively. qPCR was performed using FastStart Universal SYBR green master (Rox) (Roche) using Bio-Rad's Real-Time PCR Detection System and analyzed by Opticon 2 qPCR software. All reactions were set up in duplicates. Quantification of mRNA levels was performed using the comparative threshold cycle method (Schmittgen and Livak, 2008).

hid-F 5′- ATCGCTACGACAACTTTACGG-3′

hid-R 5′ TGGCTATCGGTATGGCAGACT -3′

rpr-F 5′- AAGCCATCGCAATGAGGATTC -3′

rpr-R 5′ TGTGTTTGGGTTTTGGGTTGG -3′

dronc-F 5′-TGAGTCCGATTCAAGGCCAC -3′

dronc-R 5′-GCTCATTCCGGAGCTTGCTA-3′

RPL32-F 5′-TGACCATCCGCCCAGCATACAGG-3′

RPL32-R 5′-TGGCGCGCTCGACAATCTCCTT-3′

Statistical Analysis

Students *t*-test was used to determine the statistical significance of the observed differences in gene expression levels (*P<0.05, ***P<0.001). Error bars indicate SD.

Results

Myo mutants display a wide range of pupal phenotypes

To gain insight into the function of *myo*, we performed a phenotypic analysis of *myo* mutants. Previous EMS mutagenesis screens on the fourth chromosome resulted in the generation of several alleles at the *myo* locus (J. Ellis and K. Arora, unpublished). 9 lethal mutations were recovered *in trans* to a small deficiency lacking *myo*, *Df(4)myo*, obtained from Dr. M. Frasch. To identify the molecular lesions in these mutants, we sequenced two of the alleles, myo^2 *and* myo^4. We identified C→T changes in positions 1521 and 1833, in myo^2 *and* myo^4, respectively, both of which result in premature termination codons (Figure 3.1). Both these changes are predicted to result in a truncated protein lacking the ligand domain, and hence myo^2 *and* myo^4 are expected to represent null alleles. In these studies, we have crossed myo^2/actin-GFP to *Df(4)myo/actin-GFP* to recover transheterozygous *myo* mutant animals. The lethal phase characterization revealed that 20% were larval lethal, while a majority of *myo* mutants die as prepupa and early pupa (60%). The remaining 20% are able to reach a pharate adult stage but fail to eclose (Figure. 3.2A). We observed that *myo* mutant larvae reared in vials fail to wander up the side of the vial and pupariate in the food. This behavior is triggered once the animal has reached

critical body size, and the larvae stop feeding and seek a dry surface to pupariate. Wandering behavior defects observed in *myo* mutants have also been described for mutants in several ecdysone pathway genes, including *usp*, the temperature-sensitive *ecdysoneless* (*ecd*^{1}) allele, and loss of ecdysone receptor B isoforms (Henrich et al., 1993; Schubiger et al., 1998; Hall and Thummel., 1998). Interestingly, Bender et al., identified a couple of mutant lines specific for EcR-B1 that are able to wander, which may be an indication that this behavior is dependent on EcR-B2 signaling. In addition, loss of *myo* results in a wide range of pupal defects. Typically, the anterior spiracles, which form part of the tracheal (respiratory) system evert upon entry to prepupal stages of development (Robertson, 1936). However, in *myo* mutants anterior spiracles fail to evert. Again in wild-type animals, a gas bubble appears in the abdomen during prepupal development, then moves towards the posterior end of the animal, and finally moves to the anterior end of the pupal case to aid in head eversion (Robertson, 1936). We also observe gas bubble translocation defects in *myo* mutants (Figure 3.2 C, E). Finally, in wild type and control $y^{-}w^{-}$ animals, head eversion and leg elongation occur shortly after the animal transitions from a prepupa to a pupa (Robertson, 1936; Figure 3.2 B). *myo* mutants display defects in both head eversion and leg elongation (Figure 3.2 C-E; Table 3.1). These metamorphosis defects are typically observed when ecdysone signaling is disrupted suggesting that *myo* may be involved in ecdysone signaling in multiple tissues (D'Avino and Thummel, 1998; Fletcher et al., 1995; Davis et al., 2005; King-Jones et al., 2005).

Embryonic and larval analysis of *myo* expression identified muscle and glia as the two main sources for *myo* (Lo and Frasch, 1999). Low levels of *myo* transcript have been reported in the trachea, salivary glands, and malpighian tubules. Moderate expression was detected in white prepupa reaching high levels at 12 hours after puparium formation (APF) (Flybase, http://flybase.org/reports/FBgn0026199.html). This expression profile indicated to us a broad requirement for Myo at multiple development stages. In addition, previous studies from our lab using a temperature sensitive homozygous myo^{KO} allele (Ellis, 2010) showed that animals die at the restrictive temperature between 96 and 108 hours after egg lay (AEL). This period corresponds to just before the onset of metamorphosis supporting a requirement for Myo during early pupal development**.**

Misexpression of *myo* results in larval growth arrest

To gain further insights into how *myo* influences growth and development during different stages of development, we used the UAS-GAL4 system to drive expression of UAS-Myo with various GAL4 drivers that target different tissues. Increased levels of Myo produced from the glia (*repo*-Gal4) results in second to third instar transition larval lethality, as they have two sets of mouth hooks (Figure 3.3). Expression using a pan neuronal *elav*-GAL4 results in larval lethality similar to that observed with the pan glial driver, indicating that increased levels of *myo* is deleterious for the animal. This is most likely due to a precocious growth response with uncoordinated behaviors that ultimately results in lethality

during a larval transition period when ecdysone levels peak. Analysis of Myo misexpression in the nervous system by targeting only a subset of cells using A9-GAL4 (neuronal and wing imaginal disc) results in pupal lethality with adult escapers (29.17%). Next, we tested *myo* misexpression using 24B-GAL4 and *dmef2*-GAL4 (muscle drivers with significant expression in the brain). We identified pupal lethality with adult escapers that had defects in leg morphology (Table 3.2). In summary, misexpression of Myo using GAL4 drivers such as A9, 24B and *dmef2*, that drive express in a range of tissues, including narrow expression in the nervous system, results in pupal lethality with adult escapers with morphological defects; while expression using broad nervous system drivers results in animals that die as larva and fail to enter pupariation (Table 3.2). Based on these findings, one interpretation is that the different stages of lethality observed may be related to the amount of Myo or the timing of ligand misexpression. Alteration in the levels of Myo may trigger defective larval molting and pupation by misregulating ecdysone signaling early on in development before the animal is ready to undergo changes.

Since Myo is a target of inhibition by Fs, we expected to be able to reverse the lethality caused by increased *myo* levels through expression of Fs. To test this we used the UAS-GAL4 system to co-express *myo* and Fs. We observed that lethality caused by increased levels of *myo* can be reversed by overexpression of Fs, using *A9*-GAL4. Fs suppresses the Myo driven lethality by 100% (Figure 3.4). These data suggest that the relationship between Myo and its homolog, Myostatin, is conserved with respect to extracellular modulation.

Myo is required for salivary gland remodeling

As described above, loss of *myo* results in a wide range of pupal defects. To determine which metamorphosis events require Myo, we selected several tissues that undergo well described changes in response to either the late larval or the prepupal ecdysone pulse. These events are: destruction of the salivary gland, fat body remodeling, abdominal muscle cell death, midgut cell death, and mushroom body remodeling. This chapter describes analysis of salivary gland degradation in activin pathway mutants, while analysis of the remaining events are described in Chapter 4.

To assess if activin signaling regulates salivary gland histolysis, we visualized salivary glands throughout pupal development in live animals using the UAS-GAL4 system. We generated stocks containing *fkh*-GAL4, a salivary gland driver, and a UAS-GFP reporter in a *myo* mutant background. During larval and pupariation stages, in control animals (*fkh*-GAL4; UAS-GFP) the salivary glands can be seen on the ventral side of the animal. Once the animal receives the second pulse of ecdysone, the head everts (12 APF) and the salivary glands move towards the dorsal region and contract. By 24 APF the salivary glands are no longer visible (Figure 3.5 A-C). In *myo* mutants, salivary glands fail to migrate, contract, and remain visible for many hours after the salivary glands of control animals have undergone cell death. Salivary gland remodeling is delayed in these mutants by at least 10 hours since we can observe salivary glands at 24 APF (Figure 3.6 D-F). These data indicate that *myo* function is required for

salivary gland remodeling. To determine if *myo* signals through the activin pathway to regulate salivary gland degradation we analyzed mutations in *babo*, which encodes the activin type I receptor. Transheterozygous *babo* mutants (*babo*^{fcl4}/*Df(2)babo)* also display defects in salivary gland remodeling (Figure 3.6 G-I). In *babo* mutants, salivary glands fail to migrate and remain visible on the ventral side at least 10 hours after the salivary glands in control animals have degraded.

Salivary gland degradation is a result of activation of cell death genes *reaper* (*rpr*), *head involution defect* (*hid*) and *Drosophila Nedd2-like caspase* (*dronc*). Expression of these genes has been shown to be decreased in the salivary glands of mutants that retain their salivary glands (Restifo and White, 1992; Broadus et al., 1999; Lee et al., 2000; Jiang et al., 2000; Lee et al., 2003; Lee et al., 2002b). Therefore we assayed whether transcript levels of apoptotic cell death genes are altered in the salivary glands of *myo* mutants. We performed qRT-PCR on salivary glands dissected at 13.5 APF from *myo* and Oregon R controls to determine if the transcript levels of *rpr*, *hid*, and *dronc* were altered. We found that *rpr*, *hid*, and *dronc* are down regulated in *myo* mutants (Figure 3.6 A-C). These data suggest that *myo* signaling acts upstream of the cell death genes required for apoptotic programmed cell death of the larval salivary glands.

Ecdysone receptor expression is not affected in *myo* mutant salivary glands

The salivary glands express both EcR-A and EcR-B1 isoforms. EcR-B1 is the dominant form in the larval salivary gland while Ecr-A is weakly expressed

(Talbot et al., 1993). EcR silencing using an RNAi line that targets all EcR isoforms result in salivary gland degradation defects (Denton et al. 2013). Even though the EcR-A isoform is weakly expressed it is also required for salivary gland degradation as a persistant salivary gland phenotype is observed in EcR-A mutants (Davis et al.,2005). Given that Myo has been shown to regulate mushroom body remodeling through regulation of EcR-B1 expression, this prompted us to ask if *myo* uses a similar mechanism to regulate salivary gland remodeling. Therefore we stained Oregon R, *myo,* and *babo* mutant salivary glands with an antibody that is specific for the EcR-B1 isoform. However, no changes in EcR-B1 expression were observed in *myo* or *babo* mutants (Figure 3.7 A-C). EcR-A was weakly detected through immunohistochemistry and differences in expression could not be determined (data not shown). Our results indicate that Myo does not regulate ecdysone responsiveness in the salivary glands through regulation of ecdysone receptor expression, and suggest that an alternative mechanism is in place for regulation of salivary gland remodeling.

Glia derived Myo is required for salivary gland cell death

To determine which of the many tissues that express Myo are critical for the salivary glands to undergo destruction, we used the GAL4-UAS system to deplete Myo in a tissue specific manner, using UAS-myo RNAi. Previously, we followed salivary gland degradation *in vivo* using *fkh*-GAL4 to drive a UAS-GFP reporter in a mutant background. We were not able to use the same approach, since the use of two GAL4 drivers, targeting different tissues, would negate the

analysis. The ideal reporter would be a salivary gland enhancer reporter that would allow us to visualize salivary glands in the animal throughout pupal development, however we have not been able to identify such a reporter. Therefore to resolve this issue, animals were collected at 0 APF, allowed to develop to 24 hours APF (when salivary glands have degraded in wild type animals), then assayed for the presence or absence of the salivary glands. We depleted *myo* from the muscle and glia, the two major sites of synthesis (Lo and Frasch, 1999; Flybase). We and others have identified a glial derived requirement for *myo* in mushroom body remodeling, while muscle derived Myo is required for other functions in the adult (Awasaki et al., 2011; Demontis et al., 2014; see Chapter 4). We observed that when Myo was depleted from glial cells, salivary glands remained present at 24 hours APF, several hours after salivary glands have degraded in control Oregon R flies. In contrast, salivary glands were not recovered at 24 hours in animals where *myo* was depleted in muscle indicating that larval salivary glands were destroyed (Table 3.3). Our data indicate that glial derived Myo, but not muscle derived Myo, is required for salivary glands histolysis. We also examined the pupal phenotypes in RNAi depleted *myo* from glia and muscle cells. Pupal phenotypes and lethality were only observed with glial loss but not with muscle (Figure 3.9 D, E). These results support the idea that animals require glial derived *myo* for pupal development.

Salivary gland cell death is controlled by signaling in the nervous system

The salivary glands express moderate levels of *babo* transcript (Flybase, http://flybase.org/reports/FBgn0011300.html). Given that *babo* has been

implicated in regulating several aspects of ecdysone signaling, we wanted to determine if salivary gland degradation is controlled directly by *babo* signaling. There are three identified *babo* receptor isoforms. The Babo-A isoform is believed to be the Myo specific activin type I receptor because this is the only RNAi depleted *babo* isoform that could rescue larval lethality caused by misexpression of *myo* (Awasaki et al., 2011). We used the GAL4-UAS system to block the response to *myo* signaling in a tissue-restricted and cell-autonomous manner and examined the effects of depleting endogenous *babo*. The salivary gland drivers *fkh*-GAL4 and *sg*-GAL4, were used to deplete *babo*-a isoform by driving UAS-*babo*-a miRNA. We collected 0 APF animals and allowed the animals to grow at 29°C for 24 hours. At this time animals were dissected, long after salivary gland have degraded in control animals and we assessed if the larval salivary gland were retained or destroyed. If Myo was directly affecting salivary gland destruction, we would expect that *babo* RNAi knockdown in the salivary glands would interfere with salivary gland cell death. However, we found that salivary glands were destroyed in the same time frame as in Oregon R control animals (see Table 3.3). Thus our data indicated that the salivary glands are not a direct target of Myo signaling for salivary gland degradation. Therefore, we extended our analysis to deplete *babo* receptor in multiple tissues including tissues known to be activin signaling responsive like the nervous system, prothoracic gland and muscles by using other GAL4 drivers (Awasaki et al. 2011, Gibbens et al., 2011; Ellis et al., 2010, Fuentes-Medel et al., 2012). As in previous experiments, staged animals were allowed to develop at 29°C and

examined for salivary gland retention or degradation at 24 hours APF. The larval salivary glands were destroyed when *babo-a* miRNA is depleted in the γ mushroom body neurons (MB247-GAL4) and in the prothoracic gland (*phm*-GAL4). However, we found that larval salivary gland were retained in animals where *babo-a* was depleted using the *dmef2*-GAL4 driver (Table 3.3). *dmef2*-GAL4 is considered to be a somatic and visceral muscle specific GAL4, however upon examination of animals carrying *dmef2*-GAL4>UAS-nRFP, we observed expression in the salivary glands and the nervous system. In the brain, UAS-nRFP driven expression by *dmef2*-GAL4 occurs in cells near the vicinity of the mushroom body neurons, antennal lobe projection neurons, and in VNC neurons (Figure 3.8 A; Ranganayakulu et al., 1996; Banovic et al., 2010; Blanchard et al., 2010; Demontis and Perrimon, 2009). We ruled out a *babo* signaling requirement in the salivary glands for cell death, since no degradation defects were detected when *babo-a* was depleted using salivary gland drivers, *fkh*-GAL4 or *sg*-GAL4. To determine if the muscle was the tissue mediating salivary gland cell death, we used 24B-GAL4, also known to be a muscle specific driver. Closer analysis of 24B-GAL4 revealed that this Gal4 also drives expression in the nervous system. Salivary glands were also retained with 24B-GAL4 (see Table 3.3), further supporting a *babo* signaling requirement in the muscle or nervous system for salivary gland cell death. We identified MHC-GAL4, as a possible candidate muscle driver, however this GAL4 drives expression late in pupal development and does not allow us to assess for a requirement for *babo* in the muscle. At this time we have not been able to identify a restricted muscle specific GAL4 driver to

resolve if Babo signaling is required in the muscles for salivary gland cell death. To test for a nervous system requirement for salivary gland degradation, we selected several nervous system drivers to deplete *babo*. Knockdown of *babo* using *repo*-GAL4 had no affect on salivary gland degradation, excluding a glial requirement. We selected a broad neuronal driver (*elav*-GAL4) that has no muscle expression to resolve if there was a neuronal *babo* signaling requirement independent of muscle. Interestingly, pan-neuronal (*elav*-GAL4) depletion of *babo-a* receptor results in defects in salivary gland degradation (see Table 3.3). Thus, our data argue that activin signaling in the brain is indirectly required for salivary gland degradation.

Next, we extended this analysis to examine the pupal phenotypes of animal in which *babo* signaling was disrupted in specific tissues. As described earlier, *myo* mutants display several pupal ecdysis defects such as gas bubble migration, head eversion, anterior spiracle eversion, and leg extension (Figure 3.9 B). Transheterozygous *babo* mutants have a stronger phenotype and stop developing shortly after entering pupariation (Figure 3.9 C). This is probably due to loss of all *babo* receptor isoforms, which are required for signaling by different activin ligands. Salivary gland (*fkh*-GAL4) *babo-a* miRNA depletion had no effect on pupal development, while *babo-a* miRNA depletion using drivers that express in neuronal cells (*dmef2*, *24B,* and *elav* GAL4) results in pupal lethality and phenotypes similar to *myo* and *babo* mutants (Figure 3.9 F-I). These results indicated that *myo/babo* signaling in the nervous system makes a significant contribution to pupal development.

Babo signaling in the CNS is required for salivary gland cell death

To identify the mechanism in the nervous system that regulates salivary gland cell death downstream of *babo* receptor signaling, we began by exploring a previous model described in mushroom body remodeling. In 2003, Zheng et al., showed that activin signaling regulates EcR-B1 expression in γ mushroom body neurons that remodel. It was later demonstrated that remodeling was dependent on Myo signaling via *babo* to activate EcR-B1 in the γ mushroom body neurons (Awasaki et al., 2011). To determine if activin signaling is required for EcR-B1 expression in the brain for salivary gland cell death, we first analyzed EcR-B1 expression in the brain of *myo* and *babo* mutants. We found that EcR-B1 expression is significantly reduced throughout the whole brain in *myo* and *babo* mutants compared to Oregon R expression in the brain (Figure 3.8 B-D). We also examined brain EcR-B1 expression in animals that have been depleted of *babo-a* in the nervous system. We found that depletion of *babo* using the pan-neuronal driver elav-GAL4 significantly reduced EcR-B1 expression in the brain, and as described earlier in this chapter, these animals also have salivary gland degradation defects (Figure 3.8 F). Based on these findings, it appears that a neuronal cell type, or a subset of neuronal cells, which expresses EcR-B1, are required for initiating salivary gland degradation at a distance. To identify the neuronal cell type(s) involved in salivary gland cell death, we analyzed the EcR-B1 expression in *dmef2*-GAL4>*babo-a* miRNA knockdown, the most narrow neuronal GAL4 driver in our hands that results in persistent salivary glands upon depletion of *babo* (see Figure 3.8 A). If these cells normally express EcR-B1 and

if upon depletion of *babo*, EcR-B1 expression is reduced or lost, these cells would be candidate neuronal cells involved in salivary gland cell death. We observed a reduction in *dmef2* positive EcR-B1 expressing cells in animals where *babo* receptor was depleted (1.3± 1.06; n=10) versus (8.4± 2.95; n=10) in controls (Figure 3.10 A-D). We then selected more narrow drivers that overlap with a subset of *dmef2*-GAL4 expressing cells. Based on the expression pattern of *dmef2*-GAL4, we tested if knockdown of *babo* type A receptor with GH146-GAL4 and MB247-GAL4 (an antennal lobe projection neuron driver and mushroom body driver, respectively), and assessed if the salivary glands were retained or degraded. The salivary glands degrade in these animals indicating that neither mushroom body neurons or antennal lobe projection neurons regulate degradation of the salivary glands (see Table 3.3). Our data suggest *myo* signaling is required for EcR-B1 expression in the brain for salivary gland degradation. Further analysis is required to determine the identity of the cells responsible for salivary gland cell death, and the signaling molecule(s) that they utilize to mediate this function.

EcR-B1 is required in the brain for salivary gland cell death

Our data suggests that regulation of EcR-B1 in the brain is the mechanism by which Myo regulates salivary gland cell death. Therefore one would expect that depletion of EcR-B1 in the nervous system should result in a persistent salivary gland phenotype. To test this, we used the GAL4-UAS system to deplete EcR-B1 and assayed for salivary gland retention or degradation at 24 APF as earlier described for *babo-a* miRNA depletion. We used *elav*-GAL4 (pan-

neuronal), *dmef2*-GAL4 (neuronal/ muscle), *24B*-GAL4 (neuronal/ muscle) to drive EcR RNAi. We used EcR RNAi line 104, which targets all three isoforms (Colombani et al., 2005). We recovered salivary glands at 24 APF from animals where ecdysone receptor was depleted using *elav*-GAL4 and *dmef2*-GAL4 (Figure 3.11 D, F; Table 3.3). Similar pupal phenotypes that have been observed with loss of activin signaling were found with loss of EcR-B1 in the brain (Figure 3.11 C, E). Interestingly, loss of EcR-B1 in the salivary gland also results in persistent salivary gland phenotype suggesting that multiple inputs regulate salivary gland cell death. While EcR-B1 expression in the brain and salivary gland appear to be required, our data argues that *myo*/activin signaling only regulates EcR-B1 in the brain, and not in the salivary glands, to promote pupal development and salivary gland degradation. EcR-B1 is a nuclear receptor therefore we predict that it regulates the expression of a signaling molecule, or a neurosecretory factor that in turn promotes salivary gland turnover.

Discussion

Drosophila metamorphosis is regulated by steroid hormone ecdysone signaling to ensure proper temporal tissue responses that allow that animal to transition from an immature larva to a mature adult form. In the absence of ecdysone signaling, animals display defects in pupal development such as in neuronal remodeling, cell death of the larval salivary glands and midgut. In the present study, we demonstrate that *myo* signaling is required for progression through pupal stages and metamorphosis. We have identified a *myo* signaling requirement for salivary gland degradation, as both *myo* and *babo* mutants retain

their larval salivary glands. However, depletion of the *myo* specific *babo-a receptor* in the salivary glands did not affect salivary gland cell death, instead pan neuronal depletion of *babo-a*, results in loss of EcR-B1 in the nervous system and a persistent salivary gland phenotype. These data argue that destruction of salivary glands is indirectly dependent on *myo* signaling in the nervous system. RNAi silencing of EcR-B1 in the CNS also results in persistent salivary gland defects, arguing that *myo* signaling dependent EcR-B1 expression in the nervous system is required to control salivary gland cell death. The signals downstream of EcR-B1 are currently unknown, but one possibility is that Myo signaling, through regulation of EcR-B1 expression, could modulate expression of neuropeptides required for specific pupal ecdysis behaviors or of a secreted protein that acts at a distance to initiate signaling in distant tissues.

Our analysis of *myo* mutant animals revealed that they are pupal lethal, with a range of phenotypes reminiscent of metamorphosis defects caused by loss of ecdysone signaling components, arguing that Myo is required for metamorphosis and could regulate ecdysone signaling in multiple tissues and/or stages in addition to neuronal remodeling. There are several lines of evidence to support the idea that EcR-B1 is downstream of *myo* signaling. First, the significant phenotypic overlap between both *myo* and EcR-B1 loss suggest that there is an epistatic relationship (this work; Bender, 1997; Schubiger, 1998). Furthermore, EcR-B1 was significantly reduced in the CNS of *myo* mutants (see Figure 3.8 C). Finally, downstream targets of EcR-B1 (*hid, rpr, dronc*), are significantly reduced in *myo* mutants. Therefore we extended our analysis to

assay additional metamorphosis events including fat body remodeling, salivary gland, larval midgut, and muscle cell death, that are all dependent on EcR-B1 expression; both to resolve whether regulation of EcR-B1 is a primary mechanism by which the activin pathway regulates ecdysone signaling, as described by (Awasaki et al. 2011), and also to establish whether Myo loss has a systemic effect on metamorphosis.

Glia and muscle are the two main sources of Myo, however glia derived Myo is required during metamorphosis, as pupal phenotypes and persistent salivary glands were only observed by RNAi depletion of Myo from glia (*repo*-GAL4) and not muscle (*dmef2*-GAL4). Our results have not revealed a role for muscle-derived *myo* in pupal metamorphosis. However studies in adults have shown that it plays an important role in aging (Demontis et al., 2014). One indication that arises from our prepupal studies where the source of Myo required is from glia and the responding cells are neurons, is the possibility that *myo* may not be very diffusible and needs to be expressed in the vicinity of responding cells. Over all these results support the idea that the nervous system provides the *myo* source required for salivary gland degradation.

The phenotypes and lethality encountered in *babo* mutants and silencing of *babo*-a isoform are more severe than loss of *myo* signaling alone (see Figure 3.9 D, G), which suggests the involvement of another ligand. Zheng et al., (2003) first identified Actβ as the ligand required for EcR-B1 expression in the γ-neurons. Later this group showed that the ligand involved was actually Myo. It is possible that Actβ may have a less significant role compared to *myo* in EcR-B1

expression, which would account for the more severe defects observed in *babo* mutants. However, it is unknown if Actβ can signal through the Babo-*A* receptor. Although Myo regulates EcR-B1 expression widely in the CNS, analysis of EcR-B1 expression in the salivary glands of *myo* and *babo* mutants revealed expression was unaltered (Figure 3.8 B, C), suggesting that *myo* signaling is not a global regulator EcR-B1 in all tissues.

We showed that *babo* and ecdysone receptor expression in the brain are required for salivary gland destruction through RNAi depletion, using GAL4 lines that drive broad (*elav*-GAL4) and narrow (*dmef2*-GAL4, and *24B-GAL4*) expression in the nervous system. These data support the idea that Myo dependent regulation of EcR-B1 transcription is a common mechanism by which Myo and Babo signaling regulates ecdysone responses. As a Myo signaling target gene, we would expect that misexpression of EcR-B1 would result in similar phenotype as Myo misexpression, which would further confirm an epistasis relationship. However, the only published misexpression analysis of ecdysone receptors was performed using heat inducible transgenes after the animals had already transitioned to a late third instar stage (Schubiger et al., 2003), which did not allow us to make this relationship. Meng et al., (2002) report that ectopic expression of Hugin, a neuropeptide involved in ecdysis and myostimulatory behavior, results in a similar larval lethal phenotype that we encountered with ectopic expression *myo*. These data suggest a possible relationship between *myo*, edysone, and neuropeptide signaling.

It remains to be resolved how Myo/activin signaling controls ecdysone

signaling in the nervous system to initiate a salivary gland cell death response. One possible mechanism is through regulation of an unidentified neuropeptide. Neuropeptides are biologically active molecules found throughout the animal kingdom, which regulate physiological and behavioral processes. The finding that *myo* is required in the nervous system for multiple responses (salivary gland cell death and wandering behavior), raises the possibility that *myo* signaling regulates expression of neurosecretory molecules, either directly or indirectly through EcR-B1. Myo may convey a signal for synthesis and secretion of neuropeptides. There is evidence that GDF11, the Myo vertebrate orthologue, regulates Neuropetide Y (NPY) expression and function for kidney development through regulation of Glial derived neurotrophic factor (GDNF) expression (Choi et al., 2009). It remains to be shown if Myo has a similar function as its vertebrate orthologue.

Many neuronal cell types show loss of EcR-B1 expression in *myo* and *babo* mutants, not just the γ mushroom body neurons, which suggests that *myo* may regulate the biological activities of these other cell types. Many of the Forty-two neuropeptide coding genes have been identified in *Drosophila* have been implicated in regulating ecdysis/molting behaviors (Nässel & Winther, 2010), thus are potential candidate neuropeptides whose activity may be regulated by *myo*, including *Drosophila* NPY. We used several criteria to select candidate neurosecretory peptides. For example, the pigment-dispersing factor (PDF) secreted from pacemaker neurons that maintain circadian rhythms shows overlaping expression with *dmef2* (Blanchard et al., 2010). Likewise the

Corazonin (*crz*) and FMRF producing Tv neurons require EcR-B1 and EcR-B2 activity to undergo pruning (Schubiger et al.,1998; Schubiger et al., 2003). Other candidate neuropeptides are those that regulate ecdysis behaviors, such as crustacean cardio active peptide (CCAP), myoinhibiting peptide, and eclosion hormone (Ewer, 2005; Zitnan et al., 2007). Ablation of CCAP neuron during metamorphosis results in pupal lethality and defects in head eversion similar to *myo* loss-of–function mutants (Park et al., 2003). We hypothesize that *myo* signaling regulates EcR-B1 to initiate ecdysone signaling to activate expression of a downstream neuropeptide that regulates salivary gland cell death and possibly other tissues. The animal may find having this secondary relay advantageous because *myo* signaling may initiate a progressive signaling cascade that cooperates with other signals at a later stage in development to elicit a biological response.

Biological responses to ecdysone are coordinated through multiple regulatory inputs. Here we have identified one such input for Myo/activin signaling in the regulation of metamorphosis. Inputs from Myo/Babo signaling, along with cohesin and β-ftz-F1, regulate EcR-B1 expression in the brain. Likewise, activin signaling is one of multiple inputs, along with nitric oxide and EcR signaling that regulates ecdysone biosynthesis (Rewitz et al., 2013). Here we show that salivary glands require both cell-autonomous and neuronal EcR-B1 expression to undergo cell death, and that *myo* is only required to regulate expression in neuronal cells. Furthermore, other inputs from the Insulin/PI3K and JUN N-terminal kinase (JNK) signaling are also known to regulate salivary gland

cell death (Mariño et al., 2014; Berry and Baehrecke, 2008). Thus signaling from the activin pathway appears to be an additional mechanism to ensure temporal coordination of salivary gland cell death.

```
1621 GTTGGGATTGGATAAGTGCTCATCAACCTGGACTTCTTGAAGAAATTAAAAAACAGCCAC
     G  W  D  W  I  S  A  H  Q  P  G  L  L  E  E  I  K  K  Q  P
1681 GTAAAGATATTGTTGTGACTATTCACCGCGCTATTAGGGTTGCAAATACAACAAGCTTTA
     R  K  D  I  V  V  T  I  H  R  A  I  R  V  A  N  T  T  S  F
1741 ATCCTAAAGTCAAAATGTTTGAGTTTCGACATAGTATTCCGTCAGGACTTGGACAATGGG
     N  P  K  V  K  M  F  E  F  R  H  S  I  P  S  G  L  G  Q  W
1801 TTGCTGTGGACTTAAAGTCTCTGCTTGGTAATCTTGGGTCTAATATGACGCAAGAAATTC
     V  A  V  D  L  K  S  L  L  G  N  L  G  S  N  M  T  Q  E  I
1861 TAATAAAGGGCGCAGAAACCTGGATGAAGTCATTAGTGGTGACCACAGACAACACATCGA
     L  I  K  G  A  E  T  W  M  K  S  L  V  V  T  T  D  N  T  S
1921 AAAATCCATTGACTGTTCACATAGAAATTGGGTCGCAAAAAAAGCATCGAAGAAAGCGCA
     K  N  P  L  T  V  H  I  E  I  G  S  Q  K  K  H  R  R  K  R
1981 GCGTATATATGGACTGCACAGAAAATGATCATGACATGCGCTGTTGTCGATATCCCCTCA
     S  V  Y  M  D  C  T  E  N  D  H  D  M  R  C  C  R  Y  P  L
2041 AAGTTAATTTCACCAGCTTTGGATGGCATTTCGTTGTAGCACCAACGTCCTTTGACGCAT
     K  V  N  F  T  S  F  G  W  H  F  V  V  A  P  T  S  F  D  A
2101 ACTTCTGCAGTGGTGACTGCAAAGTTGGTTACCTAGAGCAATATCCCCATACACATTTAG
     Y  F  C  S  G  D  C  K  V  G  Y  L  E  Q  Y  P  H  T  H  L
2161 CAGCCTTAACGACATCGGCCACACCGTGTTGCTCGCCGACAAAAATGAGTTCCTTAAGTT
     A  A  L  T  T  S  A  T  P  C  C  S  P  T  K  M  S  S  L  S
2221 TGTTATATTTTGACGATAACCATAATCTGGTTTTAAGTGTTATACCAAATATGTCTGTCG
     L  L  Y  F  D  D  N  H  N  L  V  L  S  V  I  P  N  M  S  V
2281 AGGGTTGCAGCTGTTCTTAGCGAACAAAATTCGAAAGTGTTCTTTGAAAATAGAACTAAT
     E  G  C  S  C  S  *
```

- myo_4^2 = Q381stop
- *myo* = Q485stop

Figure 3.1 Molecular characterizations of *myo* mutants.

(A) Sequence and translation of *myo* (Genbank accession no. NM_166786). Highlight in green indicates a nucleotide substitution in *myo* ^{2} (C→T) at position 1644, (Q381stop). The nucleotide highlighted in red indicates a substitution in *myo*^{4} (C→T) at position 1956, (Q485stop). These base pair substitutions are predicted to result in truncated proteins lacking the ligand domain (underlined), therefore *myo*^{2} *and myo*^{4} are expected to represent *bonafide* null alleles.

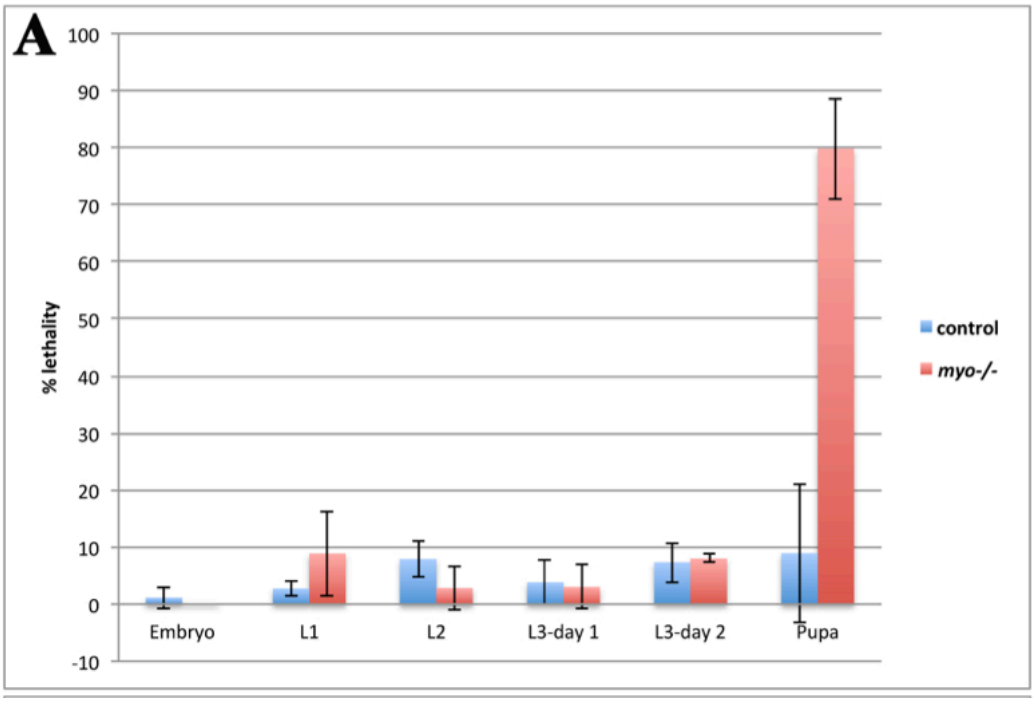
A
100
90
80
70
60
50
40
30
20
10
0
-10
% lethality
Embryo
L1
L2
L3-day 1
L3-day 2
Pupa
control
myo-/-

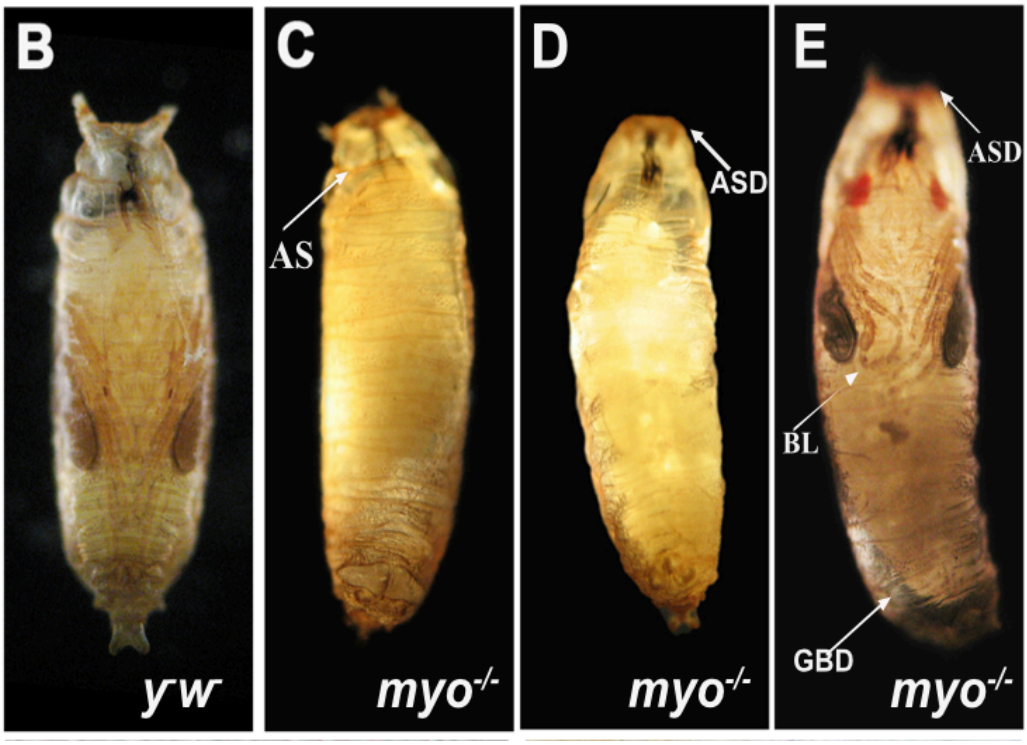
B
yw
C
AS
myo-/-
D
ASD
myo-/-
E
ASD
BL
GBD
myo-/-

Figure 3.2. Loss of *myo* leads to defects in pupal development and lethality. (A) Lethal phase analysis of $y^{-}w^{-}$ controls and *myo* mutants. The graph represents the average lethality observed from three independent trials (n=100 per genotype and trial). Majority of *myo* mutants arrest development during pupal development, while $y^{-}w^{-}$ controls eclose. Lethality observed through larval development for both *myo* mutant and controls is most likely due to animal handling. Error bars represent standard deviation. (B) $y^{-}w^{-}$ control animals with everted anterior spiracles, gas bubble at the anterior and fully extended legs. (C-E) *myo* mutants display a wide range of pupal defects. (C) A representative prepupal lethal *myo* mutant with symmetry (AS), head eversion, and gas bubble migration (GB) defects. (D) A representative pupal lethal *myo* mutant with anterior spiracle (AS) eversion and gas bubble migration defects. (E) A representative *myo* mutant pharate adult with bent legs (BL), gas bubble migration, and anterior spiracle eversion defects.

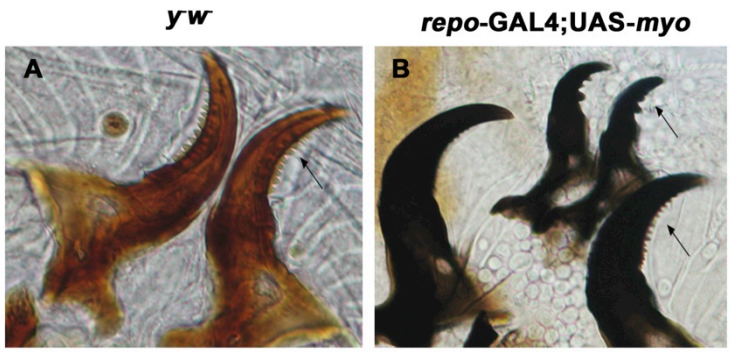
y w
repo-GAL4;UAS-myo
A
B

Figure 3.3 Misexpression of Myo results in transition stage lethality.

Bright field images of larval mouth hooks in control and ectopic expression of Myo. (A) *y⁻w⁻* 3rd instar larval mouth hooks display multiple teeth. (B) Glial (repo-GAL4) misexpression of UAS-*myo* results in animal that arrest development during 2nd/ 3rd instar transition as they display a double mouth hooks. One set has few teeth (2^{nd} instar) and the other set has many teeth (3^{rd} instar). Increased levels of *myo* in the nervous system most likely results in increased levels of ecdysone signaling.

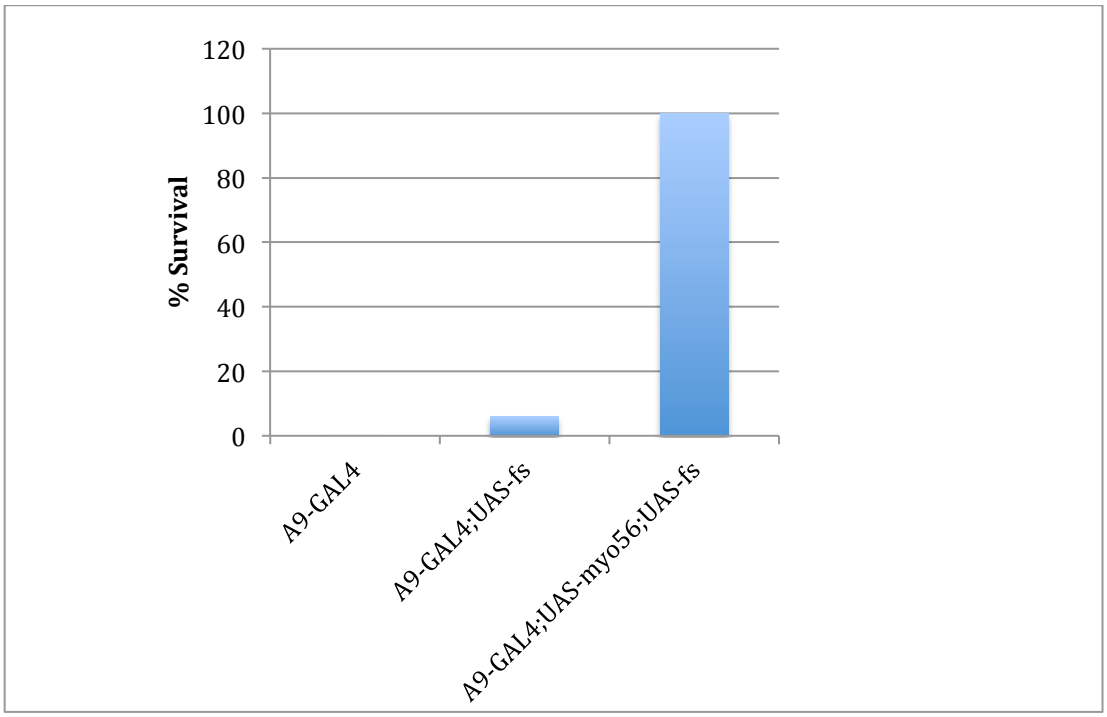
120
100
80
60
40
20
0
% Survival
A9-GAL4
A9-GAL4;UAS-fs
A9-GAL4;UAS-myo56;UAS-fs

Figure 3.4 Lethality associated of Myo misexpression can be reversed by addition of Fs inhibitor.

Graph represents average percent survival from two independent trails. Misexpression of Myo using A9-GAL4, a neuronal and wing driver, results in early larval lethality. Similar larval lethality is observed by misexpression of the activin ligand inhibitor, Fs, results in pupal lethality, with few escapers. Co-expression of Fs and Myo reverses lethality by 100%.

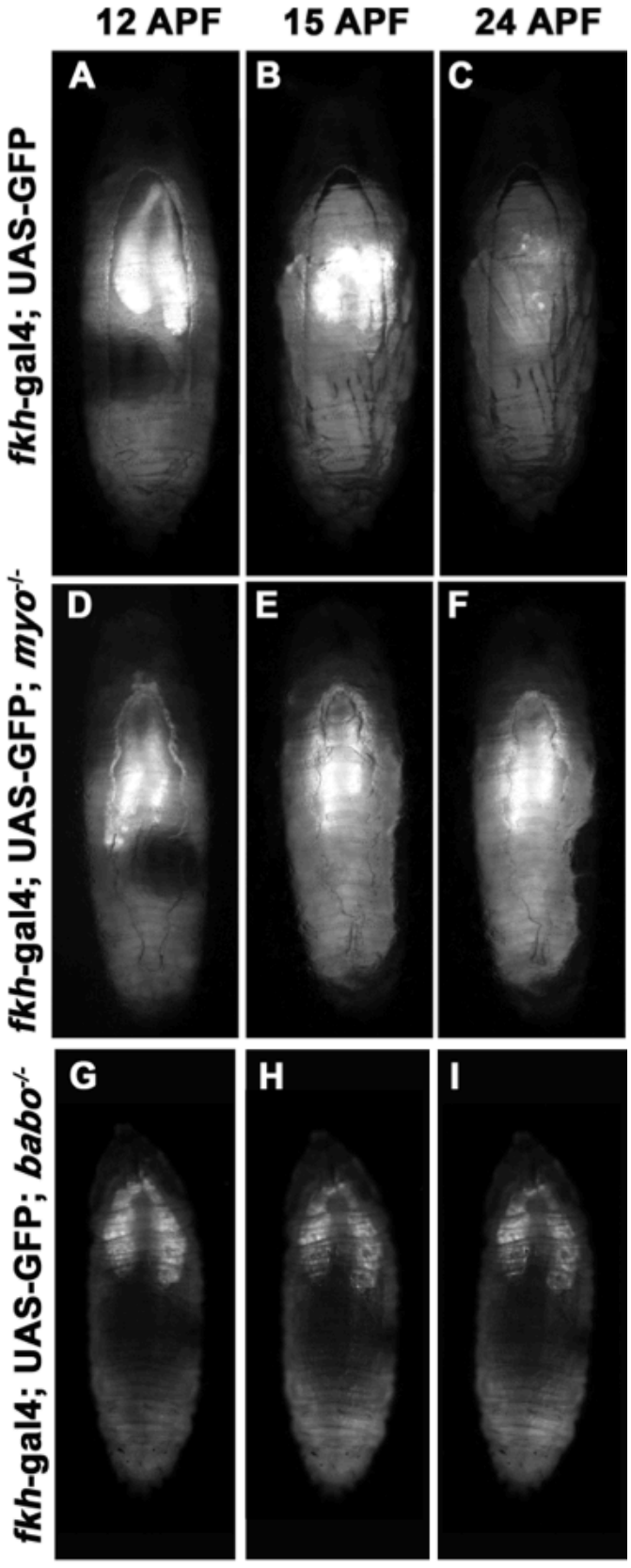
12 APF
15 APF
24 APF
A
B
C
fkh-gal4; UAS-GFP
D
E
F
fkh-gal4; UAS-GFP; myo-/-
G
H
I
fkh-gal4; UAS-GFP; babo-/-

Figure 3.5 Salivary glands fail to undergo apoptosis in *myo* and *babo* mutants.

Salivary gland degradation was visualized *in vivo* with salivary gland driver, *fkh*-GAL4 and UAS-GFP reporter through out prepupal and early pupal development. Animals were staged at 0 hours APF and imaged at 12, 15, and 24 hours APF. (A-C) *fkh*-GAL4; UAS-GFP control salivary glands are located on the ventral most side of the prepupa at 12 APF (A), but quickly start moving dorsally as the head everts. The salivary glands are condensed and curved at 15 hours APF in live animals. It should be noted that if salivary are dissected at this time, they disaggregate and cannot be recovered (B). The salivary glands are no longer visible *in vivo* at 24 APF in controls (C). (D-F) *fkh*-GAL4; UAS-GFP *myo* mutants retain their larval salivary glands. (G-I) *fkh*-GAL4; UAS-GFP *babo* mutants also display persistent salivary glands. The salivary glands of activin pathway mutants can be visualized 24 APF, long after control salivary glands have undergone cell death.

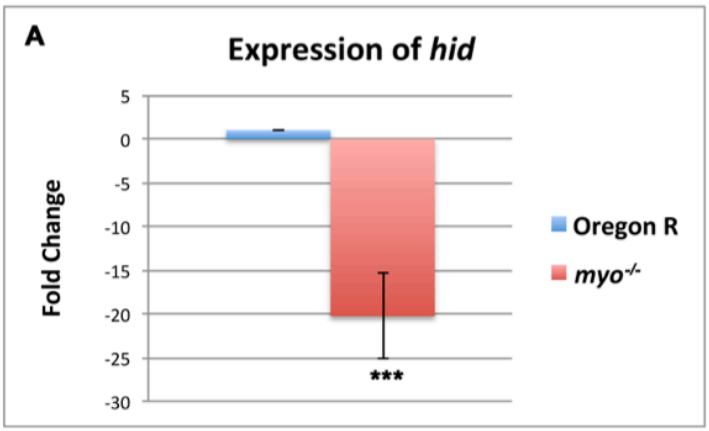
A
Expression of *hid*
Fold Change
5
0
-5
-10
-15
-20
-25
-30
***
Oregon R
myo$^{-/-}$

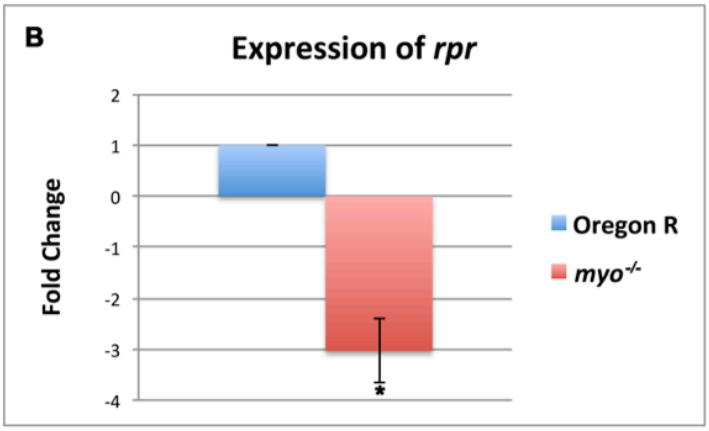
B
Expression of *rpr*
Fold Change
2
1
0
-1
-2
-3
-4
*
Oregon R
myo$^{-/-}$

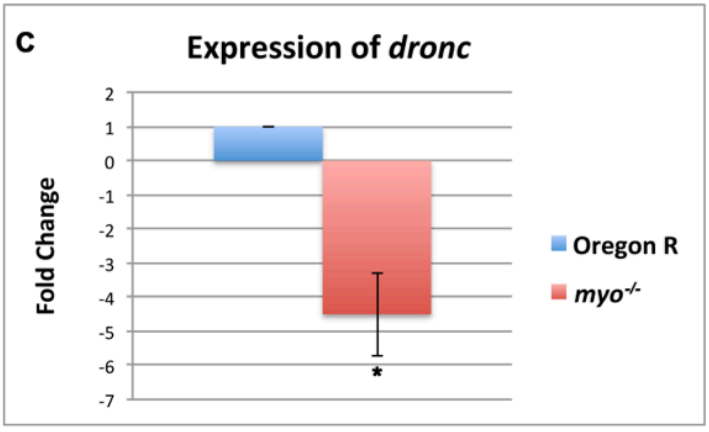
C
Expression of *dronc*
Fold Change
2
1
0
-1
-2
-3
-4
-5
-6
-7
*
Oregon R
myo$^{-/-}$

Figure 3.6 Cell death genes are down regulated in *myo* mutants.

Graphs represents quantitative expression analysis of cell death genes in the salivary glands at 13.5 APF for at least 3 independent RNA samples. The comparative CT method was used to analyze qRT-PCR data. (A) Analysis reveals that *myo* mutant salivary glands have a decrease of 20.29-fold in the pro apoptotic gene involved in salivary gland cell death *hid,* previously known as *wrinkled*. (B) Although pro apoptotic gene *rpr* play a less important role in salivary gland cell death compared hid, a 3.03-fold decrease in *rpr* was also detected in *myo* mutants salivary glands. (C) *Drosophila* caspase, *dronc* expression was 4.5-fold lower in *myo* mutant salivary glands. Data are mean±s.d. **P*<0.05, ****P*<0.001.

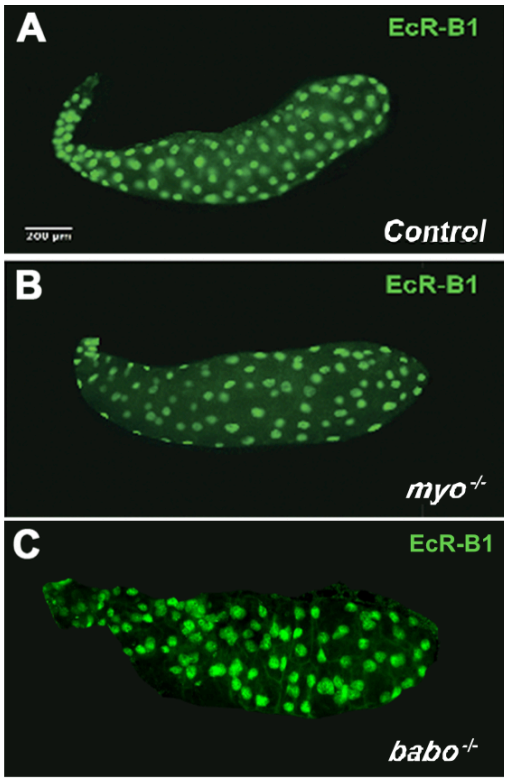
A
EcR-B1
200 µm
Control
B
EcR-B1
myo-/-
C
EcR-B1
babo-/-

Figure 3.7 EcR-B1 is expressed in the salivary glands of activin pathway mutants.

Ecdysone receptor B1 isoform expression during the late larva-prepupall ecdysone pulse (0 APF). (A) Nuclear EcR-B1 is detected in control salivary glands. Altered EcR-B1 expression was not detected in either *myo* mutants (B) or *babo* mutants (C).

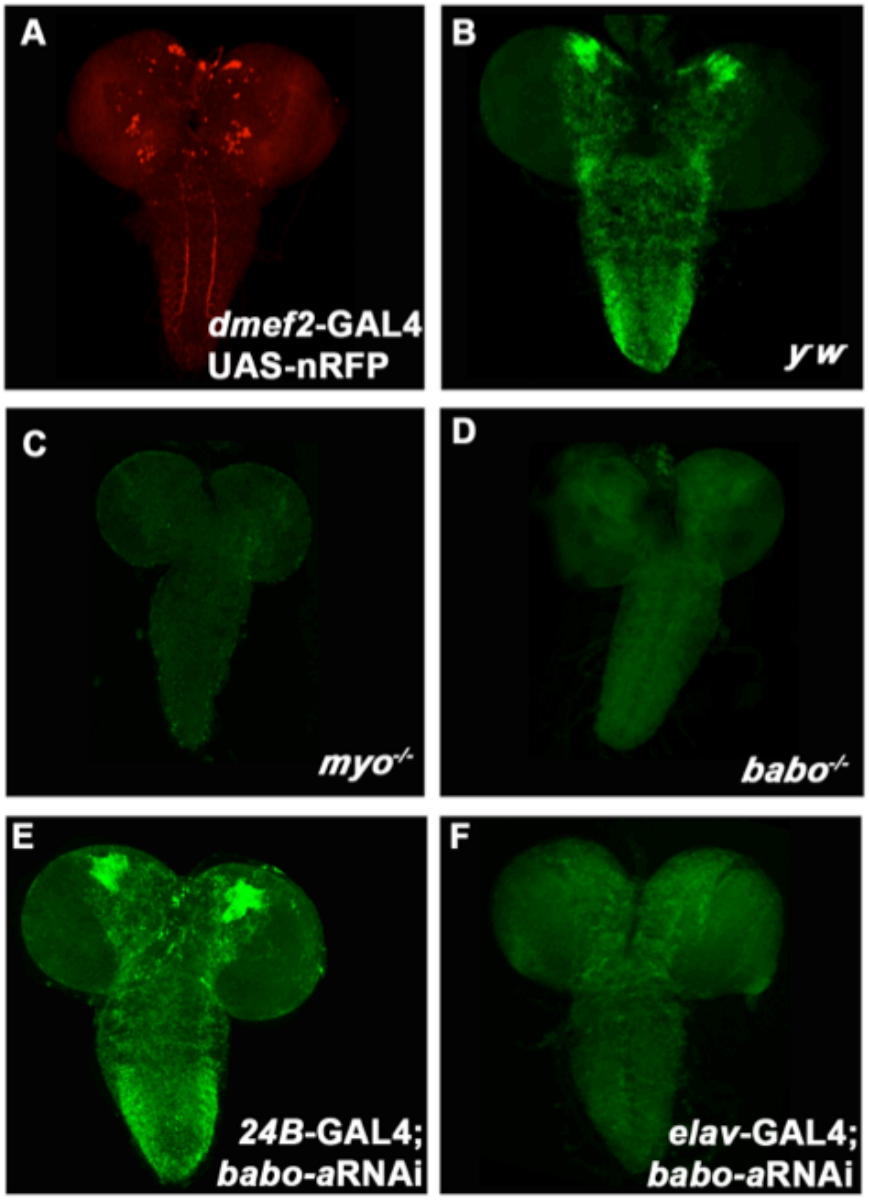
A
dmef2-GAL4
UAS-nRFP
B
yw
C
myo-/-
D
babo-/-
E
24B-GAL4;
babo-aRNAi
F
elav-GAL4;
babo-aRNAi

Figure 3.8 Reduced levels of activin signaling in the nervous system affect EcR-B1 expression throughout the whole CNS.

(A-F) Confocal images of the central nervous system at 0 hours APF (A) *dmef2*-GAL4 driven UAS-nRFP (red) expression is detected in cells near the antennal lobe projection neurons, insulin producing cells, and thoracic neurons. (B-F) EcR-B1 in the optic lobes and ventral nerve cord (VNC) of the CNS in white prepupa. (B) Controls highly express EcR-B1 in the mushroom body (MB) and ventral nerve cord (C) EcR-B1 expression in *myo* mutant is significantly reduced throughout the CNS (D) $babo^{fd4/}Df(2)babo$ mutants similarly show a significant decrease in EcR-B1 expression. (E and F) EcR-B1 expression in the CNS of animals in which *babo-a* was silenced using the following drivers (E) 24B-GAL4 *and* (F) pan-neuronal *elav*-GAL4. EcR-B1 was significantly reduced in the CNS with pan neuronal knockdown of *babo-a* but a decrease in expression could not be easily detected using a narrow neuronal driver, 24B-GAL4.

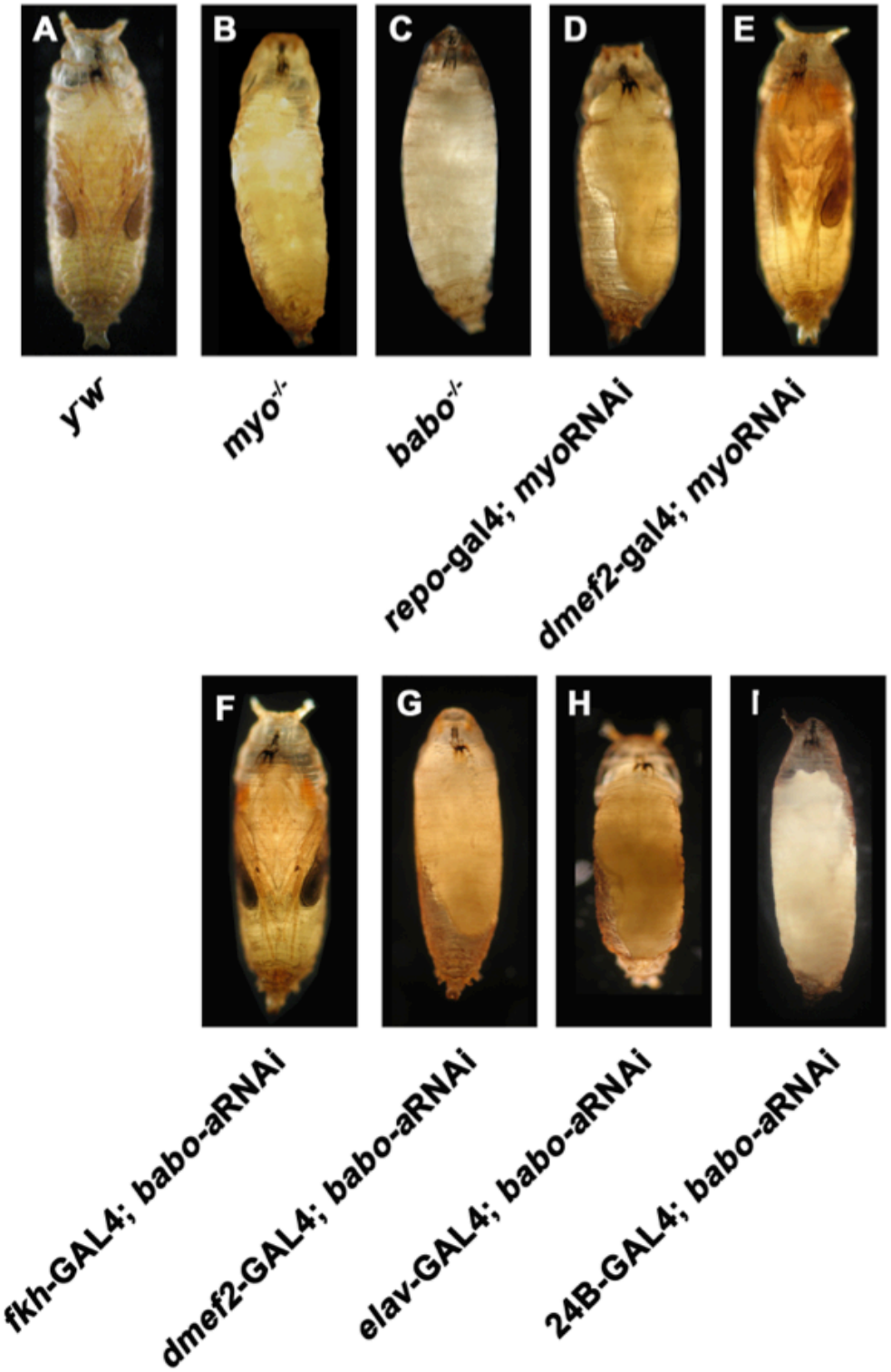
A
B
C
D
E
y w
myo-/-
babo-/-
repo-gal4; myoRNAi
dmef2-gal4; myoRNAi
F
G
H
I
fkh-GAL4; babo-aRNAi
dmef2-GAL4; babo-aRNAi
elav-GAL4; babo-aRNAi
24B-GAL4; babo-aRNAi

Figure 3.9 Disruption of activin signaling affects pupal development

(A-I) Representative pupal images of *y⁻w* controls and of animals in which activin signaling has been silenced in multiple tissue types. (A) *y⁻w⁻* control animals evert their anterior spiracles, elongate their legs, and complete metamorphosis. A subset of pupal defects described for ecdysone pathway mutants such as defects in anterior spiracle eversion, failure to shorten, gas bubble migration defects, asymmetric pupa are also observed in (B) *myo* mutants and (C) *babo* mutants. *myo* RNAi silencing in glia (repo-GAL4) results in similar pupal defects (D). No pupal defects in neuronal (*dmef2*-GAL4) silencing of *myo* (E). Pupal phenotypes described above were also observed in neuronal depletion of *myo* specific *babo-a* receptor isoform using multiple drivers: *dmef2*-GAL4 (G) elav-GAL4 (H) 24B-GAL4 (I). Pupal development was not affected when *babo* signaling was depleted in the salivary glands (fkh-GAL4) (F).

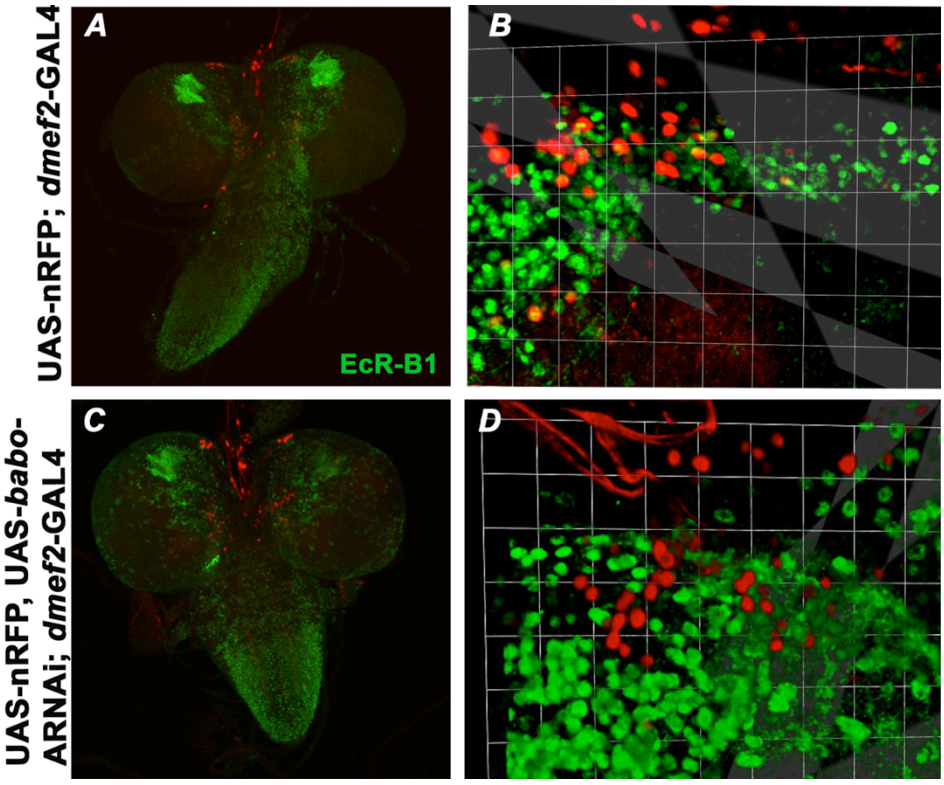
A
B
C
D
EcR-B1
UAS-nRFP; dmef2-GAL4
UAS-nRFP, UAS-babo-ARNAi; dmef2-GAL4

Figure 3.10 Depletion of *babo* in *dmef2*-GAL4 brain expressing cells affects EcR-B1 expression.

(A-D) EcR-B1 expression (green) in the brain of 0 APF animals labeled with *dmef2*-GAL4 driving UAS-nRFP (red) in control (A & B) and neuronal depleted *babo-a* animals (C & D). Confocal images at 63x of the optic lobes were submitted to Velocity imaging software for analysis. Velocity captured images reveal that an average of (8.4± 2.95; n=10) UAS-nRFP; *dmef2*-GAL4 co-express EcR-B1 cells in control animals (A & B), while only (1.3± 1.06; n=10) UAS-nRFP; *dmef2*-GAL4 co-expressing EcR-B1 cells in *babo*-a-miRNA was quantified (C & D).

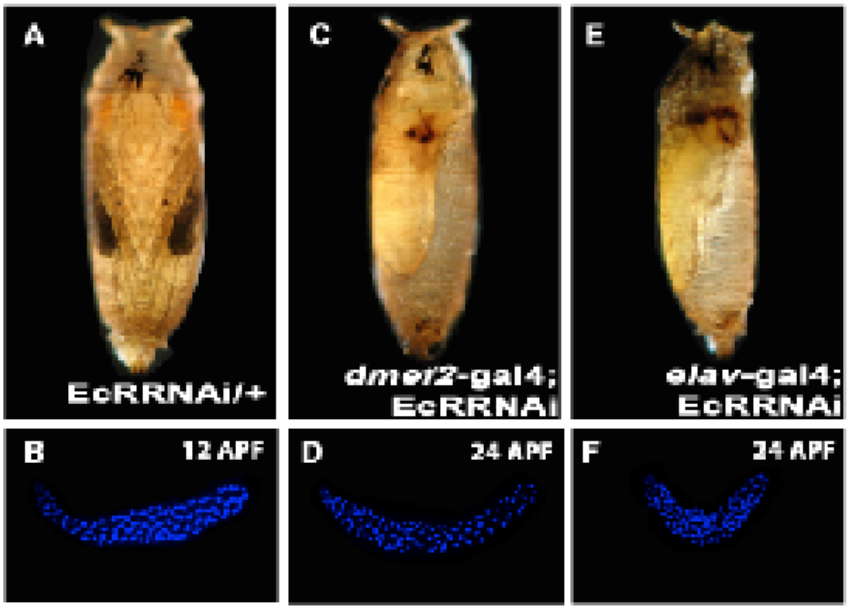
A
EcRRNAi/+
C
dmef2-gal4;
EcRRNAi
E
elav-gal4;
EcRRNAi
B
12 APF
D
24 APF
F
24 APF

Figure 3.11 Loss of EcR-B1 in the CNS results in salivary gland cell death defects.

(A,C,E) Pupal images of animals in which EcR-B1 was depleted in various tissues using UAS-GAL4. (B, D, F) Salivary glands at 12 (control) or 24 APF (experimental) stained with DAPI. (A&B) UAS-EcRRNAi/+. (C&D) *dmef2*-GAL4;EcRRNAi (E&F) *elav*-GAL4; EcRRNAi. (A) Controls display normal development with everted spiracles extended legs (C & E) Animals in which EcR-B1 was depleted in the nervous system display a wide range of pupal phenotypes including gas bubble migration defects, head everion defects, and fail to eclose. (B) At 12 APF, salivary glands are recovered from controls however at 24 APF, salivary glands are no longer present. (D& F) Persistent salivary glands observed in nervous system knockdown of EcR-B1.

Table 3.1 Myo Phenotypes

	Gas bubble defects	Asymmetric animals	Bent legs	Anterior spiracle defects	Pupal Lethal	Pharate adult	Eclosion
$y^{-}w^{-}$	0	0	0	0	8.42	16.8	74.7
myo*^{2}*/Df(4)myo	47.6	71.4	21.4	9.5	73.8	23.8	0

Number indicates the percentage of animals.

Table 3.2 Myo Misexpression Lethality Analysis

	2nd	2nd/3rd	3rd	Pupal	Eclosion
elav>myo **(pan-neuronal)**	35	65	0	0	0
repo> myo **(glia)**	0	100	0	0	0
nrv> myo **(glia & subset of neurons)**	0	100	0	0	0
24B> *myo* **(muscle & subset neurons)**	0	0	0	65	35
A9>myo **(wing disc & subset of neurons)**	0	0	0	70.83	29.17
dmef2> myo **(muscle & subset neurons)**	0	0	0	0	100

Number indicates the percentage of animals.

Table 3.3 Salivary gland cell death defects

Genotype	% of animals with Salivary gland cell death defects	n
Oregon R	0	>100
myo-/-	100	>100
Babo-/-		
***repo*-GAL4;UAS-*myo*RNAi**	100	10
***dmef2*-GAL4;UAS-myoRNAi**	0	10
***fkh*-GAL4;UAS-*babo-a* RNAi**	0	25
***Sg*-GAL4;UAS-*babo-a* RNAi**	0	25
***phm*-GAL4;UAS-*babo-a* RNAi**	0	10
***dmef2*-GAL4;UAS-*babo-a* RNAi**	100	25
***elav*-GAL4; UAS-*babo-a* RNAi**	100	10
24B-GAL4; UAS-*babo-a* RNAi	56.25	16
MB247-GAL4; UAS-*babo-a* RNAi	0	10
GH146-GAL4; UAS-*babo-a* RNAi	100	10
dmef2*-GAL4;UAS-*EcRRNAi	100	10
elav*-GAL4; UAS- *EcRRNAi	100	10
fkh*-GAL4; UAS- *EcRRNAi	100	15

Chapter 4

Role of Activin signaling in ecdysone triggered metamorphosis

Abstract

The transformation from an immature to adult form is accompanied by critical physical and behavioral changes. These events are regulated by steroid and peptide hormone signaling that impacts behavior, metabolism, sexual and neuronal development. During this period, the nervous system is also remodeled in response to hormone signaling. Previous work has shown that the activin pathway is required for remodeling of mushroom body γ-neurons, where it regulates expression of the ecdysone receptor, thus affecting the ability of these neurons to respond to ecdysone. However, the role of TGF-β/activin signaling in other hormone-regulated metamorphosis events is unknown. Our analysis of ecdysone receptor expression in the brain of activin ligand mutants (*myo*, *act*β, *daw,* and *mav*) revealed that *myo* is the only activin ligand required for EcR-B1 expression in the brain. We investigated the role of Myo in multiple tissues that undergo metamorphosis in response to ecdysone. We find that while upregulation of EcR-B1 expression in the mushroom body neurons is dependent on Myo signaling, EcR-B1 expression in other tissues, such as the larval midgut, fat body, and muscle are unaffected by loss of *myo* signaling. Furthermore, *myo* activity is not required for these tissues to undergo ecdysone signaling dependent tissue reorganization. Our data suggest that *myo* function is required in only a subset of tissues, during a discrete window of time, prior to the initiation of pupal development, providing specificity in the response to steroid signaling.

Introduction

As discussed in Chapter 3, *myo* loss-of-function analysis revealed a range of pupal phenotypes that are reminiscent of ecdysone pathway mutants, arguing that *myo* signaling may be required for several ecdysone-mediated biological responses. One of these tissues is the larval salivary glands that require *myo* signaling to undergo destruction during metamorphosis. This event depends on regulation of EcR-B1 in the brain, but not in the salivary gland itself. To further delineate the requirement for *myo* signaling in other aspects of metamorphosis, we choose several tissues that undergo morphological changes in response to the late larval or prepupal pulse of ecdysone. In this chapter, we present our studies on the following ecdysone mediated events: mushroom body γ neuron remodeling, fat body remodeling, larval midgut and muscle cell death.

During metamorphosis a subset of cells of the *Drosophila* nervous system are remodeled in response to ecdysone signaling and maintained in the adult, while the remaining undergo cell death. Mammals also reorganize neuronal circuits to form adult specific connections in response to steroid hormone signaling (Sisk and Zehr, 2005). Activin signaling is known to regulate aspects of steroid signaling in both mammals and flies (Welt et al., 2002; Zheng et al., 2003; Gibbens et al., 2011). Neuronal remodeling studies in flies have identified the activin-signaling pathway as a regulatory input for controlling the temporal response to ecdysone steroid hormone signaling during metamorphosis. Disruption of activin signaling pathway mutants or upregulation of the activin antagonist Follistatin (Fs), shows loss of EcR-B1 expression in the γ mushroom

body neurons in late third instar larval brains (Zheng et al., 2003; Pentek et al., 2009). Awasaki et al., (2011) reported loss of EcR-B1 expression in *myo* mutant γ mushroom body neurons and showed that loss of expression is linked with defects in neuronal remodeling in these animals. However, the requirement for *myo* and activin signaling in other tissues that undergo ecdysteroid mediated changes during metamorphosis remains unclear.

There are several mechanisms in place to ensure tissue specific ecdysone responses. Tissue specific responses can be achieved through regulation of expression of individual receptor isoforms. Three EcR isoforms have been identified, EcR-A, EcR-B1, EcR-B2. Different promoters control the A and B isoforms, while B1 and B2 are splice variants. Receptors differ in their N-terminal sequences, which contains the ligand independent activation function (AF-1) domain important for transcriptional activation/repression, but have the same DNA binding and ligand binding domains (Talbot et al., 1993; Mouillet et al., 2001; Warnmark et al., 2003). Isoforms are differentially expressed during metamorphosis in different tissues that have distinct metamorphic responses (Talbot et al., 1993). High levels of EcR-B1 are expressed in tissues that undergo metamorphosis related destruction while EcR-A is expressed in proliferating tissues (Cherbas et al., 2003). The larval fat body, salivary glands, muscles, midgut, epidermis, and γ mushroom body neurons all express higher levels of EcR-B1. By contrast the imaginal discs, prothoracic gland, and imaginal rings that give rise to adult salivary glands, midgut, and hindgut, express higher levels of EcR-A. Due to lack of specific antibodies, the expression profile for EcR-B2 is

unknown (Talbot et al., 1993).

In this study we focused was on defining the requirement for Myo in EcR-B1 expression in other tissues that are ecdysone responsive. We selected tissues that predominantly express the EcR-B1 isoform and tested if they require *myo* signaling to undergo their ecdysone mediated responses and for expression of EcR-B1. Here we show that upregulation of EcR-B1 in the brain and pruning of the axon and dentritic terminals of γ mushroom body neurons depends on a single activin ligand, Myo. We found that *myo* signaling is not required for fat body remodeling, larval midgut or muscle cell death, or for regulation of EcR-B1 in these tissues. These data suggest that Myo is not a global regulator of EcR-B1 expression and the responses that it triggers.

Methods

Drosophila stocks

Stocks were obtained from Bloomington Stock Center unless listed otherwise: Df (4) *myo* (M. Frash); Generation of myo^2 and UAS-mygRNAi were described in Chapter 3. We used *dmef2*-GAL4 (muscle driver), *krupple*-GAL4 (fat body driver), to express UAS-GFP on the second and third chromosomes. To study mutant animals, we introduced the GAL4s and UAS lines into a *myo* mutant background through a series of crosses.

Imaging of GFP expression in living animals

Animals of the correct genetic background were staged and collected at 0 APF.

Animals were placed on slide that was placed in a humid chamber at 25°C. Animals were imaged throughout metamorphosis. A Zeiss Axioplan 2 microscope was used to capture epiflourescence. The body wall muscle morphology was analyzed at 0, 12, 24, 36, 60 and 94 hours APF. The fat body morphology was imaged at 0, 4, 6, 8, 12, and 20 hours APF.

Imaging the larval midgut

Oregon R and *myo* mutants were selected at 0 APF and staged. Animals were dissected at 0 and 4 hours APF. The larval midguts were fixed using 4% formaldehyde and washed with 1x PBS. The midguts were mounted on a slide with 70% glycerol and imaged using dark field on a Zeiss Axioplan microscope.

Immunohistochemistry

Animals were staged and dissected in 1x PBS. Tissues were fixed in 4% formaldehyde in PBS and 0.1% Triton X-100 for 30 minutes. Fas II was detected using ID4 (1:200) from Developmental Studies Hybridoma Bank (DSHB). EcR-B1 was detected using AD4.4 (1:100) from DSHB and with a α-mouse Alexa 488 secondary. Staining protocol was previously described in chapter 3. DAPI staining was performed at 0.5 µg/ml for 10 minutes and rinsed. Tissues were mounted in Vectashield (Vector). Preparations were analyzed using an Olympus FluoView FV1000 scanning laser confocal or LSM780 confocal.

Results

We first examined the role of Myo in regulation of the mushroom body γ neuron remodeling. The mushroom bodies are structures found in the optic lobes of the larval brain that are important for olfactory learning and memory. There are three types of Kenyon cells that make up the mushroom body: γ, α/β, and α'/β' (Ito et al., 1998). The axon peduncles from these neurons project medial and dorsal lobe bundles. The γ neurons, which express EcR-B1, are the only mushroom body neurons that remodel their connections. By pupation (18 APF), the γ neurons have pruned their dorsal and medial lobes. Later, an adult medial γ lobe extends (Lee et al., 2000). The first evidence that activin signaling regulates remodeling of the γ neurons comes from studies by Zheng et al., (2003), where they showed that mutations in *babo*, the type I activin receptor, fail to prune and maintain the larval γ-neuron projections. This study also showed that the mechanism by which Babo signaling affects the behavior of the γ-neurons is through activation of EcR-B1 expression. Although these authors initially identified Actβ as the putative ligand acting through Babo, this result was based on over expression of a dominant negative form of the ligand and RNAi. Subsequently, Pentek et al., (2009). demonstrated that overexpression of the activin antagonist, Fs results in loss of EcR-B1 expression in the larval brain. Furthermore, we were able to suppress the Fs phenotypes by coexpression with Myo, arguing that the likely ligand was Myo (data not shown). When we initiated our studies, it was not clear which TGF-β /activin ligand was required for EcR-B1 expresson in the brain. To further characterize which activin signaling components are required for EcR-B1 expression we analyzed mutations in all

four activin related ligands, *actβ, daw, myo,* and *mav*. Homozygous mutant animals at white prepupal stages were stained to detect EcR-B1 expression using immunofluorescence. EcR-B1 was detected in the optic lobes and ventral nerve cord in Oregon R controls (Figure 4.1 A). Differences in EcR-B1 expression were not detected in *actβ, daw, or mav* homozygous mutants (Figure 4.1 D-F). However, *myo* loss-of-function animals display reduced levels of EcR-B1 expression in the optic lobe and ventral nerve cord (Figure 4.1 B). To determine if the source of Myo ligand was the glia, the UAS-GAL4 system was used to drive *myo* RNAi constructs specifically in glial cells. Reduced levels of EcR-B1 were detected in these animals, suggesting that glia derived Myo is required to promote EcR-B1 expression in the larval brain (Figure 4.1 C). Collectively, these data indicate that *myo* is the activin ligand that regulates expression of brain EcR-B1 expression. Interestingly, *daw* and *actβ* mutants also display lethality during metamorphosis, as do ecdysone pathway mutants. However, mutants for these ligands do not appear to have the pupal defects observed in EcR-B1 mutants. Our phenotypic analysis indicates that *myo* mutants display pupal phenotypes reported in EcR-B1 mutants, providing additional evidence that *myo* is the ligand that triggers Babo activity to regulate ecdysone signaling.

To determine if loss of EcR-B1 affects neuronal remodeling in *myo* mutants, *myo* mutants were stained with Fasciclin II (Fas II) antibody to visualize remodeling of γ neurons. By the pupal stage (18 APF), the γ larval neuron in $y^{-}w^{-}$ controls have been pruned and the α/β are the only neurons that remain (Figure

4.2 A, B). The γ neurons in a*dult y⁻w⁻* controls extend a medial projection (Figure 4.2 C). In *myo* mutants the γ neurons maintain their larval connections and fail to remodel at the pupal stage (18 APF) (Figure 4.2 D, E). *myo* mutants are pupal lethal therefore we were not able to view the adult neuronal connections. This result indicates that loss of ecdysone receptor expression correlate with loss of ecdysone responsiveness in this tissue.

We next analyzed the role of *myo* in fat body remodeling. The main function of the *Drosophila* fat body is to store energy similar to the mammalian liver and adipose tissue. When the fruit fly is ready to transition from a larva to a pupa, the animal begins to wander, finds a dry location to pupate, and stops feeding (Ashburner et al., 1989). The pupa is able to survive through many days of non-feeding because it has stored energy in fat body cells. Fat body cells change shape and dissociate in response to ecdysone pulses during metamorphosis. As pupariation commences the fat body has tightly associated polygonal cells that fill the whole body cavity. During apolysis, cells begin to change shape and take on a rounded appearance, and the fat body is no longer visible at the anterior end of the animal. The tight association of fat body cells begins to dissolve during prepupal development, between 6-12 hours APF. The head everts and individual fat body cells are visible in the head capsule at 12 APF. Individual fat body cells remain dispersed through out the whole animal for time remaining in metamorphosis. The recently eclosed adult still retains larval fat body cells but these undergo programmed cell death shortly after eclosion (Nelliot et al., 2006; Bond et al., 2011). Blocking ecdysone signaling results in fat

body remodeling defects. The fat body cells fail to change shape and do not dissociate into single cells in EcR dominant negative and βFTZ-F1 mutants (Bond, 2010).

To determine if *myo* signaling is required for ecdysone-triggered remodeling in this tissue, we analyzed the fat body during pupal development. We used the UAS/GAL4 system to visualize fat body cells in a *myo* mutant background. *kruppel*-GAL4 was used to drive UAS-GFP in the fat body. In 100% of *myo* mutant animals, the fat body retracts from the anterior and dissociates into individual cells (Figure 4.3 G-L; n=20). Fat body cells can be observed in the head capsule of *myo* mutants similar to controls (Figure 4.3 A-F). Furthermore, we observed that fat body morphology changes from polygonal to round cells in both control and *myo* mutant animals (Figure 4.3 M-P). These data suggest that *myo* signaling does not impact this aspect of metamorphosis. Additionally, EcR-B1 expression was not altered in *myo* mutant fat body cells compared to control (Figure 4.3 Q, R). Given that the ecdysone receptor involved in fat body metamorphosis EcR-B1 is not affected and the absence of a phenotype in *myo* mutant fat body, it appears that Myo does not function as a dedicated regulator of EcR-B1 expression in all tissues that undergo pupal metamorphosis.

We next analyzed the larval midgut to determine if this tissue is dependent on Myo signaling to undergo histolysis. *Drosophila* larval midgut cell death is induced by the late larval to prepupal pulse of ecdysone. Prior to the onset of metamorphosis, the larval midgut is elongated and has a proventriculus and gastric caeca. Four hours APF, the gastric caeca are no longer presents, the

proventriculus is reduced in size, and the midgut has contracted. By the prepupal-pupal, transition, the developing adult midgut cells surround the condensing larval midgut cells, known as the yellow body, which is released as the meconium in the newly eclosed fly (Jiang et al., 1997). Defects in larval midgut destruction have been observed for mutants in ecdysone response genes, BR-C and E93 (Lee et al., 2002). We observed that the larval midguts of Oregon R controls change from an elongated to a shortened gut, the 4 gastric caeca have been completely removed and a small proventriculus remains present at 4 APF (Figure 4.4 A, C; n=15) The appearance of *myo* mutant midgut resembles that of Oregon R control midguts at 4h APF (Figure 4.4 B, D; n=15). This observation suggests that *myo* signaling is not required for larval midgut histolysis. To determine if Myo signaling is required for EcR-B1 expression in the midgut, we staged and collected 0 APF animals for immunohistochemistry of the midgut. EcR-B1 is expressed in the larval midgut of *Oregon R* controls and *myo* mutants during the late larval ecdysone pulse (Figure 4.4 E, F). Our data show that *myo* signaling does not regulate an ecdysone response or EcR-B1 expression in the midgut histolysis. Preliminary analysis of midgut histolysis in $babo^{32/52}$ mutants however reveals that 87.5% of the animals do not undergo midgut histolysis (n=15). Further analysis of other activin ligands is needed to resolve which activin ligand mediates larval midgut histolysis.

We also analyzed remodeling of the larval dorsal abdominal muscles. During metamorphosis, muscle contractions are thought to be required for gas bubble expulsion, translocation to the anterior, and consequently head eversion

(Chadfield and Sparrow, 1985). *myo* mutants display defects in all three, indicating a possible defect in muscle contraction that could be linked to lack of metamorphosis of the larval muscles. The larval muscles are destroyed during metamorphosis. The anterior thoracic muscles are destroyed early in prepupal stage while the abdominal muscles are destroyed later (Robertson, 1936). Destruction of the *Drosophila* larval muscles is also dependent on ecdysone signaling. Abdominal muscles fail to degenerate in mutants for *BR-C*, an ecdysone target gene (Ward et al., 2003). In addition, Zirin et al., 2013, found that EcR-B1 and FTZ-F1 are required for abdominal dorsal exterior oblique muscle (DEOM) cell death but not for the abdominal dorsal internal oblique muscle cell (DIOM).

To determine if larval muscle cell death is dependent on *myo* signaling, we examined muscle histolysis in live animals using *dmef2*-Gal4 to drive expression of a UAS-GFP reporter in muscles and examine if they fail to degenerate in a *myo* mutant background. In control animals, the dorsal abdominal muscles begin to degrade after head eversion and adult muscles begin to take form (Figure 4.5 A-F). Larval muscles are degraded in *myo* mutants (Figure 4.5 G-L; n=22). To determine if Myo signaling is required for EcR-B1 expression in the body wall muscles, we staged and collected 0 APF animals for immunohistochemistry. EcR-B1 is expressed in the muscles of *Oregon R* controls and *myo* mutants (Figure 4.6 A, B). Our data suggest that Myo is not required for dorsal abdominal cell death, however further analysis needs to be conducted to rule out if other muscle cell types require *myo* to regulate their destruction.

In summary, we have identified a requirement for *myo* signaling in two tissues, the salivary glands (see Chapter 3) and the γ mushroom body neurons (this Chapter), that undergo morphological changes in response to ecdysone signaling, and both do so through regulation of EcR-B1 expression in the nervous system. However, loss of *myo* had no affect on the fat body remodeling, dorsal abdominal muscle cell death, and midgut cell death or EcR-B1 expression in these tissues, ruling out a dedicated role for Myo in regulation of EcR-B1 expression.

Discussion

Although there has been great effort to understand the different mechanisms that regulate distinct biological outcomes of ecdysone signaling, it remains poorly understood. Understanding how ecdysone is produced, released into the hemolymph, transported to responding tissues, how it interacts with different receptor isoforms, and the mechanism of action of ecdysone can provide insights into how different tissues could respond differently to a common signal. Expression analysis of primary and secondary response genes involved in different processes would also be informative. Studies have shown that Myo temporally upregulates EcR-B1 expression in the nervous system before the onset of metamorphosis to initiate ecdysone signaling triggered responses (Awasaki et al., 2011). In the present study, we followed the fates of multiple tissues, which undergo ecdysone triggered responses and that express high

levels of the B1 isoform of the ecdysone receptor, in an effort to determine if *myo* functions as a global regulator of EcR-B1 mediated responses.

Here we provide evidence that *myo* is not required by the larval midgut, muscle, or fat body, for regulation of EcR-B1 expression or for the response of these tissues to ecdysone signaling. This is in contrast to the loss of neuronal EcR-B1 in *myo* mutants. These data suggest that Myo is not obligately required for regulation of EcR-B1 in all tissues. Thus, it is possible that *myo* signaling is required exclusively in the nervous system as a competence signal to enhance the expression of EcR-B1 prior to the larval-pupal transition while expression in other tissues is regulated by other factors. No candidate genes have been identified thus far that upregulate EcR-B1 expression in the gut, fat body and muscle.

The events that are *myo* dependent (mushroom body remodeling and salivary gland cell death), both respond to the prepupal-pupal ecdysone pulse (Truman, 1990; Lee et al., 2000; Yin and Thummel, 2005). The observation that *myo* mutants have morphological defects in leg extension, gas bubble migration, and head eversion defects, argue that other events regulated by this prepupal-pupal ecdysone pulse are also *myo* dependent. It may be worth looking at other prepupal-pupal ecdysone events, such as wing disc elongation. Consistent with this, we did not find evidence for a *myo* role in events regulated by the early larval-prepupal ecdysone pulse (fat body remodeling and midgut cell death), However, *myo* mutants show a 9.5% incidence of spiracle defects, leaving open the possibility that it may play a less significant role during this earlier period.

The mechanism by which these processes are regulated could be linked to the loss EcR-B1 from various neurons. As discussed in Chapter 3, it remains to be determined if these neurons types require *myo* signaling to undergo morphological or developmental changes and consequently affect larval or pupal behavior.

Based on our observations, EcR-B1 expression is reduced in multiple neuronal cell types in addition to the γ mushroom body neurons, which fail to undergo remodeling, in *myo* mutants. It is not clear if all neurons depend on *myo* signaling to undergo either remodeling or cell death. Investigating the role of *myo* in ecdysone mediated neuronal responses in other neuronal cell types could reveal additional requirements for *myo* signaling.

Ecdysone signaling triggered programmed cell death is required by several tissues. Interestingly, the mode of cell death varies for different tissues. Both apoptotic and autophagy programmed cell death are required for larval salivary gland destruction (Jiang et al. 1997, 2000; Lee and Baehrecke 2001). Midgut histolysis is dependent on autophagy (Lee et al., 2002). It would be interesting to identify a *myo* signaling requirement in aspects of cell death in multiple tissues. Steroid hormones also regulate cell death in multiple mammalian tissues like the prostate and mammary glands, ovary, and testis (Kiess and Gallaher, 1998). However, the cell death signaling pathways for different tissues that undergo different forms of cell death remain poorly understood. Further analysis of Myo signaling regulation of steroid hormone

signaling in multiple tissues can provide insights into how steroid signaling is regulated in higher organisms.

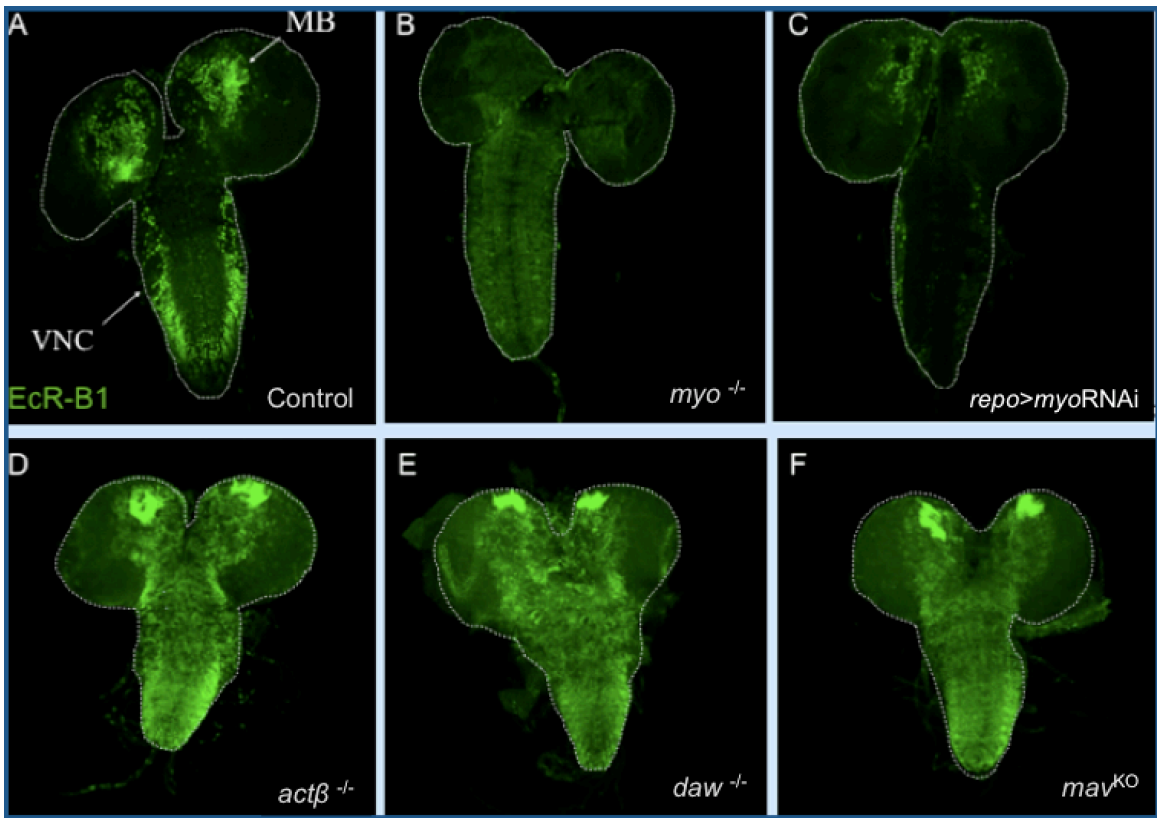
A
MB
VNC
EcR-B1
Control
B
myo -/-
C
repo>myoRNAi
D
actβ -/-
E
daw -/-
F
mav^KO

Figure 4.1 Myo is required for EcR-B1 expression in the brain.

EcR-B1 expression in the mushroom body (MB) and ventral nerve cord (VNC) of the CNS in white prepupa. (A) control (B) *myo* mutant (C) *myo*RNAi in glia cells (D) *act*β mutant (D) *daw* mutant and (F) *mav* targeted knockout.

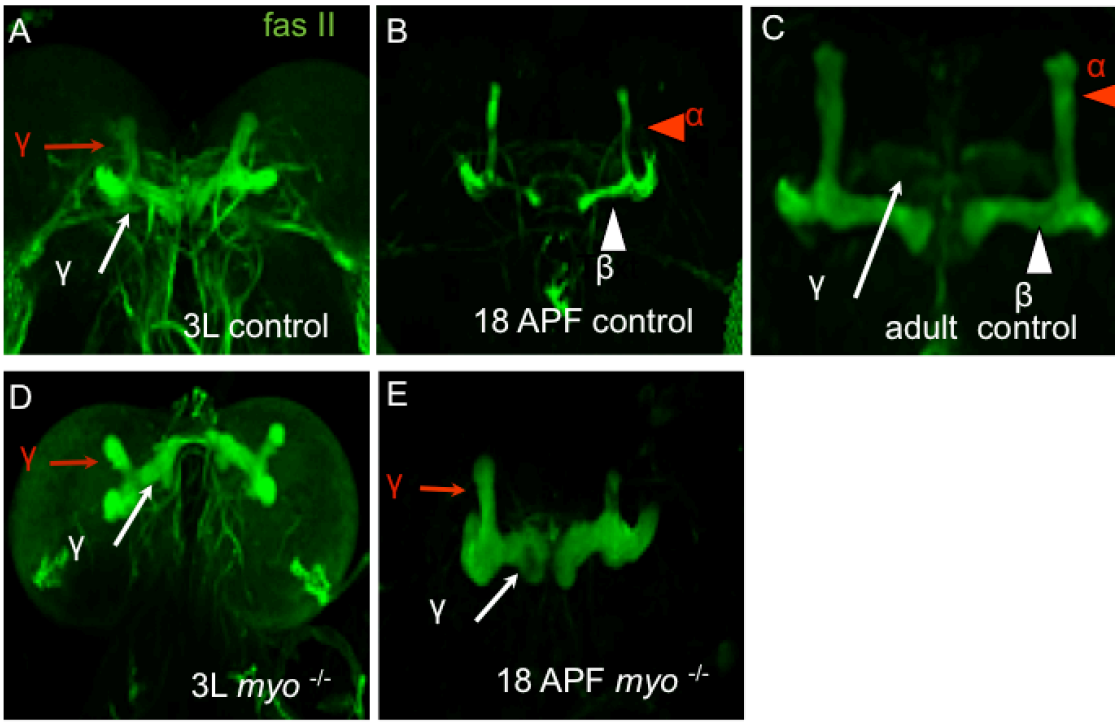
A
fas II
γ
γ
3L control
B
α
β
18 APF control
C
α
γ
β
adult control
D
γ
γ
3L myo -/-
E
γ
γ
18 APF myo -/-

Figure 4.2 Mushroom body γ neurons fail to remodel in *myo* mutants. Mushroom body γ and α/β neurons are labeled with Fas II antibody. (A-C) controls (D and E) *myo* mutants. Red arrows and arrowheads point to the dorsal lobes. White arrows and arrowheads point to the medial lobes. (A) control third instar larva with medial and dorsal γ lobe projections (B) control has pruned the medial and dorsal γ lobes and has projected the α/β lobes by 18 APF. (C) α/β and medial γ lobes are present in the adult. (D) *myo* mutant third instar larva with medial and dorsal γ lobe projections. (E) medial and dorsal γ lobe projections fail to prune by 18 APF in *myo* mutants. Myo mutants stop developing and fail eclose.

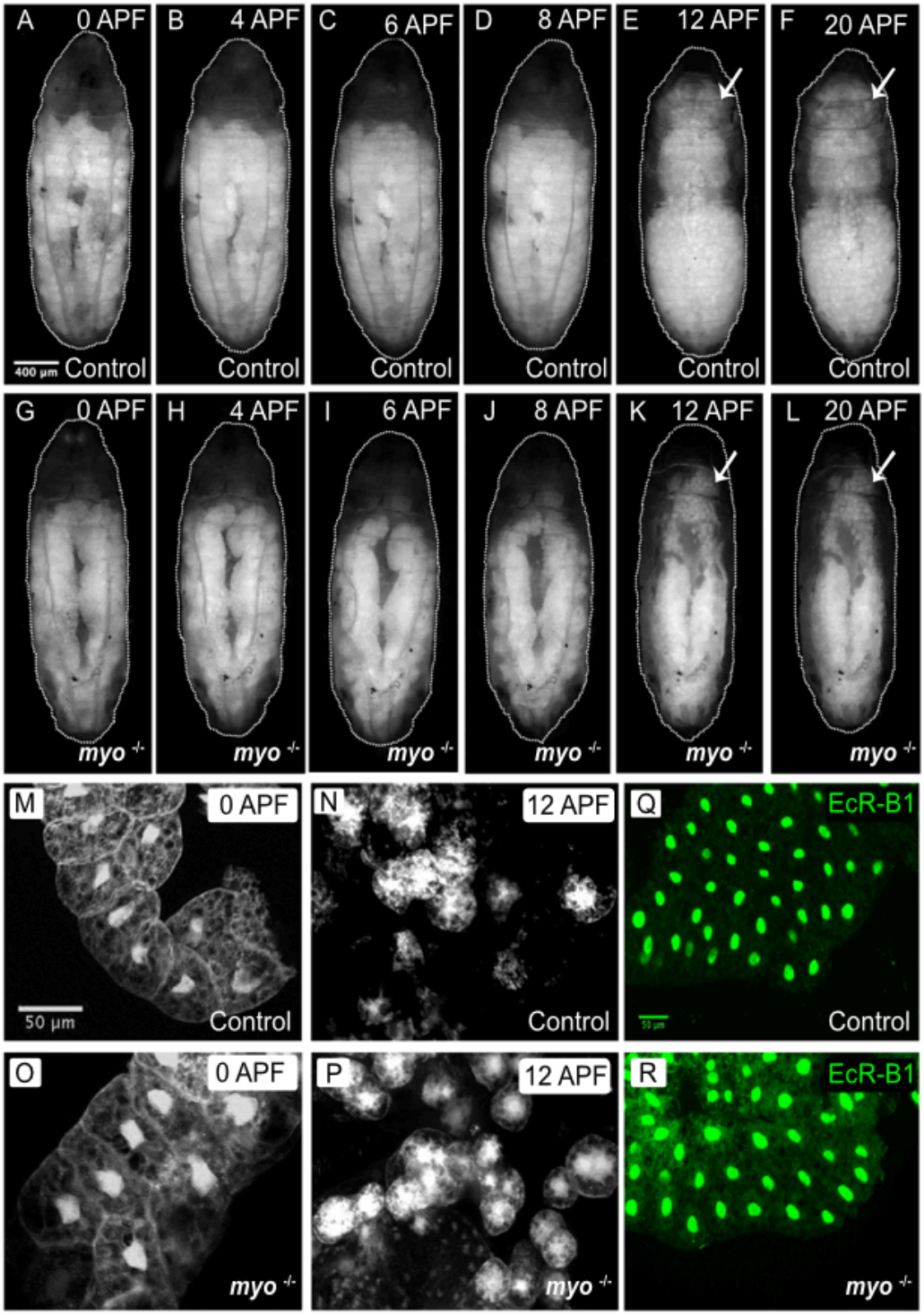
A 0 APF
B 4 APF
C 6 APF
D 8 APF
E 12 APF
F 20 APF
400 µm Control
Control
G 0 APF
H 4 APF
I 6 APF
J 8 APF
K 12 APF
L 20 APF
myo -/-
M 0 APF
N 12 APF
Q EcR-B1
50 µm Control
O 0 APF
P 12 APF
R EcR-B1

Figure 4.3 Loss of *myo* does not affect fat body remodeling.

(A-L) Fat body remodeling was visualized with a kr-GAL4 driver and UAS-GFP reporter. Animals were followed through pupal development and imaged. (A-F) Fat body in controls change shape and dissociate into round cells that move towards the head capsule (see arrow). (G-L) Fat body in *myo* mutants change shape and dissociate into round cells that move towards the head capsule (see arrow) similar to controls. (M-P) Confocal images of fat body cells marked with GFP (UAS-GFP, Kr-GAL4). In controls, fat body cells at 0 APF (M) are tightly associated and polygonal shaped which become single rounded cells by 12 APF (N). In *myo* mutants, fat body cells at 0 APF (O) are tightly associated and polygonal shaped which become single rounded cells by 12 APF (P). Similarly to controls (Q), *myo* mutants (R) express EcR-B1 during the onset of metamorphosis.

.

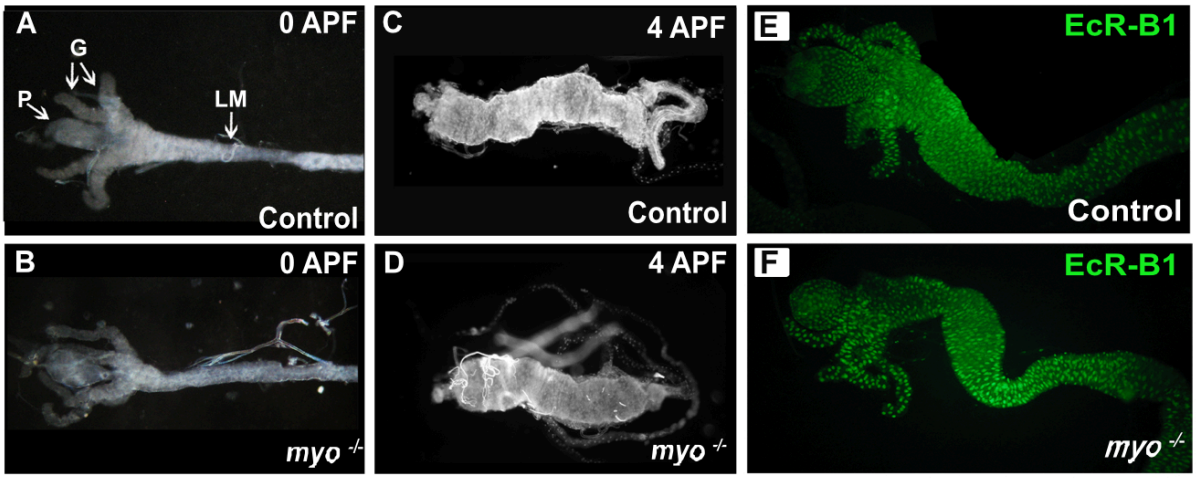
A
0 APF
G
P
LM
Control
C
4 APF
Control
E
EcR-B1
Control
B
0 APF
myo -/-
D
4 APF
myo -/-
F
EcR-B1
myo -/-

Figure 4.4 Loss of *myo* does not affect midgut cell death.

(A-D) Morphology of larval midgut (LM) undergoing remodeling. (A&C) Oregon R and (B&D) *myo* mutants were examined at 0 APF (A & B, respectively) and 4 APF (C & D, respectively). A smaller proventriculus (P), eliminated gastric caeca (G), and condensed midguts are observed in both Oregon R and *myo* mutants (C&D). EcR-B1 expression is observed at 0 APF control and *myo* mutant midguts (E&F, respectively).

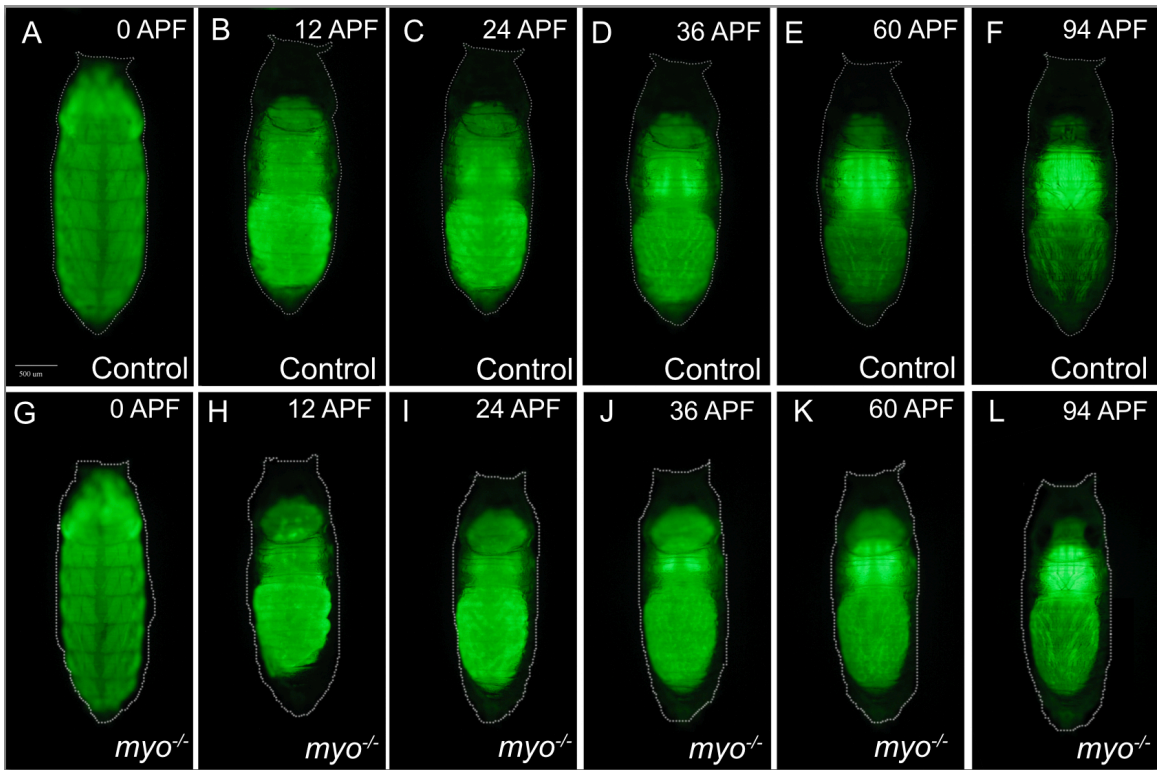
A
0 APF
Control
B
12 APF
Control
C
24 APF
Control
D
36 APF
Control
E
60 APF
Control
F
94 APF
Control
500 um
G
0 APF
myo-/-
H
12 APF
myo-/-
I
24 APF
myo-/-
J
36 APF
myo-/-
K
60 APF
myo-/-
L
94 APF
myo-/-

Figure 4.5 Dorsal muscle remodeling in *myo* mutants.

(A-R) Dorsal muscle remodeling was visualized with a *dmef2*-GAL4 driver and UAS-GFP reporter. Animals were followed through pupal development and imaged. (A-F) Dorsal muscles in control animals undergo thinning and form adult muscles prior to eclosion. (G-L) Dorsal muscles in *myo* pharate mutants undergo thinning and form adult muscles. (M-R) Dorsal muscles in *myo* prepupal mutants initiate muscle thinning.

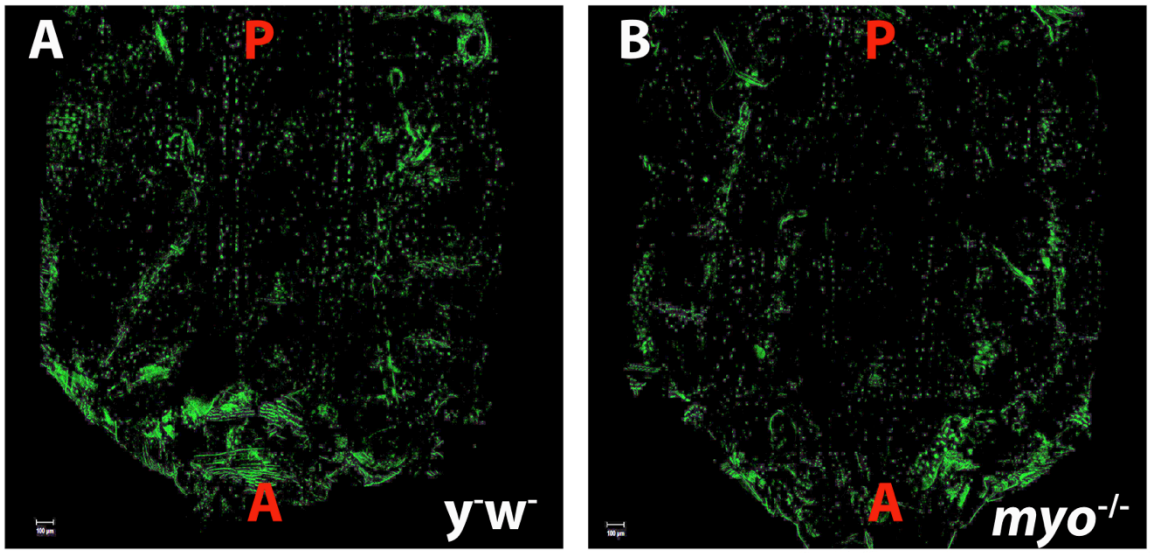
A
P
A
y-w-
B
P
A
myo-/-

Figure 4.6 Myo is not required for EcR-B1 expression in the larval body wall muscles.

White prepupa (0 APF) fillets were stained with αEcR-B1 antibody to observe expression in the inner body wall muscles. (A) Oregon R (n=5) (B) *myo* mutant (n=5). Anterior (A) and posterior (P) orientations of the animal are labeled in red.

Chapter 5

Conclusions and future directions

The evolutionarily conserved TGF-β/activin pathway has been implicated in many diverse processes including body axis formation, morphogenesis, cell proliferation and differentiation. However, it remains unclear how TGF-β/activin signaling can trigger so many contrasting cellular and biological responses. An explanation for the wide range of biological responses attributed to TGF-β/activin signaling lies in which signaling components are utilized such as specific ligand homodimers and heterodimers, the receptor combinations they bind, and the use of canonical and non-canonical intracellular signal pathways that they activate. In addition, it is becoming clear that combinatorial input from multiple signaling pathways serves to amplify or attenuate the impact of individual pathways. To better understand how different ligands of the TGF-β/activin pathway acting through a common receptor contribute to diverse responses, we investigated the requirement for two *Drosophila* activin-like ligands, Mav and Myo. Based on phenotypic and expression analysis we investigated the role of these ligands in NMJ growth and ecdysone signaling regulated events. We present evidence suggesting that although not essential for NMJ growth, Mav is sufficient to alter synapse development. Next, we found that larval salivary gland cell death and mushroom body remodeling are both dependent on activation of ecdysone receptor B1 in the brain, in response to Myo signaling. Our data points to a relay system in which ecdysone both directly and indirectly regulates tissue responses during metamorphosis.

Regulation of synaptogenesis by Mav

A requirement for TGF-β signaling in aspects of synaptogenesis is conserved in multiple organisms. For example, in *Xenopus laevis* TGF-β1 is required for synapse development. In mice, TGF-β2 is not required for synapse development but rather for synaptic transmission (Feng et al., 2008; Heupel et al., 2008). In *C. elegans*, *unc-129*, a BMP ligand, is required for motor neuron guidance (Colavita et al., 1998). Finally, as mentioned previously, several groups have demonstrated a requirement for both BMP and activin signaling in *Drosophila*.

We previously identified a requirement for Daw signaling in NMJ growth, however mutations in *babo* result in a more severe NMJ growth phenotype suggesting that a second activin ligand may function with Daw in promoting NMJ growth. We investigated the role of Mav at the NMJ based on its expression in glial cells. Excess expression of Mav in glial cells appears to have an affect on NMJ growth, as a minor increase in bouton numbers was observed (Fig. 2.3; Chapter 2). Our loss of function analysis of *mav* knockout lines did not reveal any deleterious effects on growth of the NMJ, in contrast to studies by Fuentes-Medel and colleagues (2012), who utilized depletion via RNAi to evaluate the requirement for *mav*. One possibility is that Daw could act redundantly with Mav, and compensates for loss of Mav activity. *mav* knockout mutants do not display any morphological defects and survive to adulthood. Analysis of *daw; mav* double mutants may have a stronger phenotype and reveal a role for *mav* in NMJ growth. A similar relationship between the BMP ligands, Scw and Dpp has been described previously *(*Arora et al., 1994; Ferguson and Anderson, 1992; Shimmi

et al., 2005*).* In this instance Dpp/Scw heterodimers act synergistically to specify dorsal embryonic cell fate, although excess Dpp can compensate for the loss of Scw. It remains to be determined whether Daw and Mav can form heterodimers or act synergistically for NMJ growth.

Regulation of metamorphosis by Myo

A second goal of this dissertation was to identify the role of Myo in steroid hormone regulation of maturation. We show that Myo, an activin ligand, functions as a regulator of steroid hormone metamorphic responses. In addition to the ecdysone associated morphological and behavioral defects in *myo* mutants, the salivary glands fail to degenerate and the γ mushroom body neurons fail to remodel These two responses are dependent on regulation of EcR-B1 expression in the nervous system by Myo signaling. In *myo* mutants, EcR-B1 expression is highly reduced in neurons of different identities. Furthermore, EcR-B1 expression was lost in animals in which the *myo* specific activin type I receptor, Babo-a, was depleted in the nervous system. Elimination of Babo-a, as well as EcR-B1 using neuron specific RNAi lines recapitulates the morphological defects observed in *myo* mutants. Our analysis of γ mushroom body neuron remodeling argues that activin signaling is required in these cells, however, in the case of salivary gland death, it appears that activin signaling in the nervous system indirectly regulates this ecdysone regulated biological responses. Finally, we have shown that expression of Myo in glia results in precocious larval transition defects that have been described for mutations in primary and

secondary ecdysone response genes. Taken together, our data implies that Myo signaling is required in the nervous system to regulate multiple responses to the steroid hormone ecdysone.

Potential role of Myo signaling in neuropeptide function

One possible way in which Myo signaling in the brain can indirectly affect salivary gland cell death is through influencing the production of another secreted factor from a subset of neurons, such as another growth factor, or alternatively a neuropeptide. However, in order to make a connection, future studies are required that focus on examining whether Myo regulates expression or secretion of any neurosecretory peptides and impacts associated behaviors. Currently there is no evidence that neuronal innervation or neurohormones can regulate salivary gland degradation in *Drosophila*. However, in some insects, salivary gland are known to be responsive to neuropeptide through neuronal innervation by the suboesophageal ganglion (SOG), satellite nervous system (SNS), stomatogastric nervous system (STS), and the median-transverse nervous system (MTNS) or through neurohormones serotonin and Dopamine for salivary gland function in the adults (Ali, 1997). In *myo* mutants, EcR-B1 expression is highly reduced in all neuronal populations and several of these cells produce neurosecretory peptides. One interesting possibility is that Myo regulates the expression of multiple neurosecretory peptides through regulation of EcR-B1 expression, and could therefore influence the responses of multiple non-neuronal tissues or organs in the animal and associated behaviors. There are several candidate neuropeptides that regulate ecdysis, imaginal disc eversion and

extension, cuticular tanning, wandering behavior, or muscle contractions during late third instar and metamorphosis. These include ecdysis-triggering hormone (ETH), eclosion hormone (EH), crustacean cardioactive peptide (CCAP), dFMRFamides, leucokinin, myoinhibiting peptides (MIPs), and corazonin (Crz) (Nassel and Winther, 2010; Santos et al., 2007). The type II Wit receptor is required for CCAP neuron ecdysis-associated behaviors. Wit mutants are pharate adult lethal and display head eversion, leg and wing disc extension defects, similarly to animals in which the CCAP neuron have been ablated. Furthermore, ecdysis phenotypes and lethality in *wit* mutants can be partially rescued with expression of in *wit* in CCAP neurons (Veverytsa and Allan, 2011). These data support a possible neurosecretory role for Myo. Analysis of peptide expression using existing antibodies in a *myo* mutant background would be a first step towards identifying a role for Myo signaling in neurosecretory function. The second step would be to determine if disrupting activin signaling through depletion of Babo-a using specific GAL4 lines that drive expression in those neurons results in specific morphological and behavioral defects. There is evidence in vertebrates that expression and secretion of neuronal gonadotropin-releasing hormone (GnRH) may be dependent on TGF-β1 (reviewed in Dobolyi 2012). GnRH in turn, along with inputs from activin, inhibin, and follistatin regulates the expression of FSH to influence development of gonadal tissues and pubertal development (Popovics et al., 2011).

The role of activin signaling in ecdysone biosynthesis

Our analysis of Myo in regulation of ecdysone signaling mediated responses was limited as we only analyzed how *myo* regulates tissue specific responses mediated through activation of EcR-B1. Recent studies have implicated activin signaling as one of the inputs in regulating ecdysone biosynthesis. The activin pathway was shown to affect ecdysone biosynthesis through regulation of receptors in the PTTH and insulin signaling pathways (Gibbens et al., 2011). *Drosophila* insulin–like proteins (DILPs) and PTTH hormone are synthesized in specific neurosecretory cells and act on the prothoracic gland, the site of ecdysone synthesis (Mcbrayer et al., 2007 and Gibbens et al., 2011). Identifying which of the 3 *Drosophila* activin ligands Daw, Activin β, or Myo are responsible for regulating ecdysone signaling and the mechanism used will prove useful in understanding how activin signaling regulates ecdysone hormonal response in multiple tissues. It is unlikely that Myo is the sole activin ligand that regulates ecdysone biosynthesis because not all ecdysone responsive tissues are affected in *myo mutants*. However, Myo mutants do have a wide range of pupal defects it could be a possible candidate. For example, Myo could regulate one of the pulses of ecdysone and thus affect a subset of biological events that respond to that pulse. Alternatively, *myo* may act redundantly with another activin ligand to regulate ecdysone biosynthesis.

The source of Myoglianin during pupal development

The two main sources of Myo are glial and muscle cells. However, muscle depletion or excess muscle derived *myo* does not affect the developing larva or

pupa as animals are able to eclose. A question that remains unanswered is why only glia secreted Myo has an affect on pupal development and not muscle derived Myo. One explanation may have to do with the amount of ligand available to the responding cell. Myo is in the vicinity of responding cells, while muscle *myo* is located at a distance, therefore perhaps it is possible that it does not reach the responding neuronal cells during prepupal development. The ligand may not be highly diffusible, it may have a short half-life, or the muscle is not able to make sufficient amounts. To become an active ligand, Myo must undergo proteolytic cleavage. While there is no evidence, perhaps muscle derived Myo is not processed during this period. The development of protein detection tools for immature and mature forms of Myo can provide insights into the actions of different derived forms of Myo.

Does Myo activate non-canonical Smad mediated pathways?

An approach used to find novel functions for TGF-β signaling is through identification of response elements in novel target genes. While this has worked well for the BMP pathway in many systems (Hata et al., 2000; Yao et al., 2006; Cho, 2011, Korchynskyi and ten Dijke, 2002), as well as for the activin pathway in the *Xenopus Mix.2 and goosecoid* promoters (Chen et al., 1996; Labbe´ et al., 1998), this approach has proven to be difficult as *dSmad2* responsive elements have not been identified in *Drosophila*. Currently, we know that upregulation of EcR-B1 in the CNS is dependent on Myo signaling. However, it is unknown if Myo signaling directly activates EcR-B1 expression. Identifying dSmad2

response elements in EcR-B1 may provide insights for the identification of novel Myo targets genes.

The Myo vertebrate homolog, Myostatin (MSTN) can signal through a non-Smad signaling pathway, via activation of p38, ERK 1/2, and JNK signaling independent of Smad activation (Philip et al., 2005. Huang et al., 2007; Yang, et al., 2006). Recent studies have shown that Myo signals through the Babo-a isoform in the γ mushroom body neurons (Awasaki et al. 2011). There is also evidence that dSmad2 is required for γ mushroom body remodeling and EcR-B1 expression indicating that for mushroom body remodeling Myo signals through a canonical signaling pathway (Zheng et al.,2003).One possibility is that dSmad2 has not been completely eliminated. Another possibility is that Myo signaling is independent of dSmad2 signaling, as no defects have been observed with dSmad2 RNAi depletion using several GAL4's (*nrv*, *phm*, *24B*) that drive expression in tissues that are activin signaling dependent. Therefore, we must consider that *myo* signaling may not involve Smads but rather it activates the downstream MAPK signaling pathway signal transducers as has been shown for MSTN in vertebrates. The JNK pathway mutant *DJNKK*/*hemipterous* (*hep*) has phenotypes similar to ecdysone pathway mutants and is pupal lethal (Agnès et al., 1999). To determine if a canonical intracellular signaling mechanism is used by Myo in specific tissues, immunohistochemistry using antibodies that detect phosphorylated and non phosphorylated forms of dSmad2 may prove insightful. However, successful detection of phosphorylated dSmad has only been observed in the wing disc (Hevia and de Celis, 2013). Further analysis is required

to understand the tissue specific roles and mechanism of signaling for Myo in *Drosophila* development.

Reference

Aberle, H., Haghighi, A. P., Fetter, R. D., McCabe, B. D., Magalhães, T. R., & Goodman, C. S. (2002). wishful thinking Encodes a BMP Type II Receptor that Regulates Synaptic Growth in Drosophila. *Neuron, 33*(4), 545-558.

Adler, J. H., & Grebenok, R. J. (1995). Biosynthesis and distribution of insect-molting hormones in plants—A review. *Lipids, 30*(3), 257-262.

Agnes, F., Suzanne, M., & Noselli, S. (1999). The Drosophila JNK pathway controls the morphogenesis of imaginal discs during metamorphosis. *Development, 126*(23), 5453-5462.

Ali, D. (1997). The aminergic and peptidergic innervation of insect salivary glands. *J Exp Biol, 200*(Pt 14), 1941-1949.

Arora, K., Levine, M. S., & O'Connor, M. B. (1994). The screw gene encodes a ubiquitously expressed member of the TGF-beta family required for specification of dorsal cell fates in the Drosophila embryo. *Genes & Development, 8*(21), 2588-2601.

Ashburner, M. (1989). *Drosophila: A Laboratory Handbook and Manual. Two volumes*.

Ashburner, M., Chihara, C., Meltzer, P., & Richards, G. (1974). Temporal control of puffing activity in polytene chromosomes. *Cold Spring Harbor symposia on quantitative biology, 38*, 655-662.

Awasaki, T., Huang, Y., O'Connor, M. B., & Lee, T. (2011). Glia instruct developmental neuronal remodeling through TGF-β signaling. *Nature neuroscience, 14*(7), 821-823.

Bai, H., Kang, P., Hernandez, A. M., & Tatar, M. (2013). Activin Signaling Targeted by Insulin/dFOXO Regulates Aging and Muscle Proteostasis in Drosophila. *PLoS Genetics, 9*(11), e1003941.

Ballard, S. L., Jarolimova, J., & Wharton, K. A. (2010). Gbb/BMP signaling is required to maintain energy homeostasis in Drosophila. *Developmental biology, 337*(2), 375-385.

Banovic, D., Khorramshahi, O., Owald, D., Wichmann, C., Riedt, T., Fouquet, W., et al. (2010). Drosophila neuroligin 1 promotes growth and postsynaptic differentiation at glutamatergic neuromuscular junctions. *Neuron, 66*(5), 724-738.

Bathori, M., Toth, N., Hunyadi, A., Marki, A., & Zador, E. (2008). Phytoecdysteroids and Anabolic-Androgenic Steroids - Structure and Effects on Humans. *Current Medicinal Chemistry, 15*(1), 75-91.

Bayat, V., Jaiswal, M., & Bellen, H. J. (2011). The BMP signaling pathway at the Drosophila neuromuscular junction and its links to neurodegenerative diseases. *Current Opinion in Neurobiology, 21*(1), 182-188.

Bender, M., Imam, F. B., Talbot, W. S., Ganetzky, B., & Hogness, D. S. (1997). Drosophila Ecdysone Receptor Mutations Reveal Functional Differences among Receptor Isoforms. *Cell, 91*(6), 777-788.

Berke, B., & Keshishian, H. (2009). Development of Drosophila Neuromuscular Juntions. In G. Lemke (Ed.), *Developmental Neurobiology* (pp. 520-528): Elsevier.

Berke, B., Wittnam, J., McNeill, E., Van Vactor, D. L., & Keshishian, H. (2013). Retrograde BMP Signaling at the Synapse: A Permissive Signal for Synapse Maturation and Activity-Dependent Plasticity. *The Journal of Neuroscience, 33*(45), 17937-17950.

Blanchard, F. J., Collins, B., Cyran, S. a., Hancock, D. H., Taylor, M. V., & Blau, J. (2010). The transcription factor Mef2 is required for normal circadian behavior in Drosophila. *The Journal of neuroscience : the official journal of the Society for Neuroscience, 30*(17), 5855-5865.

Bond, N. D. (2010). *The role of ecdysone signaling in fat-body tissue remodeling and pupal metabolism.* Unpublished Ph.D., University of Nevada, Las Vegas, Ann Arbor.

Bond, N. D., Nelliot, A., Bernardo, M. K., Ayerh, M. a., Gorski, K. a., Hoshizaki, D. K., et al. (2011). ßFTZ-F1 and Matrix metalloproteinase 2 are required for fat-body remodeling in Drosophila. *Developmental biology, 360*(2), 286-296.

Boulanger, A., Clouet-Redt, C., Farge, M., Flandre, A., Guignard, T., Fernando, C., et al. (2011). ftz-f1 and Hr39 opposing roles on EcR expression during Drosophila mushroom body neuron remodeling. *Nature neuroscience, 14*(1), 37-44.

Boulanger, A., Farge, M., Ramanoudjame, C., Wharton, K., & Dura, J.-M. (2012). Drosophila motor neuron retraction during metamorphosis is mediated by inputs from TGF-β/BMP signaling and orphan nuclear receptors. *PloS one, 7*(7), e40255-e40255.

Bovolenta, P. (2005). Morphogen signaling at the vertebrate growth cone: A few cases or a general strategy? *Journal of Neurobiology, 64*(4), 405-416.

Boyd, M., & Ashburner, M. (1977). The hormonal control of salivary gland secretion in Drosophila melanogaster: Studies in vitro. *Journal of Insect Physiology, 23*(4), 517-523.

Britton, J. S., & Edgar, B. A. (1998a). Environmental control of the cell cycle in Drosophila: nutrition activates mitotic and endoreplicative cells by distinct mechanisms. *Development, 125*(11), 2149-2158.

Britton, J. S., & Edgar, B. A. (1998b). Environmental control of the cell cycle in Drosophila: nutrition activates mitotic and endoreplicative cells by distinct mechanisms. *Development, 125*(11), 2149-2158.

Broadus, J., McCabe, J. R., Endrizzi, B., Thummel, C. S., & Woodard, C. T. (1999). The Drosophila βFTZ-F1 orphan nuclear receptor provides competence for stage-specific responses to the steroid hormone ecdysone. *Molecular Cell, 3*, 143-149.

Brummel, T., Abdollah, S., Haerry, T. E., Shimell, M. J., Merriam, J., Raftery, L., et al. (1999). The Drosophila Activin receptor Baboon signals through dSmad2 and controls cell proliferation but not patterning during larval development. *Genes & Development, 13*(1), 98-111.

Campos-Ortega, J. A., & Hartenstein, V. (1985). *The Embryonic development of Drosophila melanogaster*.

Chadfield, C. G., & Sparrow, J. C. (1984). Pupation in Drosophila melanogaster and the effect of the lethal cryptocephal mutation. *Developmental Genetics, 5*(2), 103-114.

Chen, X., Rubock, M. J., & Whitman, M. (1996). A transcriptional partner for MAD proteins in TGF-[beta] signalling. [10.1038/383691a0]. *Nature, 383*(6602), 691-696.

Cherbas, L. (2003). EcR isoforms in Drosophila: testing tissue-specific requirements by targeted blockade and rescue. *Development, 130*(2), 271-284.

Chng, W.-bin A., Sleiman, Maroun S. B., Schüpfer, F., & Lemaitre, B. (2014). Transforming Growth Factor β/Activin Signaling Functions as a Sugar-Sensing Feedback Loop to Regulate Digestive Enzyme Expression. *Cell Reports, 9*(1), 336-348.

Cho, J. Y. (2011). *Transcriptional regulation in response to TGF-beta signaling in Drosophila.* Unpublished Ph.D., University of California, Irvine, Ann Arbor.

Choi, J. C., Park, D., & Griffith, L. C. (2004). Electrophysiological and Morphological Characterization of Identified Motor Neurons in the Drosophila Third Instar Larva Central Nervous System. [10.1152/jn.01115.2003]. *Journal of Neurophysiology, 91*(5), 2353-2365.

Choi, Y., Tee, J. B., Gallegos, T. F., Shah, M. M., Oishi, H., Sakurai, H., et al. (2009). Neuropeptide Y functions as a facilitator of GDNF-induced budding of the Wolffian duct. *Development (Cambridge, England), 136*(24), 4213-4224.

Choi, Y.-J., Lee, G., & Park, J. H. (2006). Programmed cell death mechanisms of identifiable peptidergic neurons in Drosophila melanogaster. *Development (Cambridge, England), 133*(11), 2223-2232.

Colavita, A., Krishna, S., Zheng, H., Padgett, R. W., & Culotti, J. G. (1998). Pioneer axon guidance by UNC-129, a C. elegans TGF-beta. *Science, 281*(5377), 706-709.

Colombani, Bianchini, L., Layalle, S., Pondeville, E., Dauphin-Villemant, C., Antoniewski, C., et al. (2005). Antagonistic actions of ecdysone and insulins determine final size in Drosophila (Vol. 310).

Corrigan, L., Redhai, S., Leiblich, A., Fan, S.-J., Perera, S. M. W., Patel, R., et al. (2014). BMP-regulated exosomes from Drosophila male reproductive glands reprogram female behavior. *The Journal of Cell Biology, 206*(5), 671-688.

Cárcamo, J., Weis, F. M., Ventura, F., Wieser, R., Wrana, J. L., Attisano, L., et al. (1994a). Type I receptors specify growth-inhibitory and transcriptional responses to transforming growth factor beta and activin. *Molecular and Cellular Biology, 14*(6), 3810-3821.

Cárcamo, J., Weis, F. M., Ventura, F., Wieser, R., Wrana, J. L., Attisano, L., et al. (1994b). Type I receptors specify growth-inhibitory and transcriptional responses to transforming growth factor beta and activin. *Molecular and Cellular Biology, 14*(6), 3810-3821.

D'Avino, P. P., & Thummel, C. S. (2000). The ecdysone regulatory pathway controls wing morphogenesis and integrin expression during Drosophila metamorphosis. *Developmental biology, 220*(2), 211-224.

D'Avino, P. P. D., & Thummel, C. S. (1998). crooked legs encodes a family of zinc finger proteins required for leg morphogenesis and ecdysone-

regulated gene expression during Drosophila metamorphosis. *1745*, 1733-1745.

Das, P., Inoue, H., Baker, J. C., Beppu, H., Kawabata, M., Harland, R. M., et al. (1999). Drosophila dSmad2 and Atr-I transmit activin/TGFβ signals. *Genes to Cells, 4*(2), 123-134.

Davis, M. B., Carney, G. E., Robertson, A. E., & Bender, M. (2005a). NIH Public Access. *282*(2), 385-396.

Davis, M. B., Carney, G. E., Robertson, A. E., & Bender, M. (2005b). Phenotypic analysis of EcR-A mutants suggests that EcR isoforms have unique functions during Drosophila development. *Developmental biology, 282*(2), 385-396.

Decotto, E., & Spradling, A. C. (2005). The Drosophila Ovarian and Testis Stem Cell Niches: Similar Somatic Stem Cells and Signals. *Developmental Cell, 9*(4), 501-510.

Demontis, F., Patel, V. K., Swindell, W. R., & Perrimon, N. (2014). Intertissue control of the nucleolus via a myokine-dependent longevity pathway. *Cell reports, 7*(5), 1481-1494.

Demontis, F., & Perrimon, N. (2009). Integration of Insulin receptor/Foxo signaling and dMyc activity during muscle growth regulates body size in Drosophila. *Development (Cambridge, England), 136*(6), 983-993.

Denton, D., Aung-Htut, M. T., Lorensuhewa, N., Nicolson, S., Zhu, W., Mills, K., et al. (2013). UTX coordinates steroid hormone-mediated autophagy and cell death. *Nature communications, 4*, 2916-2916.

Dobolyi, A., Vincze, C., Pál, G., & Lovas, G. (2012). The neuroprotective functions of transforming growth factor Beta proteins. *Int J Mol Sci, 13*(7), 8219-8258.

Dunkel, L., Tilly, J. L., Shikone, T., Nishimori, K., & Hsueh, A. J. (1994). Follicle-stimulating hormone receptor expression in the rat ovary: increases during prepubertal development and regulation by the opposing actions of transforming growth factors beta and alpha. *Biology of Reproduction, 50*(4), 940-948.

Ellis, J. E. (2010). *Activin signaling in Drosophila nervous system development.* Unpublished Ph.D., University of California, Irvine, Ann Arbor.

Ellis, J. E., Parker, L., Cho, J., & Arora, K. (2010). Activin signaling functions upstream of Gbb to regulate synaptic growth at the Drosophila neuromuscular junction. *Developmental biology, 342*(2), 121-133.

Ewer, J. (2005). Behavioral actions of neuropeptides in invertebrates: Insights from Drosophila. *Hormones and Behavior, 48*(4), 418-429.

Feng, Z., & Ko, C.-P. (2008a). Schwann Cells Promote Synaptogenesis at the Neuromuscular Junction via Transforming Growth Factor-β1. *The Journal of Neuroscience, 28*(39), 9599-9609.

Feng, Z., & Ko, C.-P. (2008b). The Role of Glial Cells in the Formation and Maintenance of the Neuromuscular Junction. *Annals of the New York Academy of Sciences, 1132*(1), 19-28.

Ferguson, E. L., & Anderson, K. V. (1992a). decapentaplegic acts as a morphogen to organize dorsal-ventral pattern in the Drosophila embryo. *Cell, 71*(3), 451-461.

Ferguson, E. L., & Anderson, K. V. (1992b). decapentaplegic acts as a morphogen to organize dorsal-ventral pattern in the Drosophila embryo. *Cell, 71*(3), 451-461.

Fletcher, J. C., Burtis, K. C., Hogness, D. S., & Thummel, C. S. (1995). The Drosophila E74 gene is required for metamorphosis and plays a role in the polytene chromosome puffing response to ecdysone. *1465*, 1455-1465.

Fuentes-Medel, Y., Ashley, J., Barria, R., Maloney, R., Freeman, M., & Budnik, V. (2012). Integration of a retrograde signal during synapse formation by glia-secreted TGF-β ligand. *Current biology : CB, 22*(19), 1831-1838.

Gamer, L. W., Cox, K. A., Small, C., & Rosen, V. (2001). Gdf11 Is a Negative Regulator of Chondrogenesis and Myogenesis in the Developing Chick Limb. *Developmental Biology, 229*(2), 407-420.

Gerisch, B., Weitzel, C., Kober-Eisermann, C., Rottiers, V., & Antebi, A. (2001). A Hormonal Signaling Pathway Influencing C. elegans Metabolism, Reproductive Development, and Life Span. *Developmental Cell, 1*(6), 841-851.

Ghosh, A. C., & O'Connor, M. B. (2014). Systemic Activin signaling independently regulates sugar homeostasis, cellular metabolism, and pH balance in Drosophila melanogaster. *Proceedings of the National Academy of Sciences of the United States of America, 111*(15), 5729-5734.

Gibbens, Y. Y., Warren, J. T., Gilbert, L. I., & O'Connor, M. B. (2011). Neuroendocrine regulation of Drosophila metamorphosis requires TGFbeta/Activin signaling. *Development (Cambridge, England), 138*(13), 2693-2703.

Guo, X., & Wang, X.-F. (2009). Signaling cross-talk between TGF-[beta]/BMP and other pathways. *Cell Res, 19*(1), 71-88.

HADORN, E. (1951). Developmental action of lethal factors in drosophila. *Adv Genet, 4*, 53-85.

Haerry, T. E., Khalsa, O., O'Connor, M. B., & Wharton, K. A. (1998). Synergistic signaling by two BMP ligands through the SAX and TKV receptors controls wing growth and patterning in Drosophila. *Development, 125*(20), 3977-3987.

Hall, B. L., & Thummel, C. S. (1998). The RXR homolog Ultraspiracle is an essential component of the Drosophila ecdysone receptor. *4717*, 4709-4717.

Hamrick, M. W., Shi, X., Zhang, W., Pennington, C., Thakore, H., Haque, M., et al. (2007). Loss of myostatin (GDF8) function increases osteogenic differentiation of bone marrow-derived mesenchymal stem cells but the osteogenic effect is ablated with unloading. *Bone, 40*(6), 1544-1553.

Harvie, P. D., Filippova, M., & Bryant, P. J. (1998). Genes expressed in the ring gland, the major endocrine organ of Drosophila melanogaster. *Genetics, 149*(1), 217-231.

Hata, A., Seoane, J., Lagna, G., Montalvo, E., Hemmati-Brivanlou, A., & Massagué, J. (2000). OAZ uses distinct DNA- and protein-binding zinc fingers in separate BMP-Smad and Olf signaling pathways. *Cell, 100*(2), 229-240.

Henrich, V. C., Livingston, L., & Gilbert, L. I. (1993). Developmental requirements for the ecdysoneless (ecd) locus in Drosophila melanogaster. *Developmental Genetics, 14*(5), 369-377.

Hentze, J. L., Moeller, M. E., Jørgensen, A. F., Bengtsson, M. S., Bordoy, A. M., Warren, J. T., et al. (2013). Accessory gland as a site for prothoracicotropic hormone controlled ecdysone synthesis in adult male insects. *PloS one, 8*(2), e55131-e55131.

Heupel, K., Sargsyan, V., Plomp, J. J., Rickmann, M., Varoqueaux, F., Zhang, W., et al. (2008). Loss of transforming growth factor-beta 2 leads to impairment of central synapse function. *Neural Dev, 3*, 25.

Hevia, C. F., & de Celis, J. F. (2013). Activation and function of TGFβ signalling during Drosophila wing development and its interactions with the BMP pathway. *Dev Biol, 377*(1), 138-153.

Hillier, S. G., & MirÓ, F. (1993). Inhibin, Activin, and Follistatin Potential Roles in Ovarian Physiologya. *Annals of the New York Academy of Sciences, 687*(1), 29-38.

Hogan, B. L. (1996). Bone morphogenetic proteins: multifunctional regulators of vertebrate development. *Genes & Development, 10*(13), 1580-1594.

Huang, Z., Chen, D., Zhang, K., Yu, B., Chen, X., & Meng, J. (2007). Regulation of myostatin signaling by c-Jun N-terminal kinase in C2C12 cells. *Cell Signal, 19*(11), 2286-2295.

Ihry, R. J., & Bashirullah, A. (2014). Genetic control of specificity to steroid-triggered responses in Drosophila. *Genetics, 196*(3), 767-780.

Ito, K., Suzuki, K., Estes, P., Ramaswami, M., Yamamoto, D., & Strausfeld, N. J. (1998). The organization of extrinsic neurons and their implications in the functional roles of the mushroom bodies in Drosophila melanogaster Meigen. *Learning and Memory, 5*(1-2), 52-77.

Jiang, C., Baehrecke, E. H., & Thummel, C. S. (1997). Steroid regulated programmed cell death during Drosophila metamorphosis. *4683*, 4673-4683.

Jiang, C., Lamblin, A.-F. J., Steller, H., & Thummel, C. S. (2000). A Steroid-Triggered Transcriptional Hierarchy Controls Salivary Gland Cell Death during Drosophila Metamorphosis. *Molecular Cell, 5*(3), 445-455.

Karim, F. D., Guild, G. M., & Thummel, C. S. (1993). The Drosophila Broad-Complex plays a key role in controlling ecdysone- regulated gene expression at the onset of metamorphosis. *988*, 977-988.

Kawase, E., Wong, M. D., Ding, B. C., & Xie, T. (2004). Gbb/Bmp signaling is essential for maintaining germline stem cells and for repressing bam transcription in the Drosophila testis. *Development, 131*(6), 1365-1375.

Keshishian, H., Broadie, K., Chiba, A., & Bate, M. (1996). The Drosophila Neuromuscular Junction: A Model System for Studying Synaptic Development and Function. *Annual Review of Neuroscience, 19*(1), 545-575.

Keshishian, H., & Kim, Y. S. (2004). Orchestrating development and function: retrograde BMP signaling in the Drosophila nervous system. *Trends Neurosci, 27*(3), 143-147.

Khalsa, O., Yoon, J. W., Torres-Schumann, S., & Wharton, K. A. (1998). TGF-beta/BMP superfamily members, Gbb-60A and Dpp, cooperate to provide pattern information and establish cell identity in the Drosophila wing. *Development, 125*(14), 2723-2734.

Kiess, W., & Gallaher, B. (1998). Hormonal control of programmed cell death/apoptosis. *European Journal of Endocrinology, 138*(5), 482-491.

Kim, M.-J., & O'Connor, M. B. (2014). Anterograde Activin Signaling Regulates Postsynaptic Membrane Potential and GluRIIA/B Abundance at the <italic>Drosophila</italic> Neuromuscular Junction. *PLoS ONE, 9*(9), e107443.

Kim, M. J., & O'Connor, M. B. (2014). Anterograde Activin Signaling Regulates Postsynaptic Membrane Potential and GluRIIA/B Abundance at the Drosophila Neuromuscular Junction. *PLoS ONE, 9*(9), e107443.

King-Jones, K., Charles, J.-P., Lam, G., & Thummel, C. S. (2005). The ecdysone-induced DHR4 orphan nuclear receptor coordinates growth and maturation in Drosophila. *Cell, 121*(5), 773-784.

Kliewer, S. A., Umesono, K., Mangelsdorf, D. J., & Evans, R. M. (1992). Retinoid X receptor interacts with nuclear receptors in retinoic acid, thyroid hormone and vitamin D3 signalling. [10.1038/355446a0]. *Nature, 355*(6359), 446-449.

Koelle, M. R., Talbot, W. S., Segraves, W. A., Bender, M. T., Cherbas, P., & Hogness, D. S. (1991). The Drosophila EcR gene encodes an ecdysone receptor, a new member of the steroid receptor superfamily. *Cell, 67*, 59-77.

Korchynskyi, O., & ten Dijke, P. (2002). Identification and functional characterization of distinct critically important bone morphogenetic protein-specific response elements in the Id1 promoter. *J Biol Chem, 277*(7), 4883-4891.

Labbé, E., Silvestri, C., Hoodless, P. A., Wrana, J. L., & Attisano, L. (1998). Smad2 and Smad3 Positively and Negatively Regulate TGFβ-Dependent Transcription through the Forkhead DNA-Binding Protein FAST2. *Molecular Cell, 2*(1), 109-120.

Lee, C.-y., & Baehrecke, E. H. (2001). Steroid regulation of autophagic programmed cell death during development. *1455*, 1443-1455.

Lee, C.-Y., Cooksey, B. a. K., & Baehrecke, E. H. (2002). Steroid Regulation of Midgut Cell Death during Drosophila Development. *Developmental Biology, 250*(1), 101-111.

Lee, C.-Y., Simon, C. R., Woodard, C. T., & Baehrecke, E. H. (2002). Genetic Mechanism for the Stage- and Tissue-Specific Regulation of Steroid Triggered Programmed Cell Death in Drosophila. *Developmental Biology, 252*(1), 138-148.

Lee, S.-J. (2004). REGULATION OF MUSCLE MASS BY MYOSTATIN. *Annual Review of Cell and Developmental Biology, 20*(1), 61-86.

Lee, T., Marticke, S., Sung, C., Robinow, S., & Luo, L. (2000). Cell-Autonomous Requirement of the USP/EcR-B Ecdysone Receptor for Mushroom Body Neuronal Remodeling in Drosophila. *Neuron, 28*(3), 807-818.

Lee-Hoeflich, S. T., Zhao, X., Mehra, A., & Attisano, L. (2005). The Drosophila type II receptor, Wishful thinking, binds BMP and myoglianin to activate multiple TGFbeta family signaling pathways. *FEBS Lett, 579*(21), 4615-4621.

Li, F., Yang, H., Duan, Y., & Yin, Y. (2011). Myostatin regulates preadipocyte differentiation and lipid metabolism of adipocyte via ERK1/2. *Cell Biology International, 35*(11), 1141-1146.

Li, T., & Bender, M. (2000). A conditional rescue system reveals essential functions for the ecdysone receptor (EcR) gene during molting and metamorphosis in Drosophila. (0950-1991 (Print)).

Ling, N., Ying, S.-Y., Ueno, N., Shimasaki, S., Esch, F., Hotta, M., et al. (1986). Pituitary FSH Is Released by a Heterodimer of the [beta]-Subunits from the Two Forms of Inhibin. *Obstetrical & Gynecological Survey, 42*(2).

Liu, J.-P. (2006). The function of growth/differentiation factor 11 (Gdf11) in rostrocaudal patterning of the developing spinal cord. *Development, 133*(15), 2865-2874.

Lloyd, T. E., & Taylor, J. P. (2010). Flightless Flies: Drosophila models of neuromuscular disease. *Annals of the New York Academy of Sciences, 1184*, e1-20.

Lo, P. C. H., & Frasch, M. (1999). Sequence and expression of myoglianin, a novel Drosophila gene of the TGF-β superfamily. *Mechanisms of Development, 86*(1-2), 171-175.

Marchal, E., Vandersmissen, H. P., Badisco, L., Van de Velde, S., Verlinden, H., Iga, M., et al. (2010). Control of ecdysteroidogenesis in prothoracic glands of insects: a review. *Peptides, 31*(3), 506-519.

Marqués, G. (2005). Morphogens and synaptogenesis in Drosophila. *Journal of Neurobiology, 64*(4), 417-434.

Marqués, G., Bao, H., Haerry, T. E., Shimell, M. J., Duchek, P., Zhang, B., et al. (2002). The Drosophila BMP Type II Receptor Wishful Thinking Regulates Neuromuscular Synapse Morphology and Function. *Neuron, 33*(4), 529-543.

Massague, J. (1990). The Transforming Growth Factor-beta Family. *Annual Review of Cell Biology, 6*(1), 597-641.

Massague, J. (2012). TGF[beta] signalling in context. [10.1038/nrm3434]. *Nat Rev Mol Cell Biol, 13*(10), 616-630.

Massagué, J. (1996). TGFβ Signaling: Receptors, Transducers, and Mad Proteins. *Cell, 85*(7), 947-950.

Massagué, J. (1998). TGF-β SIGNAL TRANSDUCTION. *Annual Review of Biochemistry, 67*(1), 753-791.

McBrayer, Z., Ono, H., Shimell, M., Parvy, J.-P., Beckstead, R. B., Warren, J. T., et al. (2007). Prothoracicotropic hormone regulates developmental timing and body size in Drosophila. *Developmental cell, 13*(6), 857-871.

McCabe, B. D., Marqués, G., Haghighi, A. P., Fetter, R. D., Crotty, M. L., Haerry, T. E., et al. (2003). The BMP Homolog Gbb Provides a Retrograde Signal that Regulates Synaptic Growth at the Drosophila Neuromuscular Junction. *Neuron, 39*(2), 241-254.

McPherron, A. C., Lawler, A. M., & Lee, S.-J. (1997). Regulation of skeletal muscle mass in mice by a new TGF-p superfamily member. [10.1038/387083a0]. *Nature, 387*(6628), 83-90.

Melcher, C., & Pankratz, M. J. (2005). Candidate Gustatory Interneurons Modulating Feeding Behavior in the <italic>Drosophila</italic> Brain. *PLoS Biol, 3*(9), e305.

Meng, X., Wahlstro, G., Immonen, T., Kolmer, M., Tirronen, M., Predel, R., et al. (2002). The Drosophila hugin gene codes for myostimulatory and ecdysis-modifying neuropeptides. *117*, 5-13.

Menon, K. P., Carrillo, R. A., & Zinn, K. (2013). Development and plasticity of the Drosophila larval neuromuscular junction. *Wiley Interdisciplinary Reviews: Developmental Biology, 2*(5), 647-670.

Miech, C., Pauer, H.-U., He, X., & Schwarz, T. L. (2008). Presynaptic Local Signaling by a Canonical Wingless Pathway Regulates Development of the Drosophila Neuromuscular Junction. *The Journal of neuroscience : the official journal of the Society for Neuroscience, 28*(43), 10875-10884.

Montero, J. A., Lorda-Diez, C. I., Gañan, Y., Macias, D., & Hurle, J. M. (2008). Activin/TGFβ and BMP crosstalk determines digit chondrogenesis. *Developmental Biology, 321*(2), 343-356.

Mouillet, J.-F., Henrich, V. C., Lezzi, M., & Vögtli, M. (2001). Differential control of gene activity by isoforms A, B1 and B2 of the Drosophila ecdysone receptor. *European Journal of Biochemistry, 268*(6), 1811-1819.

Mouillet, J. F., Henrich, V. C., Lezzi, M., & Vögtli, M. (2001). Differential control of gene activity by isoforms A, B1 and B2 of the Drosophila ecdysone receptor. *Eur J Biochem, 268*(6), 1811-1819.

Nellen, D., Burke, R., Struhl, G., & Basler, K. (1996). Direct and Long-Range Action of a DPP Morphogen Gradient. *Cell, 85*(3), 357-368.

Nelliot, A., Bond, N., & Hoshizaki, D. K. (2006). Fat-body remodeling in Drosophila melanogaster. *Genesis (New York, N.Y. : 2000), 44*(8), 396-400.

Neul, J. L., & Ferguson, E. L. (1998). Spatially Restricted Activation of the SAX Receptor by SCW Modulates DPP/TKV Signaling in Drosophila Dorsal–Ventral Patterning. *Cell, 95*(4), 483-494.

Nguyen, M., Park, S., Marqués, G., & Arora, K. (1998). Interpretation of a BMP Activity Gradient in Drosophila Embryos Depends on Synergistic Signaling by Two Type I Receptors, SAX and TKV. *Cell, 95*(4), 495-506.

Nguyen, M., Parker, L., & Arora, K. (2000). Identification of maverick, a novel member of the TGF-β superfamily in Drosophila. *Mechanisms of Development, 95*(1–2), 201-206.

Nijhout, H. F. (1998). *Insect hormones*: Princeton University Press.

Nose, A. (2012). Generation of neuromuscular specificity in Drosophila: novel mechanisms revealed by new technologies. [10.3389/fnmol.2012.00062]. *Frontiers in Molecular Neuroscience, 5*.

Nässel, D. R. (2002). Neuropeptides in the nervous system of Drosophila and other insects: multiple roles as neuromodulators and neurohormones. *Progress in Neurobiology, 68*(1), 1-84.

Nässel, D. R., & Winther, A. M. E. (2010). Drosophila neuropeptides in regulation of physiology and behavior. *Progress in neurobiology, 92*(1), 42-104.

Orme, M. H., & Leevers, S. J. (2005). Flies on steroids: the interplay between ecdysone and insulin signaling. *Cell Metab, 2*(5), 277-278.

Park, D., Had iž, T., Yin, P., Rusch, J., Abruzzi, K., Rosbash, M., et al. (2011). Molecular organization of Drosophila neuroendocrine cells by dimmed. *Current Biology, 21*(18), 1515-1524.

Park, J. H., Schroeder, A. J., Helfrich-Förster, C., Jackson, F. R., & Ewer, J. (2003). Targeted ablation of CCAP neuropeptide-containing neurons of Drosophila causes specific defects in execution and circadian timing of ecdysis behavior. *Development, 130*(12), 2645-2656.

Parker, L., Ellis, J. E., Nguyen, M. Q., & Arora, K. (2006). The divergent TGF-β ligand Dawdle utilizes an activin pathway to influence axon guidance in Drosophila. *Development, 133*(24), 4981-4991.

Parker, L., Stathakis Dg Fau - Arora, K., & Arora, K. (2004). Regulation of BMP and activin signaling in Drosophila. [Review]. *Prog Mol Subcell Biol, 34:73-101*(0079-6484 (Print)).

Pentek, J., Parker, L., Wu, A., & Arora, K. (2009). Follistatin preferentially antagonizes activin rather than BMP signaling in Drosophila. *Genesis (New York, N.Y. : 2000), 47*(4), 261-273.

Philip, B., Lu, Z., & Gao, Y. (2005). Regulation of GDF-8 signaling by the p38 MAPK. *Cellular Signalling, 17*(3), 365-375.

Popovics, P., Rekasi, Z., Stewart, A. J., & Kovacs, M. (2011). Regulation of pituitary inhibin/activin subunits and follistatin gene expression by GnRH in female rats. *J Endocrinol, 210*(1), 71-79.

Prokop, A. (2006). Organization of the Efferent System and Structure of Neuromuscular Junctions In Drosophila. In R. C. Vivian Budnik and Catalina (Ed.), *International Review of Neurobiology* (Vol. Volume 75, pp. 71-90): Academic Press.

Quinn, L., Lin, J., Cranna, N., Lee, J., Mitchell, N., & R, H. (2012). Steroid Hormones in Drosophila: How Ecdysone Coordinates Developmental Signalling with Cell Growth and Division, Steroids - Basic Science, Prof. Hassan Abduljabbar (Ed.): InTech.

Ranganayakulu, G., Schulz, R. A., & Olson, E. N. (1996). Wingless Signaling Induces nautilus Expression in the Ventral Mesoderm of the Drosophila Embryo. *148*(0122), 143-148.

Reiter, L. T., Potocki, L., Chien, S., Gribskov, M., & Bier, E. (2001). A Systematic Analysis of Human Disease-Associated Gene Sequences In Drosophila melanogaster. *Genome Research, 11*(6), 1114-1125.

Restifo, L. L., & White, K. (1992). Mutations in a steroid hormone-regulated gene disrupt the metamorphosis of internal tissues in Drosophila: salivary glands, muscle, and gut. *Roux's Archives of Developmental Biology, 201*(4), 221-234.

Rewitz, K. F., Yamanaka, N., & O'Connor, M. B. (2013). Developmental checkpoints and feedback circuits time insect maturation. *Current topics in developmental biology, 103*, 1-33.

Riddiford, L. M. (1976). Hormonal control of insect epidermal cell commitment in vitro. *Nature, 259*(5539), 115-117.

Riddiford, L. M. (1993). Hormone receptors and the regulation of insect metamorphosis. *Receptor, 3*(3), 203-209.

Robertson, C. W. (1936). The metamorphosis of Drosophila melanogaster, including an accurately timed account of the principal morphological changes. *Journal of Morphology, 59*, 351-399.

Ruiz-Cañada, C., & Budnik, V. (2006). Synaptic cytoskeleton at the neuromuscular junction. *Int Rev Neurobiol, 75*, 217-236.

Santos, J. G., Vömel, M., Struck, R., Homberg, U., Nässel, D. R., & Wegener, C. (2007). Neuroarchitecture of Peptidergic Systems in the Larval Ventral Ganglion of Drosophila melanogaster. *PLoS ONE, 2*(8), e695.

Schmittgen, T. D., & Livak, K. J. (2008). Analyzing real-time PCR data by the comparative CT method. *Nature Protocols, 3*(6), 1101-1108.

Schubiger, M., Tomita, S., Sung, C., Robinow, S., & Truman, J. W. (2003). Isoform specific control of gene activity in vivo by the Drosophila ecdysone receptor. *Mechanisms of Development, 120*(8), 909-918.

Schubiger, M., Wade, A. A., Carney, G. E., Truman, J. W., & Bender, M. (1998). Drosophila EcR-B ecdysone receptor isoforms are required for larval molting and for neuron remodeling during metamorphosis. *2062*, 2053-2062.

Schuldiner, O., Berdnik, D., Levy, J. M., Wu, J. S.-y., Luginbuhl, D., Gontang, A. C., et al. (2008). NIH Public Access. *14*(2), 227-238.

Schulz, C., Kiger, A. A., Tazuke, S. I., Yamashita, Y. M., Pantalena-Filho, L. C., Jones, D. L., et al. (2004). A misexpression screen reveals effects of bag-of-marbles and TGF beta class signaling on the Drosophila male germ-line stem cell lineage. *Genetics, 167*(2), 707-723.

Shimmi, O., Umulis, D., Othmer, H., & O'Connor, M. B. (2005). Facilitated Transport of a Dpp/Scw Heterodimer by Sog/Tsg Leads to Robust Patterning of the Drosophila Blastoderm Embryo. *Cell, 120*(6), 873-886.

Sigrist, S. J., Reiff, D. F., Thiel, P. R., Steinert, J. R., & Schuster, C. M. (2003). Experience-Dependent Strengthening of Drosophila Neuromuscular Junctions. *The Journal of Neuroscience, 23*(16), 6546-6556.

Sink, H., & Whitington, P. M. (1991). Location and connectivity of abdominal motoneurons in the embryo and larva of Drosophila melanogaster. *Journal of Neurobiology, 22*(3), 298-311.

Siriett, V., Nicholas, G., Berry, C., Watson, T., Hennebry, A., Thomas, M., et al. (2006). Myostatin negatively regulates the expression of the steroid receptor co-factor ARA70. *Journal of cellular physiology, 206*(1), 255-263.

Sisk, C. L., & Zehr, J. L. (2005). Pubertal hormones organize the adolescent brain and behavior. *Frontiers in neuroendocrinology, 26*(3-4), 163-174.

Spradling, A., Fuller, M. T., Braun, R. E., & Yoshida, S. (2011). Germline Stem Cells. *Cold Spring Harbor Perspectives in Biology, 3*(11).

Stewart, B. A., & McLean, J. R. (2004). Population density regulates Drosophila synaptic morphology in a Fasciclin-II-dependent manner. *Journal of Neurobiology, 61*(3), 392-399.

Sun, M., Xing, G., Yuan, L., Gan, G., Knight, D., With, S. I., et al. (2011). Neuroligin 2 Is Required for Synapse Development and Function at the Drosophila Neuromuscular Junction. *The Journal of Neuroscience, 31*(2), 687-699.

Talbot, W. S., Swyryd, E. A., & Hogness, D. S. (1993). Drosophila tissues with different metamorphic responses to ecdysone express different ecdysone receptor isoforms. *Cell, 73*(7), 1323-1337.

Tan, C. K., Chong, H. C., Tan, E. H. P., & Tan, N. S. (2012). Getting /`Smad/' about obesity and diabetes. *Nutrition and Diabetes, 2*, e29.

Thummel, C. S. (1996). Flies on steroids - Drosophila metamorphosis and the mechanisms of steroid hormone action (Vol. 12, pp. 306-310).

Thummel, C. S. (1996). Flies on steroids — Drosophila metamorphosis and the mechanisms of steroid hormone action. *Trends in Genetics, 12*(8), 306-310.

Thummel, C. S., & Chory, J. (2002). Steroid signaling in plants and insects: common themes, different pathways (Vol. 16, pp. 3113-3129).

Toivonen, J. M., & Partridge, L. (2009). Endocrine regulation of aging and reproduction in Drosophila. *Molecular and cellular endocrinology, 299*(1), 39-50.

Veenstra, J. a. (2009). Peptidergic paracrine and endocrine cells in the midgut of the fruit fly maggot. *Cell and tissue research, 336*(2), 309-323.

Veverytsa, L., & Allan, D. W. (2011). Retrograde BMP signaling controls Drosophila behavior through regulation of a peptide hormone battery. *Development, 138*(15), 3147-3157.

Veverytsa, L., & Allan, D. W. (2013). Subtype-specific neuronal remodeling during Drosophila metamorphosis. *Fly, 7*(2), 78-86.

Wang, Z. (2011). *Endocytic trafficking is required for neuronal cell death through TGF-beta signaling in Drosophila melanogaster.* Thesis (Ph. D.)--University of Tennessee, Knoxville, 2011.

Ward, R. E., Reid, P., Bashirullah, A., D'Avino, P. P., & Thummel, C. S. (2003). GFP in living animals reveals dynamic developmental responses to ecdysone during drosophila metamorphosis. *Developmental Biology, 256*(2), 389-402.

Welt, C., Sidis, Y., Keutmann, H., & Schneyer, A. (2002). Activins, Inhibins, and Follistatins: From Endocrinology to Signaling. A Paradigm for the New Millennium. *Experimental Biology and Medicine, 227*(9), 724-752.

Wharton, K. A., Ray, R. P., & Gelbart, W. M. (1993). An activity gradient of decapentaplegic is necessary for the specification of dorsal pattern elements in the Drosophila embryo. *Development, 117*(2), 807-822.

Wolfner, M. F. (1997). Tokens of love: Functions and regulation of drosophila male accessory gland products. *Insect Biochemistry and Molecular Biology, 27*(3), 179-192.

Wolfner, M. F. (2002). The gifts that keep on giving: physiological functions and evolutionary dynamics of male seminal proteins in Drosophila. *Heredity, 88*(2), 85-93.

Wrana, J. L. (2013). Signaling by the TGFβ Superfamily. *Cold Spring Harbor Perspectives in Biology, 5*(10).

Wrana, J. L., Tran, H., Attisano, L., Arora, K., Childs, S. R., Massagué, J., et al. (1994). Two distinct transmembrane serine/threonine kinases from Drosophila melanogaster form an activin receptor complex. *Molecular and Cellular Biology, 14*(2), 944-950.

Wärnmark, A., Treuter, E., Wright, A. P., & Gustafsson, J. A. (2003). Activation functions 1 and 2 of nuclear receptors: molecular strategies for transcriptional activation. *Mol Endocrinol, 17*(10), 1901-1909.

Xie, T., & Spradling, A. C. (1998). decapentaplegic Is Essential for the Maintenance and Division of Germline Stem Cells in the Drosophila Ovary. *Cell, 94*(2), 251-260.

Yamanaka, N., Rewitz, K. F., & O'Connor, M. B. (2013). Ecdysone control of developmental transitions: lessons from Drosophila research. *Annual review of entomology, 58*, 497-516.

Yang, W., Chen, Y., Zhang, Y., Wang, X., Yang, N., & Zhu, D. (2006). Extracellular Signal–Regulated Kinase 1/2 Mitogen-Activated Protein Kinase Pathway Is Involved in Myostatin-Regulated Differentiation Repression. *Cancer Research, 66*(3), 1320-1326.

Yao, L.-C., Blitz, I. L., Peiffer, D. A., Phin, S., Wang, Y., Ogata, S., et al. (2006). Schnurri transcription factors from Drosophila and vertebrates can mediate Bmp signaling through a phylogenetically conserved mechanism. *Development, 133*(20), 4025-4034.

Yin, V. P., & Thummel, C. S. (2005). Mechanisms of steroid-triggered programmed cell death in *Drosophila*. *Seminars in Cell & Developmental Biology, 16*(2), 237-243.

Zheng, X., Wang, J., Haerry, T. E., Wu, A. Y. H., Martin, J., O'Connor, M. B., et al. (2003). TGF-β Signaling Activates Steroid Hormone Receptor Expression during Neuronal Remodeling in the Drosophila Brain. *Cell, 112*(3), 303-315.

Zhu, C. C., Boone, J. Q., Jensen, P. A., Hanna, S., Podemski, L., Locke, J., et al. (2008). Drosophila Activin-β and the Activin-like product Dawdle function redundantly to regulate proliferation in the larval brain. *Development, 135*(3), 513-521.

Zirin, J., Cheng, D., Dhanyasi, N., Cho, J., Dura, J.-M., Vijayraghavan, K., et al. (2013). Ecdysone signaling at metamorphosis triggers apoptosis of Drosophila abdominal muscles. *Developmental biology, 383*(2), 275-284.

Žitňan, D., Kim, Y. J., Žitňanová, I., Roller, L., & Adams, M. E. (2007). Complex steroid–peptide–receptor cascade controls insect ecdysis. *General and Comparative Endocrinology, 153*(1–3), 88-96.